

Ph.D. Thesis – Jun Wang; McMaster University – Civil Engineering

CONSTRUCTION SAFETY RISKS MANAGEMENT

Ph.D. Thesis – Jun Wang; McMaster University – Civil Engineering

SITUATIONAL AWARENESS FOR CONSTRUCTION SAFETY RISKS
MANAGEMENT

By JUN WANG

A Thesis Submitted to the School of Graduate Studies in Partial Fulfillment of the
Requirements for the Degree of Doctor of Philosophy

McMaster University © Copyright by Jun Wang, February 2018

Ph.D. Thesis – Jun Wang; McMaster University – Civil Engineering

McMaster University DOCTOR OF PHILOSOPHY (2018)

Hamilton, Ontario (Civil Engineering)

TITLE: Situational Awareness for Construction Safety Risks Management

AUTHOR: Jun Wang, M.Sc (Dalian University of Technology)

SUPERVISOR: Professor Saiedeh Razavi

NUMBER OF PAGES: xviii; 188

LAY ABSTRACT

Construction has the highest number of fatal injuries among all industries in Canada. Struck-by-equipment hazard (e.g., workers on foot struck by equipment or equipment struck by equipment) is one of the leading causes of construction injuries and fatalities. The primary goal of the work presented in this thesis is to reduce safety hazards based on data-driven solutions and sensed data. Specifically, this thesis pursued the following two main objectives: (i) identifying struck-by-equipment hazards with reduced false alarms in a timely manner and (ii) analyzing struck-by-equipment risk levels for individual entities (i.e., workers on foot and equipment) and construction sites. The key contributions of this research include (i) development of three spatiotemporal models to identify struck-by-equipment hazards and reduce false alarms; and (ii) development of a network-based model with three indicators to analyze struck-by-equipment risk at both entity and network (i.e., jobsite) levels.

ABSTRACT

The high number of construction injuries and fatalities resulted from struck-by-equipment hazards is one of the major challenges faced by the construction industry. Improved situational awareness assists workers to recognize hazardous situations, make decisions, and take actions in a timely manner to prevent hazards. Advanced technologies have been widely recognized as holding great promise to enable innovative applications in construction to improve situational awareness and to prevent struck-by-equipment hazards. However, existing solutions for detecting struck-by-equipment hazards generate frequent false alarms which interrupt construction and reduce site mobility and productivity. Also, there has been a need for an integrated method that can concurrently monitor and analyze the struck-by-equipment risk at both individual and system levels to enable proactive hazard prevention.

This research addresses the above-mentioned challenges by introducing the situational awareness for construction safety risks management (SA4SR), realizing timely and accurate hazard detection and dynamic risk analysis. Accordingly, the SA4SR consists of two modules: hazard detection and risk awareness. The hazard detection module focuses on identifying safety hazards in near real time with reduced false alarms. Three unsafe-proximity detection models were developed, which can not only identify struck-by-equipment hazards in a timely manner but also reduce false alarms. The effectiveness of these three models in reducing false alarms was evaluated and confirmed in both simulation and field experiments. The risk awareness module is centered on analyzing safety risk levels over time for individual entities and the whole construction

sites. A spatiotemporal network-based model with three safety leading indicators was developed to analyze the struck-by-equipment risk at both entity and network levels. The risk analysis at entity and network levels was conducted using four simulated sites, and the derived safety applications were summarized.

The developed SA4SR addressed the limitations of existing proximity detection methods and further developed a dynamic risk analysis model to comprehensively analyze struck-by-equipment risk. The situational awareness is improved by applying the developed models in the SA4SR to analyze sensed data (e.g., motions of entities). Consequently, hazards can be identified, risk evolution can be tracked and analyzed, and safety performance can be evaluated and compared. The developed SA4SR is expected to alleviate safety concerns in the construction industry and also can be extended to other types of contact collisions on sites to further enhance safety.

PREFACE

Three journal publications are included and presented in this thesis, as listed below:

- Paper #1: Wang, J., and Razavi, S. 2016a. **Low False Alarm Rate Model for Unsafe-Proximity Detection in Construction.** Journal of Computing in Civil Engineering, 30 (2), DOI: [10.1061/\(ASCE\)CP.1943-5487.0000470,04015005](https://doi.org/10.1061/(ASCE)CP.1943-5487.0000470,04015005).
- Paper #2: Wang, J., and Razavi, S. 2016b. **Two 4D Models Effective in Reducing False Alarms for Struck-by-Equipment Hazard Prevention.** Journal of Computing in Civil Engineering, 30 (6), DOI: [10.1061/\(ASCE\)CP.1943-5487.0000589,04016031](https://doi.org/10.1061/(ASCE)CP.1943-5487.0000589,04016031).
- Paper #3: Wang, J., and Razavi, S. 2018. **Spatiotemporal Network-Based Model for Dynamic Risk Analysis on Struck-by-Equipment Hazard.** Journal of Computing in Civil Engineering. 32 (2), DOI: [10.1061/\(ASCE\)CP.1943-5487.0000732](https://doi.org/10.1061/(ASCE)CP.1943-5487.0000732).

The timeline of each work and my contributions to each work are described below:

Paper #1 Presented in Chapter 2:

The work presented in paper #1 (i.e., Chapter 2) was conducted between September 2013 and July 2014. The manuscript was submitted in July 2014 and accepted in November 2014. My contributions to this paper are:

- Development of the unsafe-proximity detection model focusing on reducing false alarms in hazard identification;

- Implementation of the simulation using extended Kalman filter combined with nearest neighbor method as well as a controlled field experiment to test the developed model; and
- Development of the manuscript and working as the corresponding author of this paper.

Paper #2 Presented in Chapter 3:

The work presented in paper #2 (i.e., Chapter 3) was conducted between August 2014 and September 2015. The manuscript was submitted in September 2015 and accepted in January 2016. The model presented in Chapter 2 (which is a three-dimensional model) was improved and further developed to be two four-dimensional (4D) models which are published as the paper #2. My contributions to this paper are:

- Development of two 4D models (time-sphere model and time-cuboid model) for struck-by-equipment hazard identification and false alarm reduction;
- Implementation of simulation and field experiments to evaluate the performance of the two models; and
- Development of the manuscript and working as the corresponding author of this paper.

Paper #3 Presented in Chapter 4:

The work presented in paper #3 (i.e., Chapter 4) was conducted between October 2015 and October 2016. The manuscript was submitted in November 2016 and accepted

by the journal in August 2017. My contributions to this paper are:

- Development of the network-based model for struck-by-equipment risk analysis at both entity and network levels;
- Evaluation of the entity-level and network-level risk analysis in a simulated environment; and
- Development of the manuscript and working as the corresponding author of this paper.

Copyright Permission

I have secured written permission to include copyright material in this Ph.D. thesis from the copyright holder. The permission includes a grant of an irrevocable, non-exclusive license to McMaster University and to Library and Archives Canada to reproduce the material as part of the thesis.

ACKNOWLEDGEMENTS

I would like to express my deepest gratitude to my supervisor Prof. Saiedeh Razavi for the comprehensive guidance and continuous support of my Ph.D. study as well as professional development. No words can express my gratitude to my supervisor.

I gratefully acknowledge the Supervisory Committee members, Dr. Mohamed Attalla and Dr. Yiping Guo, for their support and advice on my research throughout my Ph.D. study.

I am grateful to Dr. Brian W. Baetz and Dr. Lydell Wiebe for their generous guidance on my professional development and to Dr. Ioannis Brilakis for his supervision during the period of my visiting study at the University of Cambridge. I am also grateful to Ms. Joanne Gadawski, Ms. Sarah Sullivan, and Ms. Carol Robinson for their administrative assist through my Ph.D. study.

It is a pleasure to thank my colleagues Wade Genders, Shuming Du, and Dr. Nazila Roofigari Esfahan for their support and professional collaborations. I am thankful to Virginia Viscardi and Wade Genders for their unfailing support and continuous encouragement throughout the years in Canada.

A very special gratitude goes out to the Natural Sciences and Engineering Research Council of Canada (NSERC) for awarding the Vanier Canada Graduate Scholarships to fund my Ph.D. study.

Finally, my profound gratitude goes to my parents, sister, and husband for their continuous love and support.

TABLE OF CONTENTS

LAY ABSTRACT	iii
ABSTRACT.....	iv
PREFACE.....	vi
ACKNOWLEDGEMENTS.....	ix
TABLE OF CONTENTS.....	x
LISTS OF FIGURES AND TABLES	xii
LIST OF ABBREVIATIONS.....	xvi
DECLARATION OF ACADEMIC ACHIEVEMENT.....	xviii
CHAPTER 1: INTRODUCTION	1
Problem Statement and Motivations	1
Research Objectives	8
Research Methodology.....	10
Thesis Organization.....	15
CHAPTER 2: HAZARD DETECTION I.....	19
Introduction	19
Paper #1: Low False Alarm Rate Model for Unsafe-Proximity Detection in Construction	20
CHAPTER 3: HAZARD DETECTION II	65
Introduction	65
Paper #2: Two 4D Models Effective in Reducing False Alarms for Struck-by- Equipment Hazard Prevention	66
CHAPTER 4: RISK AWARENESS.....	125
Introduction	125
Paper #3: Spatiotemporal Network-Based Model for Dynamic Risk Analysis on Struck- by-Equipment Hazard	127
CHAPTER 5: CONCLUSIONS	173
Summary, Contributions, and Impacts.....	173
Recommendations for Future Work.....	176

REFERENCES181

LISTS OF FIGURES AND TABLES

Chapter 1:

Fig. 1. Illustration of the dynamic interactions (a) between each pair of entities and (b) among all entities coexisting on a site	7
Fig. 2. The SA4SR framework	11
Fig. 3. Overview of the research objectives and methodology	14

Chapter 2:

Fig. 1. Framework of the unsafe-proximity detection model	28
Fig. 2. Flowchart of EKF combined with NN method for state tracking	30
Fig. 3. Illustration of the safety rules for Situations 1–5	32
Fig. 4. Flowchart of safety rules for unsafe-proximity identification.....	34
Fig. 5. Illustration of trajectories: (a) line trajectories; (b) curve trajectories; truth is the designed position with process noise; estimation is the tracked position using the EKF combined with the NN method	40
Fig. 6. Comparison of false alarm rate of estimations	46
Fig. 7. Instruments installation and real-time data review	49
Fig. 8. Obtained trajectories (map data © Google, DigitalGlobe): (a) scenarios of Groups 1 and 2; (b) scenarios of Group 3.....	50
Fig. 9. Experimental setting: (a) marked line trajectory; (b) different scenarios under line trajectories; (c) marked tangent line of curve trajectory	51

Table 1. Advantages and Limitations of Existing Proximity Detection Technologies.....	25
Table 2. Simulation Results of the Three Situations.....	41
Table 3. Validity Checking for the Three Situations	43
Table 4. Simulation Results	44
Table 5. Localization Accuracy Analysis	53
Table 6. Experiment Results Analysis	55

Chapter 3:

Fig. 1. 4D model real-world implementation (images by authors).....	75
Fig. 2. Alert zones for equipment and workers on foot: (a) time-sphere model; (b) time-cuboid model (images by authors).....	76
Fig. 3. Basic definitions: (a) local coordinate system (X - Y - Z); (b) entities' coordinate system (x - y - z).....	77
Fig. 4. (a) Geometrics of equipment alert zone for the time-cuboid model; (b) simplified case for the time-sphere model	79
Fig. 5. Overall process of the unsafe-proximity query rules used in the two 4D models..	88
Fig. 6. Unsafe-proximity query rules used in each plane (using the X - Y plane as an example).....	89
Fig. 7. Cases for already overlapped polygons: (a) four quadrants involved; (b) three quadrants involved; (c) two quadrants involved	94

Fig. 8. Unsafe-proximity query rules for polygons that will overlap: (a) one quadrant involved; (b) three quadrants involved; (c) two consecutive quadrants involved; (d) two non-consecutive quadrants involved.....	99
Fig. 9. (a) Scenario 3; (b) Scenario 4; (c) Scenario 5; (d) trajectories in Scenario 8.....	101
Fig. 10. False negative generated by the time-sphere model.....	105
Fig. 11. Entities' movement trajectories (image ©2015 DigitalGlobe Google Earth): (a) front-end loader; (b) truck tractor; (c) lift truck.....	108
Fig. 12. Experimental results: (a) Scenario 3; (b) Scenario 12.....	113
Table 1. Simulated Scenarios.....	100
Table 2. Simulation Results	103
Table 3. Experiment Scenarios	107
Table 4. Position Accuracy Analysis (m)	110
Table 5. Experimental Results	111
Chapter 4:	
Fig. 1. Network-based struck-by-equipment risk analysis model (adapted from Wang and Razavi 2017a; the images of workers and equipment in Step 2 are adopted from Wang and Razavi 2016b)	135
Fig. 2. Relative risk scores of jobsite #4 using severity thresholds as: (a) 1; (b) 0.8; (c) 0.6; and (d) adjusted and updated	152

Fig. 3. Relative risk scores of jobsite (a) #1; (b) #2; (c) #3; and (d) #4 using the same severity threshold	153
Fig. 4. Illustration of the situation at (a) frame 7 in Fig. 3(a); (b) frame 13 in Fig. 3(d); (c) frame 1117 in Fig. 3(b); and (d) frame 1441 in Fig. 3(c)	155
Fig. 5. Illustration of the situation at frame 3: (a) layout of entities on the jobsite and (b) quantified interactions presented in the network	158
Fig. 6. Degree centrality results: (a) score of each entity and (b) degree centrality expressed in the weighted network	159
Fig. 7. Eigenvector centrality results: (a) score of each entity and (b) eigenvector centrality expressed in the network.....	159
Fig. 8. Degree centrality over time: (a) entity with the highest degree centrality at each frame and (b) degree centrality ranking of one specific entity at each frame.....	160
Fig. 9. Eigenvector centrality over time: (a) entity with the highest eigenvector centrality at each frame and (b) eigenvector centrality ranking of one specific entity at each frame	161
Table 1. Summary of Frequencies of Factors	139
Table 2. Severity of Different Regions Relative to Equipment	144
Table 3. Description of Simulated Jobsites.....	150

LIST OF ABBREVIATIONS

AC: Algebraic connectivity

BBS: Behavior-based safety

BD of E: Braking distance of equipment

BIM: Building Information Modeling

CDC: Centers for Disease Control and Prevention

CPS: Cyber-physical system

EKF: Extended Kalman filter

FACE: Fatality Assessment and Control Evaluation

FAR: False alarm rate

FNR: False negative rate

FPR: False positive rate

FTR: False tracking rate

GPS: Global positioning system

IHSA: Infrastructure Health and Safety Association

IMU: Inertial measurement unit

INS: Inertial navigation system

IoT: Internet of Things

MEMS: Micro-Electro-Mechanical Systems

MFR: Model false rate

NIOSH: National Institute for Occupational Safety and Health

NN: Nearest neighbor

OSHA: Occupational Safety and Health Administration

RAP: Reduced alarms percentage

RD of E: Reaction distance of equipment

RD of W: Reaction distance of worker on foot

RFID: Radio frequency identification

RMSE: Root Mean Square Error

SA4SR: Situational Awareness for Construction Safety Risks Management

TDOA: Time difference of arrival

UAV: Unmanned aerial vehicle

WGS 84: World Geodetic System 1984

DECLARATION OF ACADEMIC ACHIEVEMENT

Ms. Wang was the main contributor and first author of all the articles presented in this thesis. The detailed contributions of the coauthor are described at the beginning of the corresponding chapter that includes the published article.

CHAPTER 1: INTRODUCTION

Problem Statement and Motivations

Overview on Construction Safety, Smart Construction, and Situational Awareness

Construction leads all industries in total worker fatal injuries in many countries such as the U.S. and Canada (BLS 2016a; AWCBC 2016). Over the 10 year period from 2007 to 2016 in Ontario, Canada, the construction sector grew by 23% and accounted for 29% (the highest traumatic fatality percentage) of the total traumatic fatalities of all industry sectors (Statistics Canada 2017; WSIB 2017). One of the major reasons causing the high fatalities and critical injuries in construction is the dynamics and complexity of construction sites. On construction sites, workers engage with dynamic resources in activities that potentially expose them to safety hazards (Zhang et al. 2013; Zhou et al. 2012; Pinto et al. 2011). Therefore, using technologies to monitor the situations occurring on sites has been identified as an effective solution to improve safety (Cheng and Teizer 2013; Hu and Zhang 2011).

In recent years, technologies have been utilized at different phases to enhance construction safety and support smart construction environments. For example, in the pre-construction phase, game technologies were used to develop a safety training platform for construction plant operations (Guo et al. 2012); location tracking and Unity3D-based data visualisation technologies were combinedly used to provide proactive training for safe

and efficient precast installation (Li et al. 2015a); an approach based on mobile eye-tracking technology was used to measure workers' situational awareness levels and further determine whether workers' situational awareness levels were improved after safety training (Hasanzadeh et al. 2016); Building Information Modeling (BIM) was used to evaluate the constructability and safety of climbing formwork systems (Kannan and Santhi 2013). During construction, wearable inertial measurement units were adopted to detect near-miss falls in ironwork (Yang et al. 2016); a wireless and wearable electroencephalography system was applied to monitor workers' vigilance states in construction activities to maintain and implement successful safety management practices (Wang et al. 2017); laser scanners, cameras, and wireless communication technologies were used to aid safe heavy equipment operations by recognizing dynamic objects from the surrounding environments in near real time (Wang and Cho 2015).

The use of robots, sensors, actuators, and a range of other Internet-enabled devices may further enable new safety applications to be used in the context of smart construction (Kochovski and Stankovski 2018). The construction industry is expected to gain significant advancements in safety management through the more widespread use of smart technologies in construction.

The occurrence of an accident is the consequence of mutual interactions of various risk factors. The vulnerability of a workforce can be described as a combination of individual and workplace factors, such as a lack of situational awareness that increases the safety risks. Temporarily losing or lacking situational awareness is a causal factor in many construction accidents (Health and Safety Executive 2015). A widely accepted

definition of situational awareness was developed by Endsley (2000) and consists of three levels (Irizarry et al. 2013):

- Level 1: perception of elements in current situation within a volume of time and space;
- Level 2: comprehension of the meanings of the elements;
- Level 3: projection of the status of the elements in the near future.

Situational awareness is depicted as the workers' internal model of the state of their surroundings. In this way, workers can decide what actions to take according to the situation (Endsley 2000). Situational awareness is represented as the main precursor to decision making and thus, improved situational awareness can lead to better decisions and avoidance of hazards on construction sites. Efforts to enhance safety through improving situational awareness have been made. For example, social network analysis was applied to investigate the relationship between worker interactions' patterns and crews' situational awareness capability (Albert and Hallowell 2014). The results showed that efficient and frequent interactions among crews can increase crews' situational awareness and consequently, the crews tend to identify more hazards. Multiple technologies also have been used in construction to improve situational awareness. For example, location tracking and data visualization technologies were used to increase the situational awareness for construction site trainees, workers, equipment operators, or decision makers to increase safety in dynamic construction site operations (Teizer et al. 2013; Cheng and Teizer 2013).

Overview on Struck-by-Equipment Hazard

The Occupational Safety and Health Administration (OSHA) identified four leading causes of construction fatalities, namely falls, struck-by, caught-in/between, and electrocutions, which are called the “Fatal Four” (OSHA 2017). Over the period of 2007-2016, fatalities of struck-by and caught-in/between objects accounted for 13% of all workplace fatalities in Ontario, Canada (WSIB 2017). Among the Fatal Four, the most serious struck-by injuries occur when a worker is struck by a piece of equipment or moving vehicle (IHSA 2017). In all equipment-involved accidents, struck-by-equipment hazards accounted for 87.7% (Hinze and Teizer 2011).

Intensive efforts from the academia and industry have been put into preventing struck-by-equipment hazards. Technology-enabled proximity warning systems using cameras, laser scanners, GPS, Bluetooth sensing, radio frequency identification (RFID), and others have been developed to alarm workers on foot and/or equipment operators about their proximity (Kim et al. 2016; Wang and Cho 2015; Teizer and Cheng 2015; Park et al. 2015; IHSA 2013). Each technology has its own advantages and limitations for the applications of proximity detection (Wang and Razavi 2016a). However, a major and common limitation of the existing proximity detection methods/systems is the high frequency of false alarms (false positives and false negatives) generated (Ruff 2010 and Teizer et al. 2010). The frequently generated false alarms will interrupt construction work, and eventually cause alarms to be ignored or disabled by participants. Furthermore, frequent and disruptive false alarms have put a limitation on the implementations of these systems/methods in real construction environments.

One of the main causes of false alarms is that the existing methods only use entities' positions for proximity detection. The distance between entities is monitored, and alarms are triggered once the distance is detected as being smaller than the predefined distance threshold (i.e., warning distance). Only using entities' positions (i.e., the distance between entities) failed to fully and accurately portray the actual situations that the entities are in. In some situations, false alarms are generated as the entities are moving apart from each other while the distance between them is smaller than the threshold. It has been suggested that positions together with other state parameters, such as speed and orientation (roll, pitch, and yaw), can describe a user's spatial context more precisely than using positions alone (Li et al. 2012; Behzadan et al. 2008). Another cause of generating false alarms is that the distance threshold (warning distance), used to determine whether an alarm is needed, is a constant value over time (Choe et al. 2014). A constant distance threshold should not apply to each pair of entities on sites due to their different dynamics. For example, a larger warning distance is needed for the entities with higher speed while slower entities need a shorter warning distance. In this way, appropriate time can be provided for entities to respond. In addition, compared with a reactive alarm, an accurate proactive (look-ahead) alarm allows entities enough time to conduct corrective actions to avoid a collision. Identification of the upcoming spatial conflicts also can assist to reduce false alarms. Development of a reliable method to foresee upcoming interferences between three-dimensional (3D) shapes (e.g., used to represent the inherent hazardous zone of an entity in the context of collision prevention) is of paramount importance and a great challenge. The prevalent methods for identifying future spatial intersections work

with three main steps: assuming a forecast time interval (e.g., 5 seconds), generating the 3D shapes corresponding to the assumed time interval, and analyzing whether the generated 3D shapes are intersected. In other words, these methods are more capable of detecting the intersections of already given 3D shapes with predefining a forecast time interval (Vahdatikhaki et al. 2015).

To address the above-identified limitations, an effective unsafe-proximity detection method that can reduce the generation of false alarms by considering the dynamics of entities and complexities of sites is needed to prevent contact collisions and save time and cost.

On dynamic and complex construction sites, each entity is simultaneously interacting with multiple other entities. The study of unsafe-proximity detection focuses on investigating the interactions between each pair of entities to prevent collisions [Fig. 1 (a)]. However, the strength of the total interactions between a single entity and all others [Fig. 1 (b)] was not considered in the existing proximity detection methods (Wang and Razavi 2016a, b; Choe et al. 2014). Modeling entities and the dynamic interactions and interrelationships among them as a system (network) promotes the full understanding of the struck-by-equipment risk from both entity and system levels and accordingly, preventive actions can be implemented from entity and system levels to avoid undesirable consequences. For example, analysis of the dynamic struck-by-equipment risk over time for each entity (entity-level risk) as well as the whole jobsite (network-level risk) assists to track the risk evolution, identify entities and sites with high risk levels, evaluate and compare safety performance for entities as well as sites, and provide insight into site

layout and activity planning.

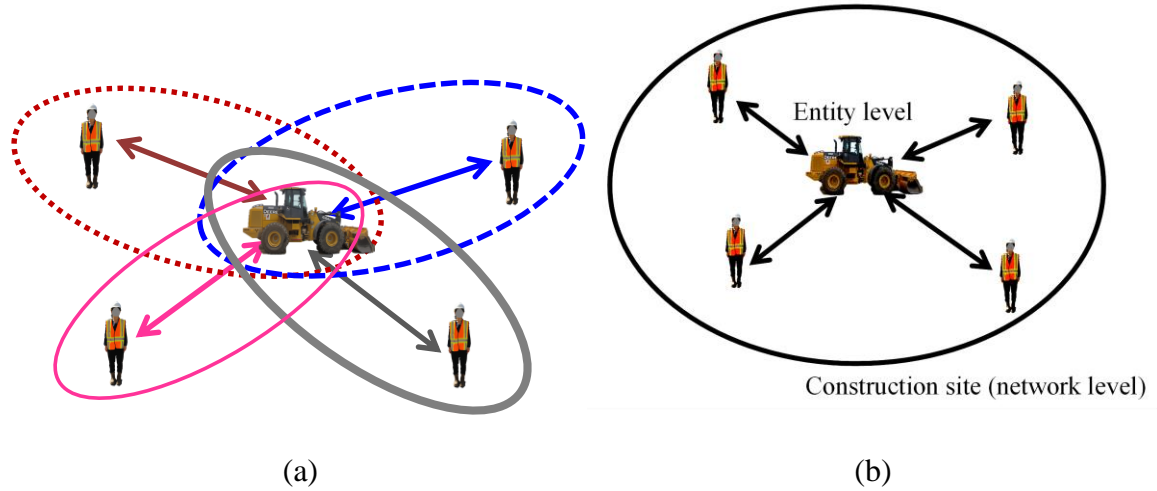


Fig. 1. Illustration of the dynamic interactions (a) between each pair of entities and (b) among all entities coexisting on a site

Some exploratory studies analyzed struck-by risks in construction. For example, the generalized linear models (Esmaeili et al. 2015a) predict the probability of occupational fatalities with respect to general struck-by accidents. Luo et al. (2016) quantified and used hazard exposure amount to assess struck-by and other safety risks by monitoring the proximity of a worker to a radiation (hazard) and his/her exposure duration. The risk trends from the perspectives of worker and hazard can be obtained. However, only data on the location of equipment and workforce were considered. The method capable of analyzing the dynamic risk at both entity and network levels, particularly for struck-by-equipment hazards, is lacking. In addition, the occurrence of a struck-by-equipment hazard is the consequence of the mutual interactions of multiple risk

factors. Therefore, instead of only considering entities' locations (proximity), other major risk factors causing struck-by-equipment hazards should also be considered in the risk analysis.

In summary, situational awareness can be improved in smart construction environments by two means:

- Applying methods to detect hazards in a timely and more accurately manner; and
- Analyzing risk at both entity and network levels over time by considering and integrating all entities and their interactions and interrelationships as a system.

Research Objectives

To address the above-identified gaps, the primary objectives of this research are to:

- Improve on-site situational awareness in smart construction context to reduce construction injuries and fatalities; and
- Develop a systematic method for proactive struck-by-equipment hazard prevention, consisting of timely and accurate hazard detection and dynamic multi-level risk analysis.

To achieve the above objectives, the following sub-objectives were pursued:

- Develop models that can not only identify unsafe proximities but also reduce false alarms; and evaluate the performance of models.

To achieve this objective, answers to the following questions need to be established:

- i. What factors should be considered to calculate dynamic warning distances

between entities?

- ii. How can false alarms (false positives and false negatives) be reduced while detecting unsafe proximities?
 - iii. How can the upcoming unsafe proximities also be identified, in addition to the identification of unsafe situations occurring on sites?
- Develop a dynamic risk analysis method that can comprehensively analyze risk at both entity and network levels to proactively prevent safety hazards from the entity and system levels (e.g., identify entities and sites with high levels of risk, evaluate and compare safety performance, and provide insight into activity and site layout planning).

To achieve this objective, answers to the following questions need to be established:

- i. What are the major risk factors causing struck-by-equipment hazards?
- ii. How can dynamic interactions among entities coexisting on the site be represented and quantified?
- iii. How can construction entities and their interactions be represented and modeled?
- iv. What indicators can be used to represent risk at entity and network levels (the used indicators should reflect observations of complex and dynamic construction environments and also can provide insight to strengthen safety practices to proactively prevent hazards)?

Based on the objectives of this thesis, the derived long-term research goals are:

- With the more widespread applications and use of IoT (Internet of Things) in smart construction, development of human-in-the-loop cyber-physical systems can assist to manage construction safety in a more effective and smarter manner.
- Applying a system-of-systems approach to model the various aspects/factors associated with construction safety to analyze and improve safety performance, by taking advantages of the benefits of smart construction, e.g., timely data collection and information sharing.

Research Methodology

The objectives of the conducted research were achieved by introducing and developing the SA4SR— situational awareness for construction safety risks management. The developed SA4SR is a systematic method to improve situational awareness by detecting hazards with reduced false alarms and analyzing risk at entity and network levels in smart construction environments. The SA4SR consists of two modules, i.e., hazard detection and risk awareness. The framework of the SA4SR is shown in Fig. 2. Fig. 3 presents the methods to achieve the stated objectives through the development of hazard detection and risk awareness modules.

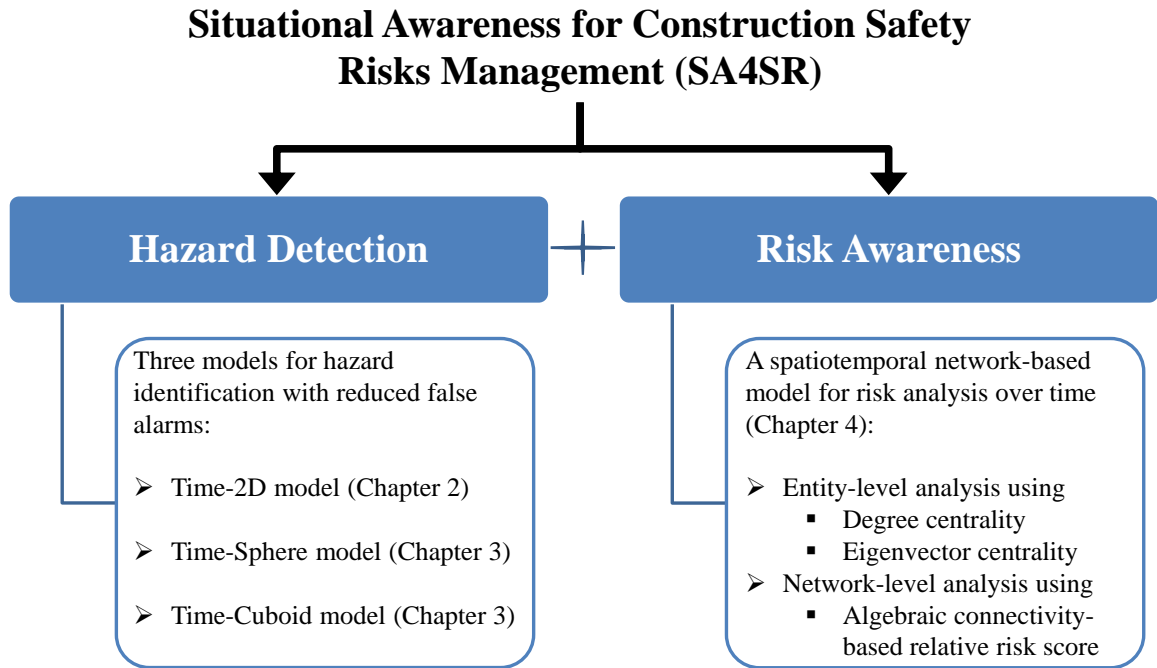


Fig. 2. The SA4SR framework

The hazard detection module focuses on identifying struck-by-equipment hazards not only in a timely manner but also with reduced false alarms. Three models (Figs. 2 and 3) including a three-dimensional (3D: two-dimensional motion and time) model and two four-dimensional (4D: three-dimensional motion and time) models were developed in this module. A numerical model of the most widely used methods for struck-by-equipment hazard detection was also examined in this module for model comparison. Verification by test was conducted to verify the developed models. Simulated scenarios and field experiments were conducted to evaluate the performance of models. Several performance indicators such as false positive rate, false negative rate, and reduced alarm percentage were used, and comparison analysis of models was conducted. Quantitative analysis, i.e.,

examining relationships between and among indicators, was applied to further compare model performance. Based on the characteristics of site and entities and the requirements of users, the corresponding model can be selected and applied for hazard detection.

The extended Kalman filter (EKF) combined with nearest neighbor method was used to track entities' motions. Dynamic warning distances between entities were adopted as thresholds to analyze the monitored situations. The equations to quantify dynamic warning distances between entities were developed for each model by considering multiple factors such as reaction distances of workers on foot and equipment (the factors considered in the quantification equations were different in each model). Based on the near real-time monitored motions of entities, the corresponding quantification equation is used and the warning distance is updated. To reduce the generation of false alarms while detecting hazards, the method (unsafe-proximity query rules, also called safety rules in the 3D model) to identify upcoming intersections of objects was developed for each model. By monitoring the distance between entities and analyzing entities' relative positions and velocity, the developed models can identify not only the occurring hazardous situations but also the upcoming unsafe proximities to reduce false alarms.

The risk awareness module (Figs. 2 and 3) focuses on analyzing the dynamic risk pertaining to struck-by-equipment hazard. A spatiotemporal network-based model including four major steps was developed in this module to analyze the struck-by-equipment risk at both entity and network levels over time. The four steps are summarized and presented in Fig. 1 in Chapter 4.

- Step 1: Content analysis was used to select the major risk factors causing struck-

by-equipment accidents.

- Step 2: The dynamic interaction associated with each of the selected risk factors was quantified by considering two parameters, i.e., the factor's weight (significance) and severity. The weight assigned to each risk factor represents the significance of the factor compared with that of other risk factors in causing a collision. Content analysis and the lagging indicator, i.e., the loss of time, were used to quantify the weight of a factor. The severity resulted from each risk factor was quantified based on the real-time detected state of the factor.
- Step 3: Graph theory was used to conceptualize and model entities and their dynamic interactions resulted from the risk factors of struck-by-equipment hazards into a weighted network as a system. Network analysis techniques were used to analyze the generated weighted network for risk analysis.

Different from lagging indicators reflecting a reactive health and safety culture, leading indicators are proactive, preventative, and predictive measures that provide information about the dynamic situations on sites and further strengthen safety performance. Two safety leading indicators, i.e., degree centrality and eigenvector centrality, were used to analyze risk at the entity level; and another safety leading indicator termed algebraic connectivity-based relative risk score was used to represent the network-level risk.

- Step 4: Four simulated sites were used to illustrate the comprehensive risk analysis at the entity and network levels with the safety leading indicators. Accordingly, safety applications were derived and explained.

Situational Awareness for Construction Safety Risks Management (SA4SR)

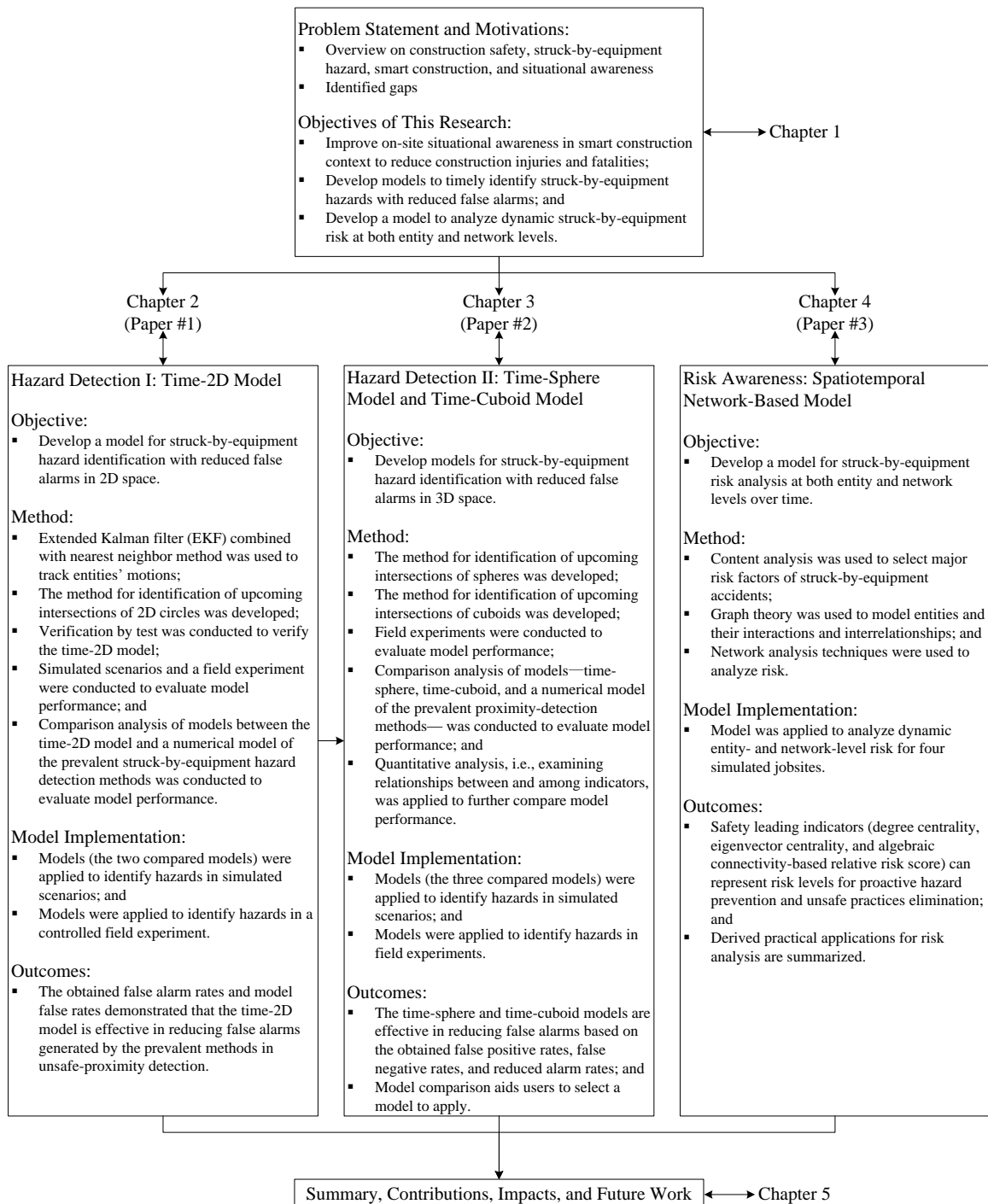


Fig. 3. Overview of the research objectives and methodology

Situational awareness can be improved by using the models developed in the SA4SR (Figs. 2 and 3) to analyze the data collected in near real-time using smart technologies. This research was conducted under the assumption that entities' (i.e. equipment and workers on foot) motions (e.g., position, velocity, and orientation) can be monitored, collected, and wirelessly transmitted to the server in near real time. The models developed for hazard detection with a low false alarm rate (hazard detection module) and dynamic risk analysis (risk awareness module) are embedded on the server to process the received data. The obtained results can be timely shared with the corresponding entities (e.g., site managers and equipment operators) if needed. For example, alarms can be triggered for operators and notifications at managerial level can be sent to site managers. The SA4SR in this thesis focuses on the development of the models for situational awareness improvement, while the solutions for reliable and robust real-time wireless data communication are not studied.

Thesis Organization

This thesis consists of five chapters as shown below:

Chapter 1 introduces an overview of the problem studied, the motivations of this research, the objectives within the scope of this thesis as well as in long term, and the methodology developed to address the identified gaps.

Chapter 2 presents an unsafe-proximity detection model (a 3D model) developed for the hazard detection module of the SA4SR. A peer-reviewed journal article is included in this chapter. The current state of proximity detection methods/systems was

reviewed. The advantages and limitations of existing proximity detection technologies were investigated and summarized. Two key reasons for existing solutions generating false alarms in proximities detection were discussed. Accordingly, the unsafe-proximity detection model (a 3D model) was developed to address the identified limitations. The developed model can not only timely identify hazards but also reduce false alarms. The safety rules for reducing false alarms were developed, and these rules fully considered entities' state information including position, heading, and speed and used dynamic warning distances. The performance of the developed unsafe-proximity detection model was evaluated in both simulation and a controlled field experiment. The extended Kalman filter combined with nearest neighbor method was used in simulation to track entities' motions. Four indicators including root-mean-square error, false tracking rate, false alarm rate, and model false rate were used to evaluate the model performance. The obtained results demonstrated the effectiveness of the developed model in detecting hazards and reducing false alarms. The corresponding contributions, limitations, and future work were summarized.

Chapter 3 presents two 4D models, i.e., time-sphere and time-cuboid models for identifying struck-by-equipment hazards with reduced false alarms. The two 4D models are also included in the hazard detection module of the SA4SR. A published journal article is included in this chapter. One of the limitations of the developed 3D model presented in Chapter 2 is that entities' motions considered in the developed safety rules were in a 2D space. Thus, the time-sphere and time-cuboid models improved the 3D model and considered entities' 3D motions. The literature about using state information

for hazard detection, detection and prediction of collisions, and generation of the dynamic warning zone for a construction entity was reviewed. Three major limitations of existing studies were identified and correspondingly, the research objectives were set. For entities, their alert zones were defined, and warning distances were quantified and updated based on their dynamic 3D motions (position, velocity, and orientation). For each 4D model, the unsafe-proximity query rules were developed to identify hazards and reduce false alarms. The developed unsafe-proximity query rules can identify not only the occurring unsafe situations but also the upcoming potential collisions. Both simulation and field experiments were conducted to evaluate the performance of the two 4D models, using the three indicators including false positive rate, false negative rate, and reduced alarm percentage. Furthermore, model analysis and comparison were conducted to provide insight into model selection and adoption in real practices. Finally, the limitations and future work of the 4D models were discussed.

Chapter 4 presents a spatiotemporal network-based model for struck-by-equipment risk analysis developed for the risk awareness module of the SA4SR. A peer-reviewed journal article is included in this chapter. A literature review on the status of hazard identification and risk analysis for struck-by hazards was conducted and presented. It was found that the dynamic risk analysis method particularly for struck-by-equipment hazard was lacking. In addition to the near real-time hazard detection presented in Chapters 2 and 3, to proactively prevent hazards on construction sites, the needs and advantages of performing comprehensive and dynamic struck-by-equipment risk analysis were discussed. Therefore, a spatiotemporal network-based model with three safety

leading indicators was developed to comprehensively analyze risk at both entity and network (i.e., the whole site) levels over time. The developed model included four major steps and each step was explained in detail. First, the key risk factors of struck-by-equipment hazards were selected from the literature and historical accident reports. Second, the method to quantify the dynamic interactions associated with the selected risk factors among entities was developed. Third, a dynamic weighted network was developed to model entities and their interactions that coexist on the site. Three safety leading indicators were developed and used to represent the struck-by-equipment risk at entity and network levels. Lastly, four simulated sites were used to explain the risk analysis at entity level (including real-time monitoring and overall performance evaluation) and network level (including analysis of one site and comparison of multiple sites). The derived safety applications, e.g., evaluation of safety performance of entities and jobsites, were summarized. The contributions, limitations, and future work of this study were discussed and summarized.

Chapter 5 summarizes the work presented in this thesis with its main contributions and impacts and provides recommendations for future research in this area.

CHAPTER 2: HAZARD DETECTION I

Introduction

Detection of hazards in an accurate and timely manner can improve on-site situational awareness. However, existing methods for detecting struck-by hazards are limited by frequently generated false alarms. As thus, the hazard detection module in the SA4SR (situational awareness for construction safety risks management) focuses on identifying struck-by-equipment hazards with reduced false alarms in a timely manner. Three models were developed and included in the hazard detection module.

In this chapter, the 3D (2D motion plus time) model for detecting unsafe proximities between construction entities and reducing false alarms is described. The other two models developed in the hazard detection module will be described in Chapter 3. The publication included in this chapter is:

Wang, J., and Razavi, S. (2016a). “**Low False Alarm Rate Model for Unsafe-Proximity Detection in Construction.**” *Journal of Computing in Civil Engineering*, 30 (2), DOI: [10.1061/\(ASCE\)CP.1943-5487.0000470](https://doi.org/10.1061/(ASCE)CP.1943-5487.0000470)

The co-author’s contributions to the above work include:

- Financial and technical supervision of the study presented in this work; and
- Review and modification of the manuscript.

Paper #1: Low False Alarm Rate Model for Unsafe-Proximity

Detection in Construction

Abstract

The research reported in this paper proposes and develops an unsafe-proximity detection model focused on decreasing false alarms. By considering three types of entity attributes [i.e., (1) position, (2) heading/moving direction, and (3) speed], more accurate unsafe-proximity identifications with reduced false alarms can be achieved. The proposed and developed model works via two modules, as follows: (1) state tracking module, and (2) safety rules module. The state tracking module collects construction entities' states (position, heading, and speed) in real time. The collected state information is analyzed in the safety rules module for unsafe-proximity identifications. Five common situations on construction sites are extracted and studied for the development of the safety rules, as follows: (1) static equipment and moving worker, (2) moving equipment and moving worker, (3) moving equipment and static worker, (4) two pieces of moving equipment, and (5) moving equipment and static equipment. The area around equipment is divided into alert and warning areas which are quantified using forklift as sample equipment. The localization accuracy of the state tracking module and the functional effectiveness of the safety rules module are evaluated, through simulation and a field experiment. Twelve scenarios and 13 sub-scenarios were designed and incorporated, in the simulation and the field experiment, respectively. The extended Kalman filter combined with the nearest neighbor method was used in the simulation and a global positioning system (GPS)-aided

inertial navigation system sensor was used in the field experiment as the state tracking module. The results suggest that the magnitude of localization accuracy of the extended Kalman filter combined with the nearest neighbor method and the adopted sensor both are less than 0.7 m. Such an accuracy level is acceptable for construction applications. Moreover, the developed safety rules have a strong capability in avoiding false alarms. In some scenarios the developed model can avoid one false alarm for each scan. The research reported in this paper also demonstrates the applicability and feasibility of implementing the model for real applications. The developed model has great promise to enhance construction safety and mobility by timely avoiding collisions, while reducing false alarms and interruptions to work.

Keywords: Unsafe-proximity detection; State tracking; Safety rules; Distance quantifications; Construction.

Introduction

It is widely known that construction sites are hazardous environments due to the continuous and dynamic interactions between various entities, such as equipment and workers on foot. Unsafe proximity of workers on foot to construction equipment or equipment to equipment has been identified as one of the distinct safety issues on construction sites (Pradhananga and Teizer 2013). Struck-by hazards are the second leading cause of construction fatalities, in which approximately 58% of fatalities resulted from being struck by equipment (Wu et al. 2013). Thus, entities on a construction site have to interact and coordinate effectively with each other to maintain a safe environment.

Such issues have been extensively studied in previous research efforts. A large number of proximity avoidance systems have been developed by utilizing various technologies, such as an ultrasonic-based sensor, radio frequency (RF) sensing technology, radio detection and ranging (i.e., radar), and global positioning system (GPS), to prevent contact accidents, particularly for accidents due to being struck by equipment (Choe et al. 2014; Teizer et al. 2010a; Chae and Yoshida 2010; Ruff 2006; Oloufa et al. 2003). However, the frequent false alarms generated by current proximity avoidance systems have put a limitation on their implementation in realistic construction environments (Ruff 2010; Teizer et al. 2010a; Ruff 2007). The published casualty statistics indicate that contact collisions remain a major problem in the construction industry. Therefore, aiming to minimize the occurrence of false alarms, the research reported in this paper proposes and develops a proactive unsafe-proximity detection model through considering entities' position, heading, and speed. In this way, workers on foot and equipment operators will have more accurate awareness of their surroundings, and further, hazards can be prevented timely.

The remainder of this paper is organized as described next. The next section describes the research background, in which the current status of proximity detection systems and the identified research gap are presented. Thereafter, an unsafe-proximity detection model which includes two modules is proposed and developed, followed by the quantification methods of alert and warning distances. The performance of the developed model is evaluated through simulation and a field experiment. Finally, the limitations, future work, and concluding remarks of this paper are discussed and summarized.

Background

Current Status of Proximity Detection Systems

The Infrastructure Health and Safety Association (IHSA) showed that contact collision remained a major cause of injury/fatality in the construction industry (IHSA 2012). Considering the high number of contact accidents on construction sites and the severity of the consequences, the states of construction entities should be properly monitored and analyzed so that potential collisions can be prevented in a timely manner. The state of a construction entity includes its position, heading/moving direction, speed, orientation (roll, pitch, and yaw), and other safety-related information. Accurate collection of entities' state information contributes to increasing situational awareness and furthermore to prevent contact accidents. The research on state tracking has made significant progress in recent years which lays a solid foundation for the development and improvement of proximity warning systems (Su et al. 2014; Shahi et al. 2013; Andoh et al. 2012; Lee et al. 2012; Duflos et al. 2010; Razavi and Haas 2010; Kang et al. 2009; Behzadan et al. 2008).

Moreover, the advancements of sensing technologies greatly prompt the development of collision avoidance systems. Studies in this regard have attracted extensive interest and multiple proximity warning systems have been developed and evaluated in the past decades. For example, Teizer et al. (2010a) used RF remote sensing technology to develop a proximity alert system. The field experiments showed the maximum recorded warning distance of a dynamic wheel forklift reached 29.87 m. The Armour system developed by Scan-Link Technologies aims to prevent struck-by injuries

on sites and has a better performance on detecting workers that are directly behind the equipment than at the side of it (IHSA 2013). A formalized framework for the evaluation of sensor-based proximity warning systems was established by Choe et al. (2013). Based on the framework, an ultrasonic-based sensor system and a pulsed radar-based system have been developed for the prevention of backing accidents in construction work zones (Choe et al. 2014).

Considering the differences of existing prevalent proximity warning systems due to their read range, cost, size, data accuracy, and other aspects, the research reported in this paper categorizes them in accordance with the adopted technology and summarizes the advantages and limitations for each of them (Table 1). Among these prevalent systems, except for the system adopting vision technology, all the others are based on distance detection to prevent potential contact collisions.

Table 1. Advantages and Limitations of Existing Proximity Detection Technologies

Technology	Advantages	Limits	References
Ultrasonic	Compact size; Low price; Light weight; Function for both daytime and night	Limited detection range; Low accuracy of data; Inconsistent detection; Several sensors are needed to cover wide equipment	Ruff 2007; Teizer et al. 2010; Choe et al. 2013; Choe et al. 2014
Radio frequency sensing technology	Varied detection range based on frequency; High signal update rate; Little data processing effort	Low accuracy of data; Multi-path signal transmission	Teizer et al. 2010; Chae and Yoshida 2010; IHS 2013; Marks and Teizer 2013
Vision	Capable of target type distinguish; Long/short detection range	Heavy computational requirements; Incapable and inefficient under night/dusty environments	Steele et al. 2003
Global Positioning System	Wide outdoor area coverage; Free of line-of-sight issue	Signal interfered by objects, such as buildings and trees	Oloufa et al. 2003; Ruff 2007; Pradhananga and Teizer 2013
Laser	High accuracy of data; High signal updated rate	High initial cost; Limited ability of ground worker detection	Allread and Teizer 2010; Wang et al. 2014
Radar	Capable of target distinguish based on materials	Inconsistent detection; Relative high cost	Ruff 2006; Ruff 2007; Choe et al. 2013
Ultra-wide band	Applicable for both outdoor and indoor sites; Real-time 3D position; Small response time	High requirement for infrastructures	Hwang 2012
Magnetic marker field	Varied proximity detection range	Magnetic field affected under the environments involving metal materials	Ruff 2010; Li et al. 2012
Infrared	Small implementation cost; Small size	High response time; Short detection range; Low accuracy of data; Highly influenced by sunlight	Benet et al. 2002; Teizer et al. 2010

Gap Identification

Such substantial studies have greatly contributed to improving the existing safety practices. However, one common limitation of current methods is the high possibility of generation of false alarms. A false alarm is an essential consideration in any safety

research and applications, as frequently generated false alarms will eventually cause alarms to be disabled or ignored by participants. The results presented in Ruff (2006) showed that 59% of the generated alarms did not signify dangerous situations in reality. The proximity warning system developed by Teizer et al. (2010a) was unable to discriminate real hazards. The generated alarms included false alarms [termed nuisance alarms in the work of Teizer et al. (2010a)]. Searching for effective methods to reduce frequent false alarms has been identified as a significant task to improve existing proximity detection methods (Ruff 2010; Teizer et al. 2010a; Ruff 2007).

One reason for the frequently generated false alarms is that the distance between entities is the only factor taken into consideration but the headings and speed of involved entities are ignored. In some cases, the distance between two entities could be flagged and alarmed as an unsafe proximity as the distance between the two entities is smaller than the predefined distance threshold, while in reality the entities are moving apart from each other with no risks presenting. Such a generated alarm is a false alarm. It has been suggested by Behzadan et al. (2008) that position and other information, such as orientation (roll, pitch, and yaw) together, can define a user's spatial context with much greater precision than with position alone. Li et al. (2012) also pointed out that simply sensing the proximity between entities is inadequate for safety control. To this end, another two significant pieces of information [i.e., (1) heading, and (2) speed], which should not be neglected for safety control are selected to be continuously tracked along with position in the research reported in this paper.

Another limitation of the current methods (Marks and Teizer 2013b; IHSA 2013;

Teizer et al. 2010a) is that the approach to determining the distance threshold for unsafe-proximity identification is not described. Distance threshold should be calibrated with respect to some essential factors (such as brake distance and reaction time), allowing appropriate distance and time for corrective actions (Marks and Teizer 2013b; Teizer et al. 2010a). Otherwise, a short detection range would result in too short of a time for equipment operators to respond and a long detection range would result in a higher false alarm rate (Hwang 2012; Chae and Yoshida 2010). The distance threshold used for unsafe-proximity identification should be different when the piece of equipment is moving as opposed to staying stationary. However, current methods either have not fully considered these factors, or have not described the relationship between the distance threshold and these essential factors (Choe et al. 2014; Marks and Teizer 2013b; IHSA 2013; Chae and Yoshida 2010). As thus, the research reported in this paper identifies and discusses the key factors that should be considered in quantification of the distance threshold. The quantification method introduced in this paper also contributes to reducing generation of false alarms.

Aiming to resolve the limitations discussed previously, the primary objective of this paper is to provide an effective and innovative approach to prevent unsafe proximities of workers on foot to equipment, and equipment to equipment, with a low false alarm rate.

The main contributions of this paper are: (1) development of a low false alarm rate unsafe-proximity detection system, (2) development of the safety rules for unsafe-proximity identification in five common situations on construction sites (by considering

entities' position, heading, and speed), (3) identification of the essential factors that should be considered in the quantification of warning distance (the developed quantification method allows for both long-distance detection at higher speed and close-in detection at lower speed), and (4) evaluation of the developed model through simulation and a controlled field experiment.

Unsafe-Proximity Detection Model

The proposed and developed unsafe-proximity detection model works via two modules: (1) state tracking module, and (2) safety rules module. The real-time information describing entities' states is obtained using the state tracking module. Thereafter, the collected states are analyzed in the safety rules module to identify unsafe proximities. The framework of the developed model is shown in Fig. 1.

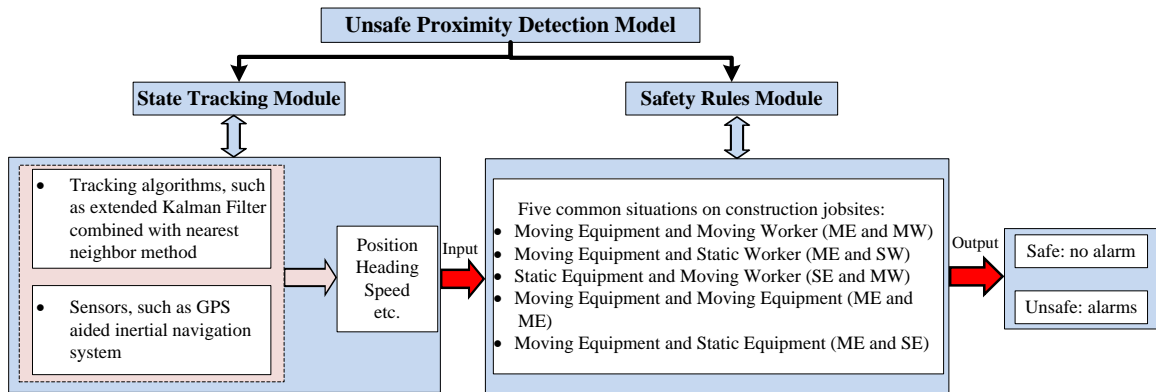


Fig. 1. Framework of the unsafe-proximity detection model

State Tracking Module

In this paper, the extended Kalman filter (EKF) combined with the nearest neighbor (NN) method is adopted as the state tracking module to track entities' state information in simulation (performed in *MATLAB*). The EKF is a state estimation algorithm for nonlinear motion model with good dynamic performance and noise suppression. In the real world, due to the complexity of construction sites, occasionally no detection/measurement is generated or some undesirable detections/measurements (interferential measurements) are generated. To replicate this phenomenon, the research reported in this paper utilizes two parameters to reflect the complexity of real construction environments: (1) probability of detection and (2) probability of undesirable detection. As a result, at some scans more than one measurement could be obtained. Measurements are observations related to the state of a target, such as direct estimation of position, range and azimuth from the sensor, and time difference of arrival (TDOA) of a signal between two sensors. Thereby, data association method is needed to estimate the most accurate measurement obtained with the EKF. The NN method is adopted in the research reported in this paper as the data association method due to its good performance and less computation effort consumed. The flowchart of the EKF combined with the NN method is illustrated in Fig. 2.

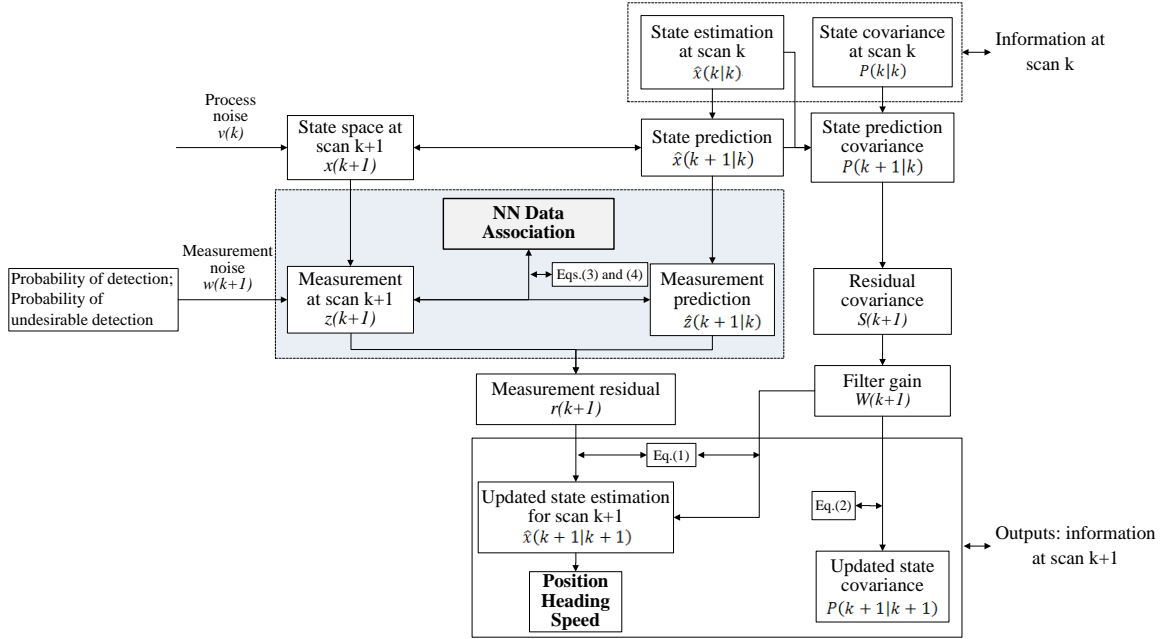


Fig. 2. Flowchart of EKF combined with NN method for state tracking

In Fig. 2, $(k + 1|k)$ denotes the use of information at scan k to estimate the corresponding information at scan $k + 1$. The information at scan k is summarized using the state estimation $\hat{x}(k|k)$ and the associated covariance $P(k|k)$. The main idea of EKF is to update state estimation $\hat{x}(k + 1|k + 1)$ by associating measurement $z(k + 1)$ with measurement prediction $\hat{z}(k + 1|k)$ as per Eq. (1) and simultaneously to update the state covariance $P(k + 1|k + 1)$ as per Eq. (2) (Bar-Shalom and Li 1995).

$$\hat{x}(k + 1|k + 1) = \hat{x}(k + 1|k) + W(k + 1)r(k + 1) \quad (1)$$

$$P(k + 1|k + 1) = P(k + 1|k) - W(k + 1)S(k + 1)W(k + 1)' \quad (2)$$

where $\hat{x}(k + 1|k + 1)$ is the updated state estimation; $\hat{x}(k + 1|k)$ is the state prediction; W represents the filter gain; r is the measurement residual; $P(k + 1|k + 1)$ is the updated state covariance; $P(k + 1|k)$ means the state prediction covariance; and S is the

residual covariance.

The NN determines the nearest valid measurement $z(k+1)$ from the measurement prediction $\hat{z}(k+1|k)$ to update the state estimation $\hat{x}(k+1|k+1)$, as shown in Fig. 2. Filter gating is a threshold-based solution used to determine whether a measurement is valid. A valid measurement will be in the validation region ν with the probability determined by the gate threshold γ [Eq. (3)] (Habtemariam et al. 2011). The valid measurements are determined based on the distance measurement D [Eq. (4)]. By comparing the calculated distance with the filter gating, the valid measurements can be determined. Among all valid measurements, the one with the least distance is selected as the nearest one.

$$\nu(k+1, \gamma) = \{z: [z - \hat{z}(k+1|k)]' S(k+1)^{-1} [z - \hat{z}(k+1|k)] < \gamma\} \quad (3)$$

$$D(z) = [z - \hat{z}(k+1|k)]' S(k+1)^{-1} [z - \hat{z}(k+1|k)] \quad (4)$$

where z is the measurement at scan $k+1$; and $\hat{z}(k+1|k)$ represents the measurement prediction at scan $k+1$.

Safety Rules Module

The states of entities obtained in the state tracking module will be analyzed in the safety rules module. Five types of situations are considered and studied to develop the safety rules, as follows: (1) static equipment (SE) and moving worker (MW), (2) moving equipment (ME) and moving worker, (3) moving equipment and static worker (SW), (4) two pieces of moving equipment, and (5) moving equipment and static equipment (Fig. 3). According to the scope of this paper, preventing the unsafe proximity of workers on foot to equipment, and equipment to equipment, the considered five situations are enough to

reveal real construction field situations.

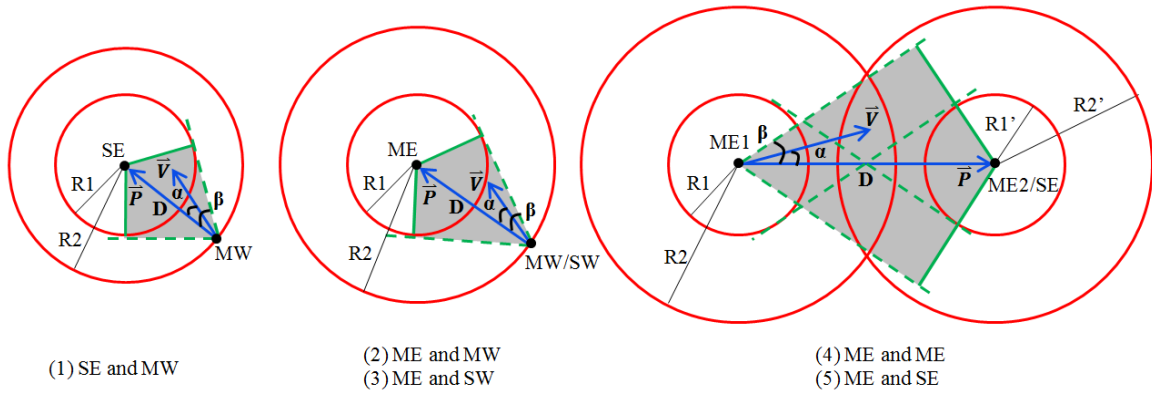


Fig. 3. Illustration of the safety rules for Situations 1–5

In this paper (Fig. 3), the alert area is defined as the hazardous area around equipment which is the inherent unsafe area around the equipment. Hence the size of the alert area depends on the type of equipment. A hazard refers to a situation that an entity is within the alert area. The warning area is the area that has the potential to become hazardous under certain conditions. For the proof of concept, circles are adopted as an approximation of the alert and warning areas of equipment, and equipment is denoted as a single point, without considering equipment operations (e.g., dig or swing). Different equipment exhibits different alert distance ($R1$) and warning distance ($R2$). As alert area is the inherent hazardous area of equipment and equipment is considered as a single point in this paper, for specific equipment the alert distance $R1$ is the same regardless of its static or moving state.

A significant majority of proximity detection methods in the current state of

research are based on distance detection, only considering the warning distance (as explained in the Background section). Therefore, these prevailing methods (denoted as Method 1) based on distance detection are selected as the benchmark for comparison with the method developed in the research reported in this paper. Method 1 is a numerical model of these prevailing methods and thus works as the benchmark in simulation and the field experiment. In Method 1, if the distance between entities is monitored and identified as being smaller than warning distance, the system will trigger an alarm. The warning distance determined by users generally includes equipment braking distance, defined as the distance the equipment will travel from the point when its brakes are fully applied to the point when it comes to a complete stop. If the entities are within the warning area but are moving apart from each other, the generated alarm by Method 1 is a false alarm since no hazard presents itself. To avoid the high false alarm rate, an alarm should not be triggered only because the entity is located within the warning area. The unsafe-proximity detection model developed in this paper, denoted as Method 2, not only utilizes the attribute of distance but also considers the headings and speed of the entities. The developed safety rules are used to determine whether an alarm should be sent out while entities are in the warning area. An alarm will be triggered only if the distance between entities is smaller than the warning distance and the involved entities are getting closer to each other given the current states of their movements. Method 2 is an improved method of Method 1 and serves as a foundation for further study.

The developed safety rules for the five situations are explained in Fig. 4. Based on the collected state information, the developed safety rules will be performed between any

two entities. Even though multiple workers and/or multiple pieces of equipment are involved, the model will be applied to each pair of entities to prevent potential collisions.

In Figs. 3 and 4, D is the Euclidean distance between two entities. α is an angle between two vectors [i.e., (1) \mathbf{P} , and (2) \mathbf{V}]. Under Situations 1–3, \mathbf{P} represents the relative position of equipment to worker and \mathbf{V} is the relative velocity (heading and speed) of worker to equipment. Under Situations 4 and 5, \mathbf{P} represents the relative position of one piece of equipment (Equipment 2) to the other piece of equipment (Equipment 1) and \mathbf{V} is the relative velocity of Equipment 1 to Equipment 2. The shaded area in Fig. 3 is called the dangerous angle, which presents a range of headings that can eventually place the moving entity in the hazardous area. β is half of the dangerous angle.

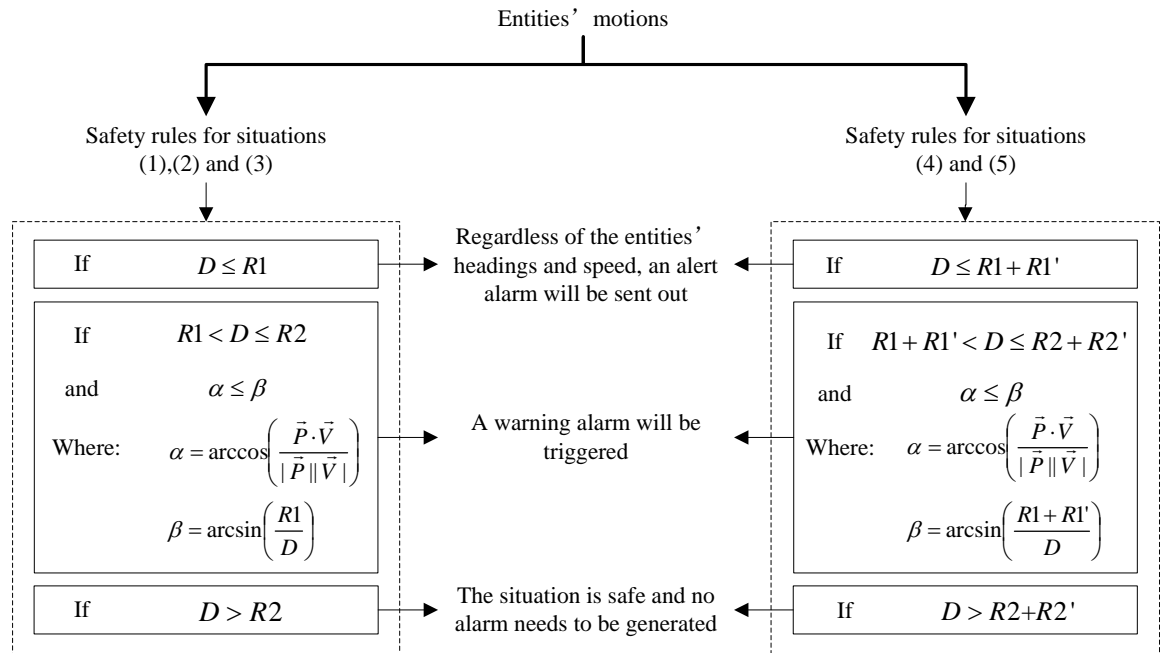


Fig. 4. Flowchart of safety rules for unsafe-proximity identification

As the developed safety rules consider entities' speed, a moving worker can be considered as a static worker when the speed of the worker is monitored as 0. As thus, Situation 3 can be considered as one sub-situation of Situation 2. Likewise, Situation 1 also can be considered as one sub-situation of Situation 2, and Situation 5 can be considered as one sub-situation of Situation 4. Therefore, this paper takes Situations 2 and 4 as sample situations studied in the simulation. Also, as quantification of warning distance $R2$ is different when equipment is moving as opposed to staying stationary, Situation 1 (i.e., SE and MW) is also studied as an independent sample situation in the simulation. The verification of the safety rules is discussed in the “Verification of the Safety Rules” section.

Quantification of Alert and Warning Distances

For specific equipment, alert distance $R1$ is the same regardless of its static or moving state. The warning distance $R2$ for static equipment differs from the one for moving equipment. Accurate quantification of $R1$ and $R2$ can improve the effectiveness of proximity detection methods and assist in better utilization of construction sites. Consequently it contributes to enhancing construction safety, mobility, and productivity.

Forklifts lift, stack, and transfer resources, and can be frequently seen on construction sites. Two primary incident types [i.e., (1) forklift overturns, and (2) worker on foot struck by forklift] have fatality rates at 22% and 20%, respectively (NIOSH 2001). The research reported in this paper uses a fully laden 2.5-t (metric ton) forklift as sample equipment to explain the process of quantification of $R1$ and $R2$. The selected forklift model (2.5-t capacity) is referred from the report on reducing forklift safety risks

(Government of South Australia 2010).

It is expected that an entity should stay outside of the alert area when the forklift comes to a complete stop. This paper adopts 2 m as the alert distance for the forklift with a 2.5-t capacity. The determined 2 m includes the length of the fork attached to the forklift. Thus $R1$ is 2 m for Method 2. Warning distance is treated differently in Method 1 as opposed to Method 2. In Method 1, $R2$ is the distance threshold where an alarm should be triggered, indicating an unsafe proximity is detected. However, in Method 2, $R2$ is the boundary point where the method starts to identify the entities' moving directions and speed. The difference between $R1$ and $R2$ is denoted as the buffer distance (BD). The definitions of BD for the selected three situations [i.e., (1) Situation 1, (2) Situation 2, and (3) Situation 4] are described in Eqs. (5)-(7), respectively. Three key factors are considered in determining BD, as follows: (1) reaction distance of worker on foot (RD of W), (2) reaction distance of equipment (RD of E), and (3) braking distance of equipment (BD of E ; not to be confused with buffer distance in this context).

$$BD_{(1)} = \text{RD of } W \quad (5)$$

$$BD_{(2)} = (\text{RD of } W) + (\text{RD of } E) + (\text{BD of } E) \quad (6)$$

$$BD_{(3)} = (\text{RD of } E1) + (\text{BD of } E1) \text{ and } BD'_{(3)} = (\text{RD of } E2) + (\text{BD of } E2) \quad (7)$$

where

$$\text{RD of } W = \text{reaction time of worker} \times \text{speed of worker} \quad (8)$$

$$\text{RD of } E = (\text{reaction time of operator} + \text{execution time}) \times \text{speed of equipment} \quad (9)$$

$$\text{BD of } E = \frac{(\text{speed of equipment})^2}{2 \times \text{deceleration of equipment}} \quad (10)$$

Eq. (10) is transferred from the kinetic equation [Eq. (11)] which expresses

uniformly retarded rectilinear motion:

$$v_1^2 - v_2^2 = 2 \cdot a \cdot s \quad (11)$$

where v_1 is the initial speed which is the equipment speed; v_2 is the end speed which is 0; a is the deceleration of the equipment; and s is the distance that equipment travels which is the BD of E .

For Situations 1 and 2, $R2$ is defined as

$$R2 = R1 + BD \quad (12)$$

For Situation 4, $R2$ and $R2'$ are defined as

$$R2 = R1 + BD \text{ and } R2' = R1' + BD' \quad (13)$$

On average, the reaction time for a typical person is approximately 0.7 s regardless of their background and training (Technology Associates 2014). The execution time is 1 s after subtracting 1.5 s of perception and reaction time from 2.5 s of total braking reaction time (Technology Associates 2014; Hunter-Zaworski et al. 2003). The deceleration of a fully laden 2.5-t forklift is 1.9 m/s^2 and its speed ranges from 6–32 km/h (Government of South Australia 2010). In the research reported in this paper, 14 km/h is selected as the speed of the forklift. The speed of a worker on construction sites is assumed as 1.46 m/s, which is the mean of the actual comfortable gait speed of men between 30 and 49 years of age (Bohannon 1997). As thus, for the forklift with a 2.5-t capacity, $R1$ is determined to be 2 m for all the selected three situations [i.e., (1) Situation 1, (2) Situation 2, and (3) Situation 4]. The value of $R2$ is calculated to be 3.05 m for Situation 1, 13.65 m for Situation 2, and 25.20 m for Situation 4 [Eqs. (5)–(13)].

The value of $R2$ can be updated using Eqs. (5)–(13) if the values of the parameters

are changed. The quantification process for Situation 3 also adopts the proposed equations for Situation 2, but the speed of worker is 0. Likewise, the quantification process for Situation 5 is the same as Situation 4, but the speed of the other piece of equipment is 0. The obtained $R1$ and $R2$ for the forklift will be used in the simulation. In the field experiment, $R1$ also is 2 m while $R2$ is updated with the collected state information.

The blind spot area is one major cause of accidents on construction sites. The obtained $R2$ can be analyzed in tandem with the research on equipment with three-dimensional (3D) blind spots measurement. The blind spot area for a forklift is 96.71 m^2 at a 12-m radius on the xy -plane (Ray and Teizer 2013). Even though the type of forklift along with its technical details was not pointed out by Ray and Teizer (2013), it can be inferred from their work that the blind area covered by radii of 13.65 and 25.20 m is close to or greater than 96.71 m^2 . For a moving forklift, such warning distances are conducive to safety control. More contents on how to measure blind spots for equipment are available (Ray and Teizer 2013; Marks et al. 2013; Teizer et al. 2010b; Hefner 2003). The practitioners are encouraged to evaluate their obtained value of $R2$ in tandem with the measured blind spot area. This practice works as a complementary method to confirm the rationality of $R2$ for the unsafe-proximity control problem. Since the $R2$ includes reaction distance as well as braking distance, an alarm should not be activated once the entity is within the warning area. This is the primary reason for the development of Method 2 to conduct more accurate proximity identifications and to avoid the high false alarm rate.

Simulation and Model Evaluation

Simulation Setting

A true alarm indicates a real unsafe situation exists. The generated alarm is a true alarm if the following two conditions are satisfied simultaneously: (1) entity is located within the warning area, and (2) entity will be located in the alert area in the near future if the involved entities maintain their current moving patterns or states (heading and speed).

Three situations have been set up and selected for simulation. There are four different scenarios (sub-situations) for each situation. First, the trajectory of the involved entities is categorized as either a line or curve (Fig. 5). Setting up two types of trajectories facilitates better evaluation of the tracking performance of the EKF combined with the NN method under different motion models. Second, the number of true alarms is divided into two groups [i.e., (1) equal to 0, and (2) greater than 0]. Therefore, the four scenarios associated with each situation are as follows:

1. Line trajectories, number of true alarms = 0;
2. Curve trajectories, number of true alarms = 0;
3. Line trajectories, number of true alarms > 0; and
4. Curve trajectories, number of true alarms > 0.

Setting up 12 scenarios enables researchers to evaluate the performance of the developed unsafe-proximity detection model. The simulation of 12 scenarios is performed in *MATLAB*. Cartesian coordinates (x , y) are used to express position. The probability of detection is set as 0.9 which indicates that at each scan the target can be detected with a probability of 0.9. The number of undesirable detections is in accordance with a Poisson

distribution and is randomly determined at each scan with a probability of 1×10^{-4} per unit volume of the detection space. The determinations of the probability of detection and probability of undesirable detection depend on many factors, such as the complexity of application environments and the adopted technology. More descriptions on the probability of detection and the probability of undesirable detection can be found in the work of Clark (2005). The process noise and measurement noise are also randomly generated with a Gaussian distribution. To decrease the impact of randomness on the results, each scenario was performed using Monte Carlo simulation and the average outcome was used as the final result.

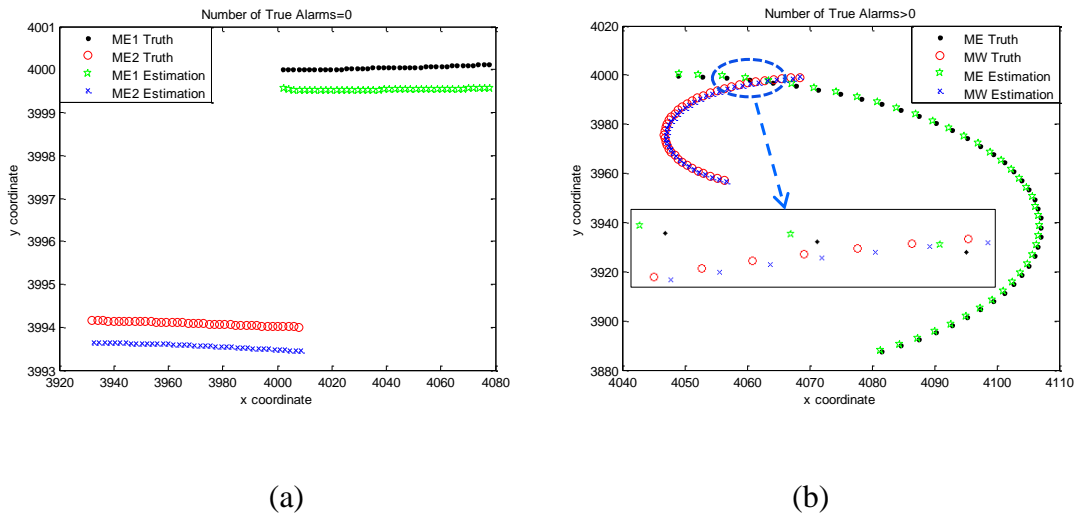


Fig. 5. Illustration of trajectories: (a) line trajectories; (b) curve trajectories; truth is the designed position with process noise; estimation is the tracked position using the EKF combined with the NN method

Verification of the Safety Rules

The safety rules need to be verified first. Table 2 gives the simulation results of the three proposed situations [i.e., (1) Situation 1, (2) Situation 2, and (3) Situation 4]. Under each situation the number of true alarms is greater than 0 with curve trajectories. The distance between the two entities is not smaller than RI at any scan.

Table 2. Simulation Results of the Three Situations

Curve trajectories and number of true alarms>0			
Situations	Items	Method 1	Method 2
SE and MW	Number of Alarms	8	1
	i th scan	2,3,5-7, and 37-39	3
ME and MW	Number of Alarms	7	2
	i th scan	1-4,37,38, and 40	37 and 38
ME and ME	Number of Alarms	9	1
	i th scan	1-5 and 37-40	37

Situation ME and MW is selected as an example to explain the verification process. Table 2 shows that the Method 1 generates seven alarms as it localized the worker within the warning area at seven scans [i.e., (1) Scan 1, (2) Scan 2, (3) Scan 3, (4) Scan 4, (5) Scan 37, (6) Scan 38, and (7) Scan 40]. Method 2 generates only two alarms, indicating the situation is identified as unsafe at two scans [i.e., (1) Scan 37, and (2) Scan 38]. The unsafe situation in Method 2 is flagged when the worker is within the warning area and the worker and equipment are getting closer to each other with their current moving patterns.

If the safety rules comply with the requirements of unsafe-proximity detection (i.e., identification of real unsafe situations), the alarms generated with Method 2 (Scans

37 and 38) should be true alarms while all the remaining alarms obtained with Method 1 (Scans 1–4 and 40) should be false alarms. In such case, the two conditions for a true alarm can both be met at the Scans 37 and 38. The worker will be located within the alert area in the near future if both entities keep moving forward with no change in their headings and speed, as detected at Scans 37 and 38, respectively. Therefore, make the entities maintain movement with the same headings and speed obtained at Scan 37 for another 50 continuous observations. Over these 50 observations, the distance (D) between entities is monitored and checked to see if

$$D \leq R1 \quad (14)$$

The total number of times that Eq. (14) has been met was recorded and the result shows that the Eq. (14) was met three times, which is greater than 0 (Table 3). This means in the near future the MW would be within the alert area. As thus the alarm activated at the Scan 37 is a true alarm. Apply the same process to all other scans (Scans 1–4, 38, and 40). Table 3 shows that the alarm generated at Scan 38 is a true alarm because the number of times is 7. The alarms generated at Scans 1–4 and 40 are false alarms since the number of times all are 0. The results suggest that all alarms obtained with Method 2 are true alarms and all the remaining alarms obtained with Method 1 are false alarms. Apply the same verification process to the other two situations. The results demonstrate that the developed safety rules can meet the requirements of unsafe-proximity detection for Situations 1, 2 and 4.

Table 3. Validity Checking for the Three Situations

Situations	i th scan	Number of ($D \leq R1$)
SE and MW	2,5-7, and 37-39	0
	3	$6 > 0^a$
	1-4 and 40	0
ME and MW	37	$3 > 0^a$
	38	$7 > 0^a$
	1-5 and 38-40	0
ME and ME	37	$7 > 0^a$

^a Alarm generated at the i th scan is a true alarm.

Evaluation of the Accuracy of the EKF Combined with the NN Method

Two indicators are used to evaluate the accuracy of the state tracking module, as follows: (1) root-mean-square error (RMSE) and (2) false tracking rate (FTR).

RMSE

According to the RMSE formula (Liang et al. 2013), the obtained RMSE of each scenario is around 0.5 m (Table 4). The mean of the RMSE of all simulated scenarios is 0.53 m. The obtained RMSE boxplot presents no outlier, which signifies a high stability of the tracking algorithm. In addition to the complexity of construction sites taken into consideration, the adopted state space equations and measurement equations, and the adopted distribution of process noise and measurement noise, also have an effect on the localization accuracy (Fig. 2).

False Tracking Rate (FTR)

The FTR is designed as a supplemental indicator to reflect the localization accuracy. Through discovering whether the entity is located within the warning area or not, FTR emphasizes on calculating the percentage of incorrect localization [Eq. (15)]. It can deliver the information of false-positive tracking ($FTR > 0$) or false-negative tracking

(FTR < 0; Table 4). The FTR also enables users to confirm whether the accuracy is acceptable for construction applications.

$$FTR = \frac{\tilde{a}_1 - a_1}{a_1} \quad (15)$$

where a_1 is the number of warning alarms generated by Method 1 using true positions; and \tilde{a}_1 is the number of warning alarms generated by Method 1 using estimated positions. Eq. (15) only deals with the alarms generated with Method 1 as this indicator is especially designed for the localization accuracy analysis.

Table 4. Simulation Results

Number of true alarms	Entities	Trajectory	Accuracy of Tracking		Effectiveness of Model		
			RMSE (m) i.e., E, W (or E)	FTR	FAR, truth	FAR, estimation	MFR
Number of true alarms=0, no hazards present	SE and MW	Line	-,0.4895	0.0012	1	0.9987	0.0012
	ME and MW	Curve	-,0.5537	0.0925	1	0.9559	0.0062
	ME and MW	Line	0.4986,0.5012	0.0012	1	0.9986	0.0012
	ME and MW	Curve	0.5771,0.6254	-0.0196	1	0.9853	0.0694
	ME and ME	Line	0.4994,0.5117	0	1	1	0
	ME and ME	Curve	0.5231,0.5998	0	1	0.9971	0.0071
Number of true alarms>0, hazards present	SE and MW	Line	-,0.5521	0.0625	0.2500	0.3307	-0.0048
	ME and MW	Curve	-,0.5763	0.0400	0.6667	0.6493	0.0116
	ME and ME	Line	0.4762,0.5006	0.0588	0.8210	0.7717	0.0925
	ME and ME	Curve	0.5228,0.5149	0.1300	0.6000	0.6574	-0.004
	ME and ME	Line	0.4917,0.4862	-0.0639	0.8333	0.8144	-0.0275
	ME and ME	Curve	0.5421,0.5845	-0.0131	0.5000	0.4984	-0.0014

Note: E =equipment, W =workers on foot.

In Table 4, the FTR is close to 0 under all scenarios. This indicates the accuracy of the tracking algorithm is acceptable for the unsafe-proximity detection problem. To further confirm whether the tracking performance of the EKF combined with the NN method is stable under different motion models (line trajectory and curve trajectory), the

hypothesis test of paired data using the Student's t distribution is conducted (Devore 2004). The obtained results provide convincing evidence that the tracking method's performance is not different between line trajectory and curve trajectory. It suggests the strong robustness of the tracking method.

Assessment of the Functional Effectiveness of the Model

Two indicators used to assess the functional effectiveness of the developed model are (1) false alarm rate (FAR), and (2) model false rate (MFR).

False Alarm Rate (FAR)

The FAR is an indicator specifically to demonstrate the effectiveness of the developed safety rules [Eqs. (16) and (17)]. The FAR represents the capability of the safety rules to avoid false alarms. A larger FAR indicates that the safety rules are more capable in decreasing false alarms.

$$\text{FAR, truth} = \frac{a1-a2}{a1} \quad (16)$$

$$\text{FAR, estimation} = \frac{\tilde{a}1-\tilde{a}2}{\tilde{a}1} \quad (17)$$

where $a2$ is the number of warning alarms generated by Method 2 using true positions; and $\tilde{a}2$ is the number of warning alarms generated by Method 2 using estimated positions. The definitions of $a1$ and $\tilde{a}1$ are the same as in Eq. (15).

All acquired FAR are greater than 0 and 67% of them are close to 1 (Table 4). That indicates the safety rules can significantly decrease false alarms. There are 16 results indicating that Method 2 can nearly avoid one false alarm for each scan since their FAR are quite close to 1 (bold in Table 4). Fig. 6 shows the paired data under the same

situation with the same trajectory. There are six groups of pairs generated from the 12 scenarios. Fig. 6 suggests that the safety rules function better when the number of true alarms is 0.

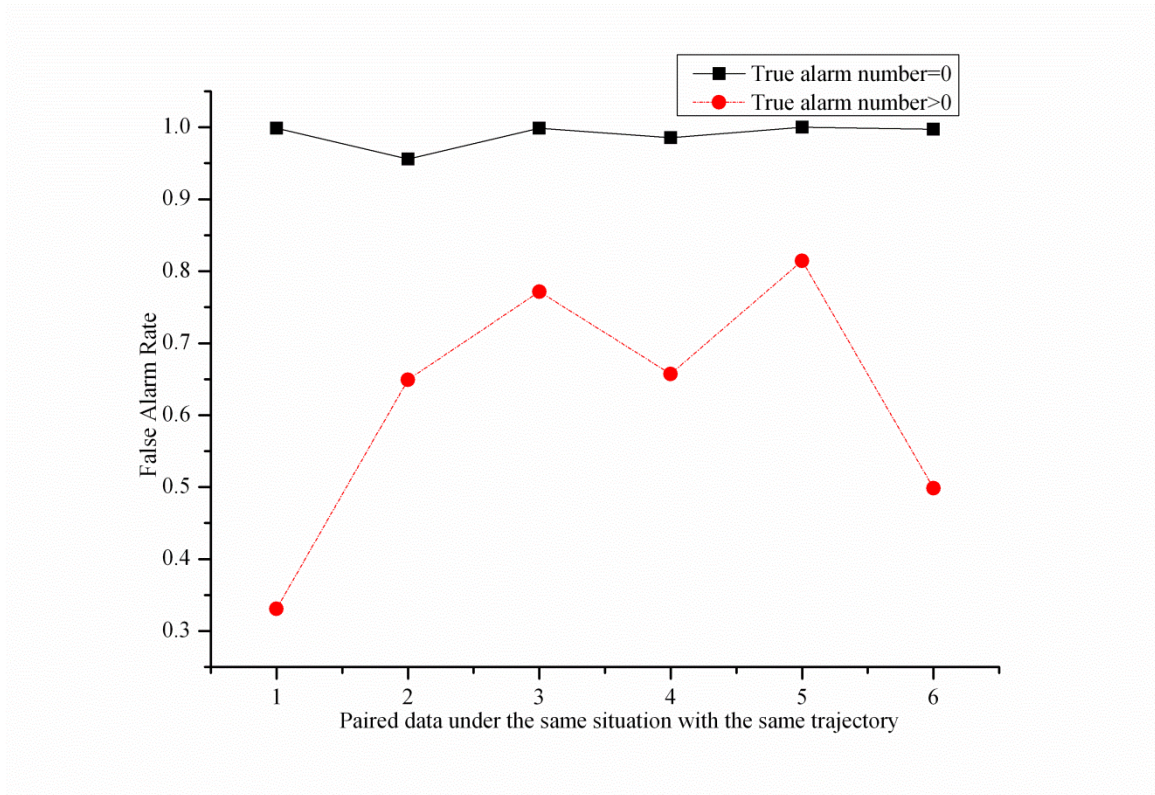


Fig. 6. Comparison of false alarm rate of estimations

Model False Rate (MFR)

The MFR is an assessment of the overall performance of the Method 2 [Eq. (18)]. It reflects both the accuracy of tracking algorithm and the effectiveness of the safety rules. Method 2 has better overall performance in detecting unsafe proximities if the MFR is closer to 0.

$$MFR = \frac{(\tilde{a}_2 + \tilde{a}_3) - (a_2 + a_3)}{a_1 + a_3} \quad (18)$$

where a_3 is the number of alert alarms using true positions; and \tilde{a}_3 is the number of alert alarms using estimated positions. Other parameters have the same definitions as in Eqs. (15)-(17). The value of the sum $a_1 + a_3$ is the number of effective scans under one scenario. An effective scan means the distance between entities is smaller than warning distance while collecting their state information.

All the calculated MFRs are close to 0 (Table 4), which sufficiently denotes the strong functionality of Method 2. The four indicators provide convincing evidence that Method 2 has good performance in avoiding false alarms compared with Method 1.

Field Experiment and Results Analysis

The controlled field experiment aims to demonstrate the applicability and feasibility of the developed model for real applications. The experiment was conducted on a wide-open parking lot of McMaster University. The IG-500N, a GPS-aided miniature inertial navigation system (INS) was used in the state tracking module to collect entities' state information.

Sensor Introduction

The IG-500N is a miniature INS with an embedded GPS. Using its onboard EKF, the IG-500N combines an embedded 50 channels GPS receiver and an inertial measurement unit (IMU) to provide accurate and robust 3D position, velocity, and orientation at high update rates (e.g., 100 Hz). The integrated IMU is composed of three-axis gyroscopes, three-axis accelerometers, and three-axis magnetometers. The synchronization output pin in the sensor allows data to be synchronized with the coordinated universal time (UTC) reference. Due to its high accuracy and robustness,

light weight (44 g), small size ($36 \times 49 \times 25$ mm), and low power consumption, it has been widely used in multiple application fields such as aerospace industry, car motion analysis, and performance sailing (SBG 2014). The real-time data describing entities' states can be collected and logged in a universal serial bus (USB) data logger, a laptop, or other USB interface devices. If wireless data transmission can be well-achieved on construction sites, all of the acquired data can be transmitted to one or some data process centers for timely decision making. The research reported in this paper introduces a GPS-aided INS sensor into construction applications which constitutes a considerable improvement to the state-of-the-art in this area.

Experimental Setting

Situation 4 (i.e., ME and ME) under both line and curve trajectory was performed in the experiment. A small sport utility vehicle (SUV) acted as a forklift. A frequency of 50 Hz is selected for data collection. The acquired data for the research reported in this paper include position (latitude and longitude), speed, heading (angle between moving direction and the geographic north), and time. The GPS-aided INS was attached inside the car (at the middle bottom of the windshield) and a connected GPS antenna was attached to the surface of the car (Fig. 7). The collected data [two-dimensional (2D) position, velocity, and orientation] can be reviewed in real time using graphs. The sensor was connected to a laptop for data review and recording. The distance between the sensor and the edge of car is 0.9 m. The car is approximately considered as a circle, of which the center is the sensor and radius is 0.9 m. This circle is the point shown in Fig. 3.

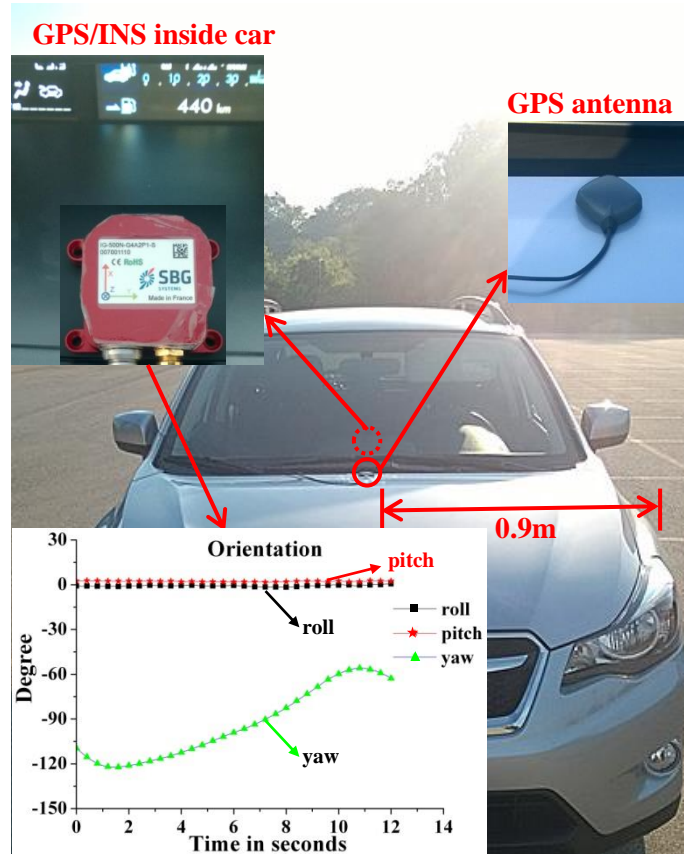


Fig. 7. Instruments installation and real-time data review

There are 13 sub-scenarios set for the experiment which are categorized into three groups (Fig. 8), as follows (the alert distance R1 is 2 m for both pieces of moving equipment):

1. Trajectories of both ME1 and ME2 are a line. The distance between ME1 and ME2 is 1.5 and 3 m in two sub-scenarios, respectively, which means the number of true alarms is greater than 0.

2. Trajectories of both ME1 and ME2 are a line. The distance between ME1 and ME2 is 4.5, 5, 6, 7, 8, 9, 10, 12, and 15 m in nine sub-scenarios, respectively, which

means the number of true alarms is 0.

3. Trajectory of ME1 is a line, and trajectory of ME2 is a curve. The distance between the line trajectory and the tangent line of the curve which is parallel to the line trajectory is 6.8 m (Curve 1) and 8.8 m (Curve 2) in two sub-scenarios, respectively.

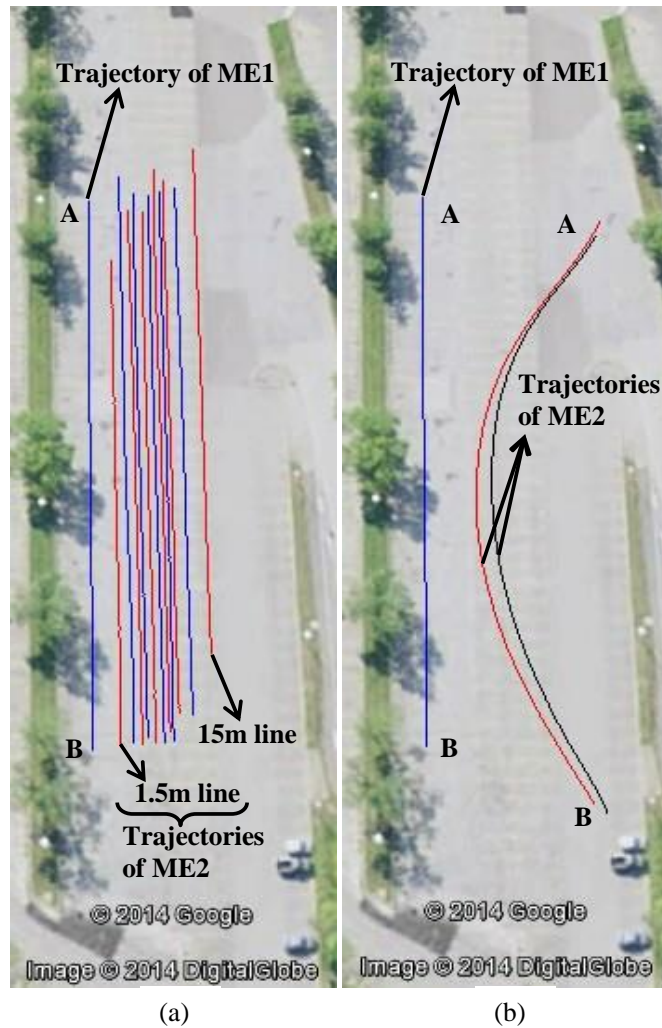


Fig. 8. Obtained trajectories (map data © Google, DigitalGlobe): (a) scenarios of Groups 1 and 2; (b) scenarios of Group 3

Fig. 8 shows the obtained trajectories uploaded on Google Earth. Fig. 8(a) shows scenarios of Groups 1 and 2, and Fig. 8(b) shows scenarios of Group 3.

Each line trajectory was marked on parking lot using duct tape as shown in Fig. 9(a). The length of each line trajectory is 78 m. The sensor was kept moving along the marked trajectory. In this case, the position of the sensor represents the position of the car and is the position of the line trajectory.

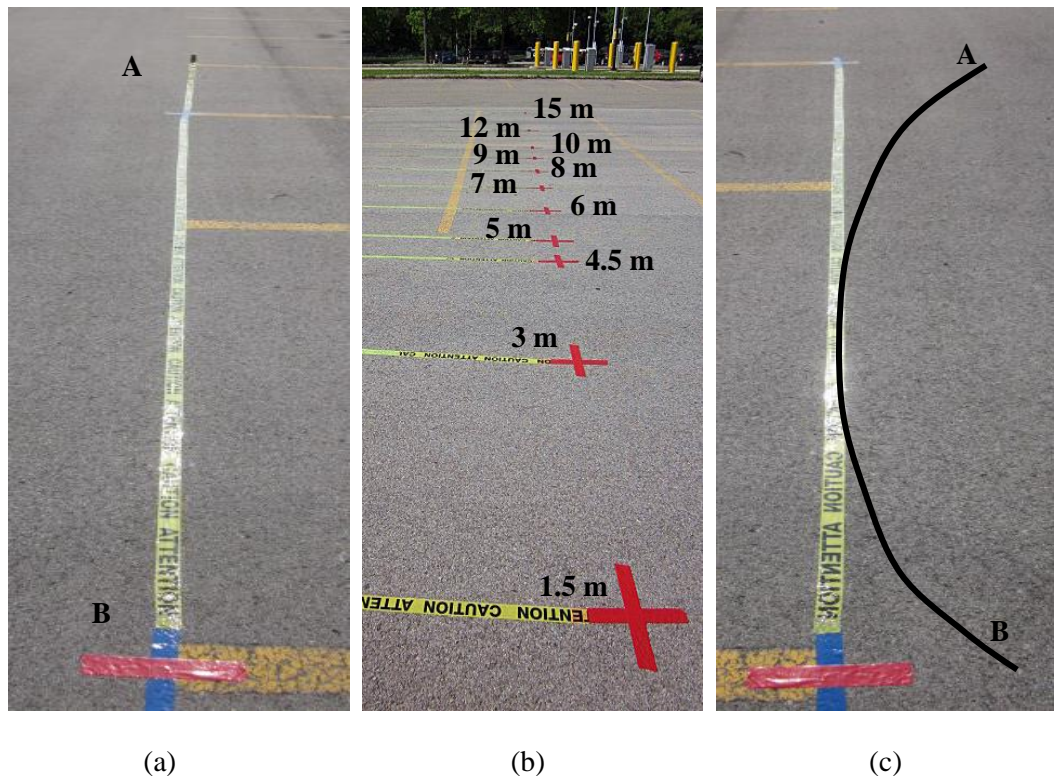


Fig. 9. Experimental setting: (a) marked line trajectory; (b) different scenarios under line trajectories; (c) marked tangent line of curve trajectory

The line trajectory of ME1 is termed the original line in the research reported in

this paper. Under all scenarios ME1 always moved along the same line (original line) and in the same direction (from Point A to Point B). The trajectory of ME2 was either a line or a curve and ME2 always moved in the opposite direction (from Point B to Point A). Fig. 9(b) shows all the designed line trajectories of ME2. Each value marked with cross represents the distance between ME1 and ME2. Each value with its corresponding line is a trajectory of ME2. Since the distance between the sensor and the edge of car is 0.9 m, the distance between the original line and line trajectory of ME2 is the corresponding value shown in Fig. 9(b) plus 1.8 m. Correspondingly, the 6.8 and 8.8-m values mentioned in Group 3 mean that the smallest distance between ME1 and ME2 is 5 and 7 m, respectively. The tangent line, which is parallel to the original line, was also marked onsite using duct tape [Fig. 9(c)]. The only requirement to obtain a curve trajectory is the car should pass parts of the marked tangent line while other sections of the curve were freely determined by the driver.

Results Analysis

Evaluation of the Localization Accuracy

The obtained state information includes position, forwarding speed, and heading. Fig. 8 presents the recorded positions and the trajectories uploaded on Google Earth. The trajectories of ME2 are the 1.5-m line and 3-m line to the 15-m line from the left to the right [Fig. 8(a)]. Even though the length of all marked line trajectories is 78 m, the length of obtained line trajectories ranges from 75 to 88 m. That is because the start and finish points for data collection were slightly different in the 13 sub-scenarios.

The research reported in this paper uses an indirect method to evaluate the

localization accuracy of the adopted sensor. The distance between any two lines marked onsite is known. By comparing the distance between lines shown in Fig. 8(a) with its corresponding true distance, the localization performance of the sensor can be assessed. For a more comprehensive evaluation, the distance between the selected lines ranges from 0.5 to 10 m. The results (Table 5) positively exhibit that the GPS-aided INS has a good performance in localization with an average accuracy of 0.30 m. Such good performance is primarily resulted from the onboard EKF and the integrated IMU. The onboard EKF fuses the data collected from the embedded GPS with the data collected from the IMU to perform optimal position, speed, and heading estimations. The data collected from IMU conducive to more accurate position estimations mainly include 3D accelerations and orientation. The high localization accuracy of the sensor is beneficial for the implementation of the developed model in construction applications.

Table 5. Localization Accuracy Analysis

Selected line trajectories ^a	Distance between two lines (m)	Measured distance between two lines (m)	Error (m)	Mean of errors (m)
4.5-m L versus 5-m L	0.5	0.7178	-0.2178	0.30
8-m L versus 9-m L	1.0	0.7620	0.2380	
1.5-m L versus 3-m L	1.5	1.6893	-0.1893	
10-m L versus 12-m L	2.0	1.9082	0.0918	
4.5-m L versus 7-m L	2.5	3.0631	-0.5631	
12-m L versus 15-m L	3.0	3.3342	-0.3342	
Original L versus 1.5-m L	3.3	3.6943	-0.3943	
5-m L versus 9-m L	4.0	3.9347	0.0653	
1.5-m L versus 6-m L	4.5	4.8923	-0.3923	
5-m L versus 10-m L	5.0	4.6276	0.3724	
3-m L versus 10-m L	7.0	6.6845	0.3155	
6-m L versus 15-m L	9.0	8.6366	0.3634	
5-m L versus 15-m L	10.0	9.6600	0.3400	

^aL refers to line.

Assessment of the Model Effectiveness

The acquired state information is entered into Methods 1 and 2. The results are shown in Table 6. In Table 6, the total number of scans obtained in the corresponding sub-scenario expressed in the first column is denoted as $n1$. The number of alarms obtained using Methods 1 and 2 are denoted as $n2$ and $n3$, respectively. The high frequency at 50 Hz in the experiment is the primary reason for the generation of hundreds of alarms. A lower frequency (2–10 Hz) is suggested in real construction applications. Since the speed of ME1 and ME2 are not constant as in the simulation, the warning distance $R2$ is updated over time using Eqs. (5)–(13). For a speed of 32 km/h (the upper limit of a fully laden-2.5 t forklift) for both pieces of equipment, $R2$ can reach 75.6 m. However, during the experiment the speed was controlled between 25 and 40 km/h. Consequently ME1 and ME2 would be within warning area shortly after starting data collection. Such controlled condition aims to make most of the obtained scans under each scenario the effective scans (explained in the “Model False Rate” section). This is why the percentage of total scans [percent of total scans ($n2/n1$)] in Method 1 is high. As warning distance needs to be updated with real-time speed, alarms will be triggered for a high speed even though pieces of equipment are far from each other. This also serves as a method to monitor whether equipment speed is within the allowable range on construction sites. The value of speed does not affect the function of the model. It also does not influence the model effectiveness evaluation because the FAR indicating the model effectiveness is not associated with speed.

Table 6. Experiment Results Analysis

Trajectories	Sub-scenarios S	Total number of scans, n_1	Number of true alarms	Number of alarms obtained using Method 1, n_2	Percentage of total scans, n_2/n_1	Number of alarms obtained using Method 2, n_3	Percentage of total scans, n_3/n_1	FAR	
Line versus Line	S1,1.5m: warning area	327	163	259	85.3	163	66.0	0.3707	
	S1,1.5m: alert area	327	20	20	85.3	20	66.0	-	
	S2,3m: warning area	384	54	330	88.5	54	16.7	0.8364	
	S2,3m: alert area	384	10	10	88.5	10	16.7	-	
	S3,4.5m	378	0	340	89.9	0	0	1	
	S4,5m	401	0	350	87.3	0	0	1	
	S5,6m	381	0	331	86.9	0	0	1	
	S6,7m	391	0	347	88.7	0	0	1	
	S7,8m	373	0	338	90.6	0	0	1	
	S8,9m	391	0	369	94.5	0	0	1	
	S9,10m	357	0	336	94.1	0	0	1	
Line versus Curve1	S10,12m	336	0	319	94.9	0	0	1	
	S11,15m	351	0	348	99.1	0	0	1	
	S12,5m: warning area	435	101	367	84.5	101	23.2	0.7248	
	S12,5m: alert area	435	0	0	84.5	0	23.2	-	
	Line versus Curve2	S13,7m: warning area	435	42	357	82.1	42	9.6	0.8824
		S13,7m: alert area	435	0	0	82.1	0	9.6	-

For each of the scenarios from S3–S11, the number of alarms generated with Method 2 equals the number of true alarms which is 0. The MFR under each scenario equals 0. The alarms generated with Method 1 are false alarms with FAR equal to 1. For the other four scenarios ([i.e., (1) S1, (2) S2, (3) S12, and (4) S13], the number of true alarms is not known before conducting this experiment. By applying the verification process described in the “Verification of the Safety Rules” section, the alarms that are generated by Method 1 but not by Method 2 are proved to be false alarms. As shown in Table 6, the number of true alarms for these four scenarios are expressed in bold and each

FAR is greater than 0. The results positively exhibit that implementation of Method 2 is conducive to avoiding false alarms in unsafe-proximity detections.

Discussions

On detecting a hazardous proximity, except for activating an alarm, time to collision also can be calculated based on the distance and speed. The type of an alarm could be visual, auditory, vibrating, or a combination of them. A user can define the time to collision threshold for each type of alarm. According to the obtained value of time to collision, a corresponding type of alarm (visual, auditory, vibrating, or a combination of them) can be triggered. On triggering an alarm, a record of the hazardous proximity can be kept. The record of a hazardous proximity includes the alarmed time, entities' detailed states, time to collision, and other information. The obtained and saved records are important information to assist further safety management procedures, decisions, policies, training, and education.

When compared with other technologies adopted for unsafe-proximity detections (Table 1), a GPS-aided INS sensor has the advantages of ease of use and high accuracy in performance. A GPS-aided INS sensor can provide 3D position, velocity, and orientation directly to meet the demands of the model, which can be considered as a limitation of technologies such as ultrasonic, infrared, and RF sensing technologies. Additionally, its small size and light weight also enable its future and wide adoption on construction sites. Thus, a GPS-aided INS is a user-friendly instrument to implement Method 2 in realistic environments. Moreover, entities' heading and speed are essential information in the implementation of Method 2. A GPS-aided INS heading accuracy is 0.5° and the speed

accuracy is on a scale that is less than 0.1 m/s, which enhance the accuracy performance in real applications.

Limitations and Future Work

At the current stage, the developed model only considers the entities including equipment and workers on foot in 2D space; other important factors (such as site layout, entities' altitude, and equipment operations) are not taken into account. The future work will consider and incorporate these factors into the safety rules to further improve the functionality of the model.

Theoretically, the developed model can be applied to each pair of multiple entities even with irregular curve trajectories. However, implementing the model in real-world scenarios involving multiple pieces of equipment and workers to further improve its applicability and scalability is the future work of this study. In addition, the selected site for the controlled field experiment was an open area where good GPS signals were available. As such, applying the model on real construction sites to further evaluate and confirm model performance is also needed for the future work of the research reported in this paper.

Conclusions

Considering the high frequency of contact collisions on construction sites and the limitations of existing proximity detection methods, an unsafe-proximity detection model including two modules is proposed and developed in the research reported in this paper aiming on decreasing false alarms. The safety rules for unsafe-proximity identification in five common situations involving workers on foot and equipment are developed. Entities'

headings and speed along with the distance between entities are considered, which facilitate participants to have more accurate understanding of the circumstances. The verification of the safety rules is performed in simulation. The essential factors that need to be considered in quantification of the warning distance are discussed, and the warning distance is formulated for different situations. Using the data collected in the state tracking module, the warning distance can be updated in real time. The developed quantification method allows for both long-distance detection at higher speed and close-in detection at lower speed. Accurately quantifying the distance can assist in better and safer utilization of the workspace. The performance of the developed unsafe-proximity detection model is evaluated through simulation and a field experiment. The controlled field experiment demonstrates the feasibility and applicability of the developed model in realistic environments. The introduced technology, a GPS-aided INS, enables implementation of the model in the real world. The developed model exhibits great prospect to enhance construction safety and mobility by timely avoiding collisions, and to improve the productivity by reducing false alarms and interruptions to work. Moreover, implementation of real-time states collection and transmission contributes to establishing more advanced construction sites.

References

- Allread, B. S., and Teizer, J. (2010). "Blind spot measurements for realtime pro-active safety in construction." *Proc., Construction Research Congress*, ASCE, Reston, VA, 132–141.
- Andoh, A., Su, X., and Cai, H. (2012). "A framework of RFID and GPS for tracking

- construction site dynamics.” *Proc., Construction Research Congress*, ASCE, Reston, VA, 818–827.
- Bar-Shalom, Y., and Li, X. R. (1995). *Multitarget-multisensor tracking: Principles and techniques*, 3rd Ed., YBS Publishing, Storrs, CT.
- Behzadan, A. H., Aziz, Z., Anumba, C. J., and Kamat, V. R. (2008). “Ubiquitous location tracking for context-specific information delivery on construction sites.” *Automation in Construction*, 17(6), 737–748.
- Benet, G., Blanes, F., Simó, J. E., and Pérez, P. (2002). “Using infrared sensors for distance measurement in mobile robots.” *Rob. Autom. Syst.*, 40(4), 255–266.
- Bohannon, R. W. (1997). “Comfortable and maximum walking velocity of adults aged 20–79 years: Reference values and determinants.” *Age Ageing*, 26(1), 15–19.
- Chae, S., and Yoshida, T. (2010). “Application of RFID technology to prevention of collision accident with heavy equipment.” *Autom. Constr.*, 19(3), 368–374.
- Choe, S., Leite, F., Seedah, D., and Caldas, C. (2013). “Application of sensing technology in the prevention of backing accidents in construction work zones.” *J. Comput. Civ. Eng.*, 557–564.
- Choe, S., Leite, F., Seedah, D., and Caldas, C. (2014). “Evaluation of sensing technology for the prevention of backover accidents in construction work zones.” *Journal of Information Technology in Construction*, 19, 1–19.
- Clark, G. A. (2005). “Probability density and CFAR threshold estimation for hyperspectral imaging.” <https://e-reports-ext.llnl.gov/pdf/312003.pdf> (Mar. 4, 2014).

- Devore, J. D. (2004). *Probability and statistics for engineering and the sciences*, 6th Ed., Cole-Thomson Learning, Belmont.
- Duflos, E., Vanheeghe, P., Razavi, S. N., and Haas, C. T. (2010). “Belief function based algorithm for material detection and tracking in construction.” *Proc., Workshop on the Theory of Belief Functions*, Brest, France.
- Government of South Australia. (2010). “Forklift safety—Reducing the risks.” SafeWork, SA, (http://www.safework.sa.gov.au/uploaded_files/forklift_safety.pdf) (Apr. 3, 2014).
- Habtemariam, B. K., Tharmarasa, R., and Kirubarajan, T. (2011). “Multiple detection probabilistic data association filter for multistatic target tracking.” *Proc., Int. Conf. on Information Fusion*, IEEE, New York, 1–6.
- Hefner, R. (2003). “Construction vehicle and equipment blind area diagrams.” (<http://www.cdc.gov/niosh/topics/highwayworkzones/BAD/pdfs/catreport1.pdf>) (Sep. 17, 2014).
- Hunter-Zaworski, K., et al. (2003). “Transportation engineering online lab manual.” (http://www.webpages.uidaho.edu/niatt_labmanual/chapters/geometricdesign/theoryandconcepts/BrakeReactionTime.htm) (Apr. 3, 2014).
- Hwang, S. (2012). “Ultra-wide band technology experiments for real-time prevention of tower crane collisions.” *Autom. Constr.*, 22, 545–553.
- IHSA (Infrastructure Health and Safety Association). (2012). “Health and safety advisory-reversing vehicles: Personnel detection systems.” (http://www.ihsa.ca/images/pfiles/548_W453.pdf) (Mar. 27, 2014).

- IHSA (Infrastructure Health and Safety Association). (2013). “Can new technologies prevent struck-by injuries?” *IHSA Mag.*, 3(13), 20–21.
- Kang, N. G., Park, J. S., Hong, T. M., Lee, B. K., and Pyeon, M. W. (2009). “Development of RTLS access point allocation prototype for location tracking in construction sites.” *Proc., Int. Conf. on Networked Computing, Advanced Information Management and Service, and Digital Content, Multimedia Technology*, IEEE, New York, 943–948.
- Lee, H. S., Lee, K. P., Park, M., Baek, Y., and Lee, S. (2012). “RFID-based real-time locating system for construction safety management.” *J. Comput. Civ. Eng.*, 10.1061/(ASCE)CP.1943-5487.0000144, 366–377.
- Li, J., Carr, J., and Jobes, C. (2012). “A shell-based magnetic field model for magnetic proximity detection systems.” *Safety Science*, 50(3), 463–471.
- Liang, Q., Zhang, B., Zhao, C., and Pi, Y. (2013). “TDoA passive localization: Underwater versus terrestrial environment.” *IEEE Trans. Parallel Distrib. Syst.*, 24(10), 2100–2108.
- Marks, E., and Teizer, J. (2013a). “Evaluation of the position and orientation of (semi-) passive RFID tags for the potential application in ground worker proximity detection and alert devices in safer construction equipment operation.” *J. Comput. Civ. Eng.*, 645–652.
- Marks, E., and Teizer, J. (2013b). “Method for testing proximity detection and alert technology for safe construction equipment operation.” *Constr. Manage. Econ.*, 31(6), 636–646.

- Marks, E. D., Cheng, T., and Teizer, J. (2013). “Laser scanning for safe equipment design that increases operator visibility by measuring blind spots.” *J. Constr. Eng. Manage.*, 10.1061/(ASCE)CO.1943-7862.0000690, 1006–1014.
- MATLAB R2012b* [Computer software]. Natick, MA, MathWorks.
- NIOSH (National Institute for Occupational Safety and Health. (2001). “Preventing injuries and deaths of workers who operate or work near forklifts.” <http://www.cdc.gov/niosh/docs/2001-109/>) (Apr. 3, 2014).
- Oloufa, A. A., Ikeda, M., and Oda, H. (2003). “Situational awareness of construction equipment using GPS, wireless and web technologies.” *Autom. Constr.*, 12(6), 737–748.
- Pradhananga, N., and Teizer, J. (2013). “Automatic spatio-temporal analysis of construction site equipment operations using GPS data.” *Autom. Constr.*, 29, 107–122.
- Ray, S. J., and Teizer, J. (2013). “Computing 3D blind spots of construction equipment: implementation and evaluation of an automated measurement and visualization method utilizing range point cloud data.” *Autom. Constr.*, 36, 95–107.
- Razavi, S. N., and Haas, C. T. (2010). “Multisensor data fusion for on-site materials tracking in construction.” *Autom. Constr.*, 19(8), 1037–1046.
- Ruff, T. M. (2006). “Evaluation of a radar-based proximity warning system for off-highway dump trucks.” *Accid. Anal. Prev.*, 38(1), 92–98.
- Ruff, T. M. (2007). *Recommendations for evaluating and implementing proximity warning systems on surface mining equipment*, Centers for Disease Control and

Prevention (CDC), Atlanta, GA.

Ruff, T. M. (2010). “Overview of proximity warning and technologies and approaches.” *National Institute for Occupational Safety and Health (NIOSH) Workshop on Proximity Warning Systems for Mining Equipment*, Centers for Disease Control and Prevention (CDC), Atlanta, GA.

SBG Systems. (2014). “IG-500N: GPS aided miniature INS.” (<http://www.sbg-systems.com/products/ig500n-miniature-ins-gps>) (Jul. 5, 2014).

Shahi, A., West, J. S., and Haas, C. T. (2013). “Onsite 3D marking for construction activity tracking.” *Autom. Constr.*, 30, 136–143.

Steele, J., Debrunner, C., Whitehorn, M., and Center, W. M. R. (2003). “Stereo images for object detection in surface mine safety applications.” *Technical Rep. TR20030109*, Western Mining Resource Center, Colorado School of Mines, Golden, CO.

Su, X., Li, S., Yuan, C., Cai, H., and Kamat, V. (2014). “Enhanced boundary condition-based approach for construction location sensing using RFID and RTK GPS.” *J. Constr. Eng. Manage.*, 10.1061/(ASCE)CO.1943-7862.0000889, 04014048.

Technology Associates. (2014). “Reaction time.” (<http://www.technology-assoc.com/articles/reaction-time.html>) (Apr. 3, 2014).

Teizer, J., Allread, B. S., Fullerton, C. E., and Hinze, J. (2010a). “Autonomous proactive real-time construction worker and equipment operator proximity safety alert system.” *Autom. Constr.*, 19(5), 630–640.

Teizer, J., Allread, B. S., and Mantripragada, U. (2010b). “Automating the blind spot

measurement of construction equipment.” *Autom. Constr.*, 19(4), 491–501.

Wang, J., Zhang, S., and Teizer, J. (2015). “Geotechnical and safety protective equipment planning using range point cloud data and rule checking in building information modeling.” *Autom. Constr.*, 49, 250–261.

Wu, W. W., Yang, H. J., Li, Q. M., and Chew, D. (2013). “An integrated information management model for proactive prevention of struck-by-falling-object accidents on construction sites.” *Autom. Constr.*, 34, 67–74.

CHAPTER 3: HAZARD DETECTION II

Introduction

One of the limitations of the developed unsafe-proximity detection model presented in Chapter 2 (a 3D model) is that the model considered entities' motions and alert zones (an entity's inherent hazardous zone) in 2D space. Therefore, to portray real situations on sites and identify hazards more accurately, two 4D (3D motion plus time) models, i.e., time-sphere model and time-cuboid model, were developed in the hazard detection module of the SA4SR (situational awareness for construction safety risks management) to improve on-site situational awareness. The developed two 4D models made improvements to the 3D model and also focused on identifying struck-by-equipment hazards and reducing false alarms. The work included in this chapter explains the two 4D models. It is published as:

Wang, J., and Razavi, S. (2016b). “**Two 4D Models Effective in Reducing False Alarms for Struck-by-Equipment Hazard Prevention.**” *Journal of Computing in Civil Engineering*, 30 (6), DOI: [10.1061/\(ASCE\)CP.1943-5487.0000589](https://doi.org/10.1061/(ASCE)CP.1943-5487.0000589)

The co-author's contributions are:

- Technical supervision of the study presented in this paper; and
- Review and modification of the manuscript.

Paper #2: Two 4D Models Effective in Reducing False Alarms for Struck-by-Equipment Hazard Prevention

Abstract

Over the past decade, several smart and automated systems have been developed to address the issue of struck-by hazards in construction—that is, workers on foot struck by equipment or equipment struck by equipment. False alarms (false positives and false negatives) are common in such systems, but methods for limiting false alarms have not yet been thoroughly studied or tested for real-world implementations. This study presents two novel four-dimensional (4D) [time and three-dimensional (3D) space] models, a time-sphere model and a time-cuboid model, that are effective in reducing the rate of false alarms. In each developed 4D model, (1) entities' state information, including 3D position, orientation (roll, pitch, and yaw), and velocity, is acquired and analyzed over time; (2) the hazardous area around equipment or workers is represented by a sphere or a cuboid with the warning distance adjusted and updated according to the entities' collected state information; and (3) unsafe-proximity query rules identify and predict contact collisions using relative position and velocity and a pairwise 3D unsafe-proximity query. The effectiveness of the developed 4D models was evaluated through simulation and field experiments; however, the data were not wirelessly communicated because the focus of the study was on development, analysis, and comparison of two models for safety hazard identification. The obtained false positive and false negative rates indicate that the two developed 4D models have a strong capability for reducing false alarms. The obtained

reduced alarm percentages imply that on average 65% of the alarms triggered by the most prevalent method can be averted by using the time-sphere model and 81% can be reduced by using the time-cuboid model. Furthermore, three major categories of findings are summarized: model comparison, model analysis, and the relationship between alert zone dimensions and model performance. The developed rigorous 4D models can also be employed for several types of contact collisions that involve temporal and permanent site facilities, materials transported in air, and equipment and workers on foot. Reduced false alarms will improve construction safety, productivity, and mobility.

Keywords: Construction safety; Struck-by hazard; False alarm; Spatial interference; Four-dimensional (4D) models; Warning distance; Alert zone; Unsafe-proximity query rules.

Introduction

Construction entities, such as equipment and workers on foot, are generally in a dynamic status and can be in close proximity to each other on unstructured construction sites. Consequently, unsafe spatial interferences between construction entities can potentially lead to contact collisions. In 2013, 16% of fatal occupational injuries resulted from hazardous contact with equipment and objects (BLS 2015). Based on the statistics published by the Occupational Safety and Health Administration (OSHA), from 1995 to 2008, struck-by-equipment hazards accounted for 58% of total struck-by accidents (Wu et al. 2010). In 2008 and 2009, construction equipment operator fatalities accounted for 4 and 6% of total construction fatalities, respectively, in the United States. (Gürçanlı et al.

2015). Therefore, contact collision between workers on foot and equipment or between equipment and equipment is a great threat to the safety and health of construction personnel.

Several proximity warning methods have been developed to prevent struck-by-equipment accidents (Teizer et al. 2010; Hwang 2012; Pradhananga and Teizer 2012; Choe et al. 2014). The most widely used, however, use distance detection to determine potential contact collisions (IHSA 2013; Marks and Teizer 2013a; Choe et al. 2014). Generally, an alarm is triggered and sent to the involved entities if the set or obtained distance threshold (warning distance) is violated. Many of these alarms, though, may be false (false positive or false negative), failing to correctly indicate and reveal actual dangerous situations (Ruff 2010; Wang and Razavi 2016a). False positives bring disruptions to work and eventually cause alarms to be disabled or ignored by participants. False negatives fail to signal actual risks when entities are involved in hazardous situations. For these reasons, the primary objectives of this paper are: (1) developing time-sphere and time-cuboid models by fully considering entity state—that is, 3D position, orientation (roll, pitch, and yaw) and velocity—to reduce false alarms; (2) generation of a sphere or cuboid alert zone (inherent hazardous zone) and a dynamic warning distance for each construction entity to enhance space utilization, construction mobility, and productivity; and (3) accurate identification of future potential 3D space conflicts in addition to current spatial interferences.

The structure of this paper starts with a literature review and the most widely used methods for contact collision prevention are presented. Three major aspects of frequent

false alarms are extracted and summarized, followed by the research scope and objectives. Afterward, development of the two four-dimensional (4D) [time and three-dimensional (3D) space] contact-collision prevention models (i.e., time-sphere and time-cuboid) is explained. To demonstrate the effectiveness of these models, both simulation and field experiments were conducted, and the analytical results are presented and discussed in detail here. Finally, the limitations of the research are summarized and concluding remarks are presented.

Literature Review

State Information

In the context of construction safety, an entity's state information refers to its position, orientation, acceleration, velocity, and other safety-related information. Most proximity warning methods are based only on the distance between entities and neglect other pieces of state information, which leads to frequent, disruptive false alarms (Ruff 2010; Teizer et al. 2010). Examples of such methods are found in some proximity warning systems that use radio frequency (RF) sensing, ultrasonic-based sensing, Bluetooth sensing, and others (Park et al. 2015; Wang et al. 2015; IHSA 2013; Marks and Teizer 2013b; Choe et al. 2013; Ruff 2007). According to the adopted technology, nine categories of existing prevalent proximity warning systems were summarized and presented in the work of Wang and Razavi (2016a), including the advantages and limitations of each one. Kim et al. (2006) developed a 3D workspace-modeling method to avert collisions of equipment and site obstacles by calculating the actual minimum distance between them. Nevertheless, distance does not fully and accurately portray the

actual situation that the entities are in. In many instances, two-dimensional (2D) or 3D workspaces may have intersections (Li et al. 2012; Vahdatikhaki and Hammad 2015), so additional information, such as 3D orientation, velocity, and/or acceleration, is needed to ensure more accurate situational awareness and to make more reliable safety decisions [Endsley 1995; Teizer et al. 2007; Taneja et al. 2011; Ahn et al. 2015; V. R. Kamat, et al., “Estimating three-dimensional position and orientation of articulated machine using one or more image-capturing devices and one or more markers,” U.S. Patent No. 20150168136 (2015)]. R. L. Burns [“Dynamic safety envelope for autonomous-vehicle collision avoidance system,” U.S. Patent No. 6393362 (2002)] developed a function to specify safety envelopes for autonomous vehicles based on position, speed, trajectory, and other predetermined parameters, but this involved only two-dimensional examples. The SAFEmine collision avoidance system was developed for vehicles using GPS to collect position, heading, and speed, but this system also mainly focuses on finding out whether vehicles’ 2D paths will converge in the future (HEXAGON Mining SAFEmine 2015).

To overcome the downfalls of these early methods, this paper develops two 4D contact-collision prevention models that completely account for an entity’s 3D position, orientation, and velocity to more accurately reveal actual situations and to proactively identify hazardous 3D space conflicts between entities.

Detection and Prediction of Collisions

Another way to reduce the generation of false alarms is to develop a method that can not only efficiently detect actually occurring spatial interferences but also identify

potentially imminent spatial conflicts (Zhang and Hammad 2012; Talmaki and Kamat 2014; Talmaki et al. 2015). Compared with a reactive alarm, an accurate look-ahead (proactive) alarm allows operators and workers on foot enough time to perform countermeasures to avoid a hazard. In the work conducted by Burns [“Dynamic safety envelope for autonomous-vehicle collision avoidance system,” U.S. Patent No. 6393362 (2002)], a method for identifying future potential overlaps between generated 2D safety envelopes was developed. However, this method requires a time interval for each forecast iteration to be determined and provided in advance. The SAFEmine collision avoidance system mentioned earlier focuses on discovering whether there will be a conflict between vehicles’ 2D paths in the future (HEXAGON Mining SAFEmine 2015).

Compared with the projection of conflicts in two dimensions, development of a reliable method of foreseeing impending interferences between 3D spaces remains of paramount importance and a great challenge. A number of methods for 3D workspace generation and conflict detection have been developed in which upcoming 3D space intersections are identified using predictively generated spatial shapes. In other words, foreseeing future spatial interferences is based on the premise that the predicted 3D spaces have been created (Cohen et al. 1995; Tantisevi and Akinci 2007; Moon et al. 2014b, c; Vahdatikhaki et al. 2015). In a recent study, Vahdatikhaki and Hammad (2015) developed a dynamic equipment-workspace generation method in which the line-segment intersection algorithm was used to realize collision detection. A collision was identified if the edges of the workspaces were actually intersecting. In summary, these approaches were more capable of identifying the intersections of already given 3D workspaces even

though those workspaces were created based on predictions. In general, generating a predicted 3D space indicates necessary assumptions of an entity's future motion patterns, such as assuming its speed and moving direction in a predefined time interval.

This study developed two 4D models that not only can detect actual spatial interferences but also can foresee impending spatial conflicts without predefining a prediction time interval and generating the corresponding predicted 3D spaces.

Generation of the Dynamic Warning Zone for a Construction Entity

The warning zone is the area around a construction entity that has the potential to incur a hazard under certain conditions. It is also called the warning workspace or warning area and generally is represented using warning distance. In various studies, 2D shapes have been used to signify the equipment warning area (Chae and Yoshida 2010; Han et al. 2014; Wang and Razavi 2016a; Awolusi et al. 2015). Bounding boxes (cubes and cuboids), cylinders, spheres, cones, and other 3D shapes have also been widely used to stand for equipment workspaces and site obstacles (Jimenez et al. 2001; Chavada et al. 2012; Cheng and Teizer 2013; Moon et al. 2014a). Another advantageous way to decrease false alarms is to define 2D or 3D shapes around each entity in a more dynamic and accurate manner. Overconservative, constant, or not enough warning zones not only lead to false alarms but also hinder the efficient use of congested sites (Vahdatikhaki and Hammad 2015; Roofigari Esfahan et al. 2015). Thus, a more accurate method for estimating warning zones is needed for practical applications. It was pointed out that the warning zone should be calibrated with respect to some essential attributes, such as equipment speed and personnel reaction time, allowing appropriate distance and time for

corrective actions (Teizer et al. 2010; Marks and Teizer 2013b). Several dynamic workspace generation methods have been developed in which equipment workspaces are dynamically adjusted using equipment movement characteristics (e.g., speed and motion vector) but personnel reaction time and other parameters are neglected [Burns, “Dynamic safety envelope for autonomous-vehicle collision avoidance system,” U.S. Patent No. 6393362 (2002); Zhang and Hammad 2012; Vahdatikhaki and Hammad 2015]. As indicated in the study conducted by Vahdatikhaki and Hammad (2015), not all identified collisions represent real safety threats because the 3D equipment workspace is generated without considering the geometry and motion characteristics of equipment along the vertical axis.

Along with entities’ motion characteristics, including vertical movement, this paper takes into account personnel reaction time and operator execution time to update the warning distance for both equipment and workers on foot. In this way, false alarms can be effectively avoided. Also, the adjusted warning distance achieves both long-distance detection for higher speed and short-distance detection for lower speed, and in turn provides appropriate time for entities to respond.

Research Scope and Objectives

To effectively prevent struck-by-equipment hazards in construction—workers on foot struck by equipment or equipment struck by equipment—time-sphere and time-cuboid models are developed that are effective in reducing false alarms. The focus of this paper is on development, analysis, and comparison of two models for safety hazard identification. Thus, the research objectives include (1) defining equations to dynamically

adjust and update the adopted distance threshold (i.e., warning distance); (2) developing unsafe-proximity query rules that not only detect actual 3D spatial interferences but also foresee impending spatial conflicts; and (3) evaluating the developed time-sphere and time-cuboid models' effectiveness in reducing false alarms through simulation and field experiments.

4D Contact-Collision Prevention Models

In this section, two 4D contact-collision prevention models, time-sphere and time-cuboid, are developed. Each model includes three major components: (1) the corresponding 3D shape (i.e., sphere or cuboid) representing an entity's alert zone and the formulas used to update the state information (3D position, orientation, and velocity) associated with each 3D shape; (2) the equations to quantify the essential distance thresholds (alert distance and warning distance); and (3) the unsafe-proximity query rules for each model to perform the pairwise 3D unsafe-proximity query and identify hazardous contacts.

The framework for ideal implementation of the 4D models in the real world is shown in Fig. 1. Three major steps are involved: (1) real-time state information is acquired by attaching sensors to individual entities; (2) sensed data are wirelessly transmitted through the Internet to the cloud, and the cloud is integrated with the 4D models; and (3) results regarding unsafe situations are sent back to the associated entities, which are uniquely identified, and corresponding actuator(s) are activated for alarms. The alarms can be visual, audible, and/or vibrating.

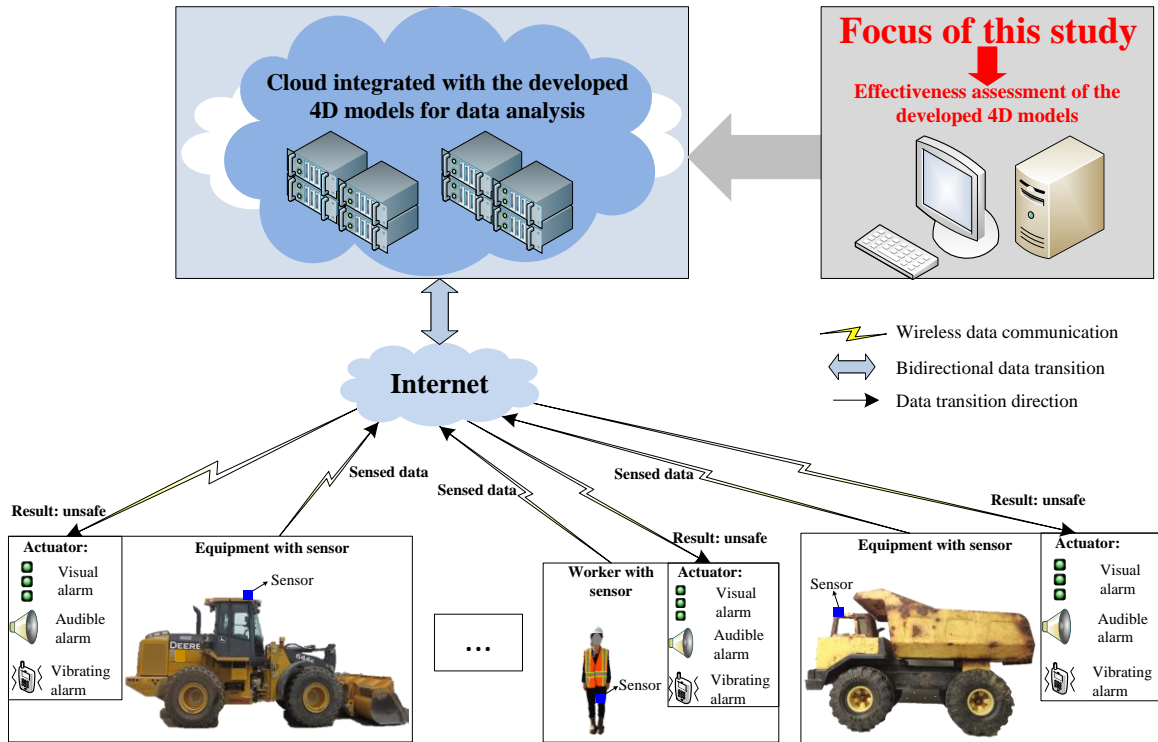


Fig. 1. 4D model real-world implementation (images by authors)

In this study, the data were not wirelessly communicated because the focus was on development, analysis, and comparison of two models for safety hazard identification. Instead, the sensed data were transmitted through a data logger to a desktop for post-analysis and assessment of the models' effectiveness in reducing false alarms. Wireless communication of the sensor and actuator systems represents future work with the proposed framework.

3D Shape and State Calculation

Basic Definitions

The alert zone is the inherent hazardous zone of an entity within which no other

entities are allowed without authorizations. Two 3D shapes, sphere and cuboid, are adopted in this paper to respectively represent an entity’s alert zone in the time-sphere and time-cuboid models (Fig. 2). Determination of the size of the alert zone is described in the later section “Quantification of Distance Thresholds.” For the same entity, the longest side of the cuboid equals the diameter of the sphere. A cuboid comes closest to the abstraction of an entity’s alert zone (without considering equipment operations) (Chang et al. 2010; Vahdatikhaki et al. 2015). Thus, the time-sphere model, compared with the time-cuboid model, using a sphere to represent an entity’s alert zone, potentially generates more alarms. The defined sphere or cuboid alert zone can also be adopted as the hazardous zone of temporary and permanent site elements.

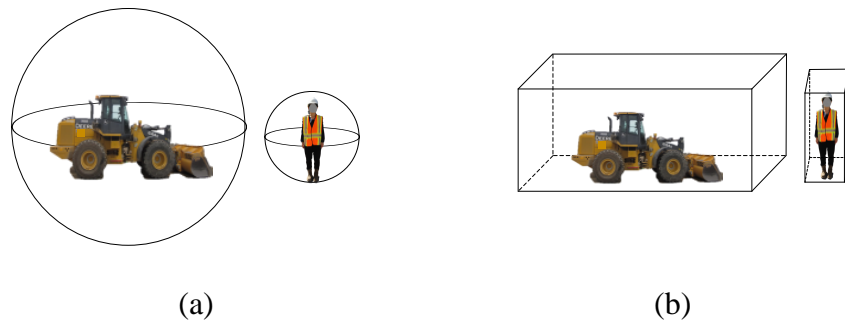


Fig. 2. Alert zones for equipment and workers on foot: (a) time-sphere model; (b) time-cuboid model (images by authors)

Two major coordinate systems are adopted to establish the two 4D models. The first is a local coordinate system (represented by X - Y - Z) in which geographic east and north and up are referred as the X -, Y -, and Z -axes and a selected point works as the origin

[Fig. 3(a)]. The second (represented by x - y - z) is established on an entity's body. Taking the cuboid around equipment as an example [Fig. 3(b)], the positive y -axis (roll axis) is aligned with the cuboid length and oriented toward the equipment's forward direction. The positive x -axis (pitch axis) is aligned with the cuboid width and oriented 90 degrees clockwise to the positive y -axis. The positive z -axis (yaw axis) is aligned with the cuboid height and points down. Generally an entity's state information is acquired by attaching a sensor to it. The sensor has the same coordinate system as the one on the entity and is used to represent it. Roll, pitch, and yaw angles are used to describe a rigid body's spatial rotations with respect to a reference frame. In this paper, the local coordinate system (X - Y - Z) works as the reference frame to measure an entity's orientation. In real-world applications, an initial orientation of the sensor is recorded and used for further model calibration if the sensor cannot be perfectly attached to an entity. A perfect sensor installation is defined by the initial roll and pitch, which are as close to zero as possible, and the sensor's y -axis is aligned with the entity's y -axis when the entity is static on horizontally flat ground.

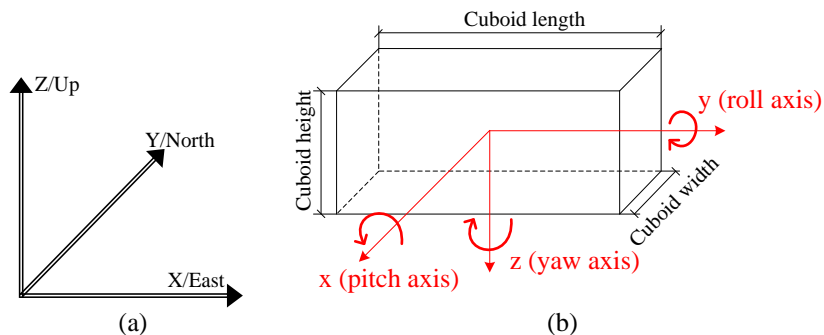


Fig. 3. Basic definitions: (a) local coordinate system (X - Y - Z); (b) entities' coordinate system (x - y - z)

Some basic examples are provided to describe yaw, pitch, and roll generation. Yaw changes if the entity is making a turn; pitch is generated when an entity is moving upward or downward on a slope; and a (slight) roll is generated if the altitude of the equipment tires on one side is different from that on the other side.

State Calculation

The theoretical calculations explained in this section are based on the assumption that a sensor is attached to an entity in a perfect way. Consequently, an entity's state can be represented by the state information collected by the sensor:

$$\text{State information} = [p_X, p_Y, p_Z, v, R, P, Y] = [p_X, p_Y, p_Z, v_X, v_Y, v_Z, R, P, Y] \quad (1)$$

where $[p_X, p_Y, p_Z]$ represents 3D position in the local coordinate system; R , P , and Y are roll, pitch, and yaw respectively (all R , P , and Y in the equations in this paper are expressed as angles); and v is moving velocity; and $[v_X, v_Y, v_Z]$ is corresponding velocity decomposition in the local coordinate system.

As expressed in Eq. (1), v refers to moving velocity at the entity's y -axis (i.e., forward or backward speed). The entity's vertical movement (i.e., speed and z -axis) is also considered in this paper and is explained at the end of this section.

To correctly and effectively apply the developed 4D models, the states of the sphere center [Fig. 2(a)] and the cuboid vertices and center [Fig. 2(b)] need to be calculated, including (1) 3D positions of the sphere center, cuboid vertices, and center and (2) sphere center and cuboid vertices' velocity decompositions in the local coordinate system. The entity's 3D orientation needs to be considered in the corresponding

calculation process. The velocity of the sphere center and the cuboid vertices includes not only linear velocity, which is the same as the sensor's, but also the angular velocity resulting from the rigid body's orientation (Chen and Huang 1987; Liu and Wang 2005; McFarland et al. 2014). The developed 4D models can be effectively applied to any scenario regardless of the sensor's installation position on the entity. The complexity of the calculation depends on the sensor's installation state (Fig. 4). S_W , S_H , S_L [Fig. 4(a)] are determined by the geometry of the cuboid alert zone and the sensor's installation location. Because none of these dimensions is a half of the respective cuboid width, height, and length, and the sensor's installation location cannot be considered on any of the cuboid surfaces, the calculation associated with the case shown in Fig. 4(a) is more complicated; generally other cases are simpler. Multiple real-world cases can be simplified, and one simplified case with the calculation equations is presented in this paper.

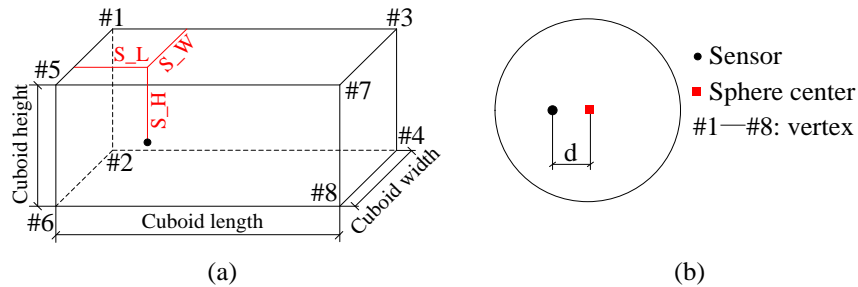


Fig. 4. (a) Geometrics of equipment alert zone for the time-cuboid model; (b) simplified case for the time-sphere model

The simplified example [Fig. 4(b)] is for an entity on which the sensor's location is the horizontal central line of the 3D shape, but is obviously offset from the sphere center (e.g., the dump truck). The calculation equations for this case are expressed in Eqs. (2)–(10). Eqs. (2)–(4) also represent the method of calculating the 3D position of the cuboid center for the time-cuboid model.

$$pX' = p_X - d \cdot \cos P \cdot \sin Y - d \cdot \sin P \cdot \sin R \cdot \cos Y \quad (2)$$

$$pY' = p_Y - d \cdot \cos P \cdot \cos Y + d \cdot \sin P \cdot \sin R \cdot \sin Y \quad (3)$$

$$pZ' = p_Z - d \cdot \sin P \cdot \cos R \quad (4)$$

$$vX' = v \cdot \cos P \cdot \sin Y - (\Delta Y/\Delta t) \cdot d \cdot \cos R \cdot \cos Y - (\Delta Y/\Delta t) \cdot d \cdot \sin R \cdot \sin P \cdot \sin Y - (\Delta P/\Delta t) \cdot d \cdot \sin R \cdot \cos Y + (\Delta P/\Delta t) \cdot d \cdot \cos R \cdot \sin P \cdot \sin Y \quad (5)$$

$$vY' = v \cdot \cos P \cdot \cos Y + (\Delta Y/\Delta t) \cdot d \cdot \cos R \cdot \sin Y - (\Delta Y/\Delta t) \cdot d \cdot \sin R \cdot \sin P \cdot \cos Y + (\Delta P/\Delta t) \cdot d \cdot \sin R \cdot \sin Y + (\Delta P/\Delta t) \cdot d \cdot \cos R \cdot \sin P \cdot \cos Y \quad (6)$$

$$vZ' = v \cdot \sin P + (\Delta Y/\Delta t) \cdot d \cdot \sin R \cdot \cos P - (\Delta P/\Delta t) \cdot d \cdot \cos R \cdot \cos P \quad (7)$$

$$\Delta Y/\Delta t = (Y \text{ at time } t_2 - Y \text{ at time } t_1) \cdot 2 \cdot \pi/360/(t_2 - t_1) \quad (8)$$

$$\Delta P/\Delta t = (P \text{ at time } t_2 - P \text{ at time } t_1) \cdot 2 \cdot \pi/360/(t_2 - t_1) \quad (9)$$

$$\Delta R/\Delta t = (R \text{ at time } t_2 - R \text{ at time } t_1) \cdot 2 \cdot \pi/360/(t_2 - t_1) \quad (10)$$

where p_X, p_Y, p_Z , and v have the same definition as in Eq. (1); $[pX', pY', pZ']$ is 3D position of the sphere center; $[vX', vY', vZ']$ is the center's decomposed velocity aligned with the X -, Y -, and Z -axes of the local coordinate system; and d is the distance between

the sensor and the sphere center. To indicate the respective radian change per second, $(\Delta Y/\Delta t)$, $(\Delta P/\Delta t)$, and $(\Delta R/\Delta t)$ are expressed in rad/s.

As mentioned previously, movement characteristics along the vertical axis have not been fully considered in some work (e.g., Vahdatikhaki and Hammad 2015). In real-world situations, however, workers need to complete some tasks at height, which requires them to move to different elevations. Therefore, in addition to forward and backward velocity, the vertical velocity of workers on foot (an entity moving along the z -axis) is considered in the developed 4D models to reduce the generation of false alarms. In this case, the equations for 3D position calculation are still applicable and the velocity decompositions aligned with the X - and Y -axes are considered to be zero.

In summary, using the sensor's state information along with the developed equations and the determined geometric 3D shape, the required state information can be updated accordingly. In this paper, the distance between entities is represented by the distance between the centers of the involved 3D shapes. In real-world applications, the distance between entities can be simplified and approximated as the distance between two sensors if applicable. Additional calibrations on coordinate system transformation are needed if the sensor's coordinate system is not perfectly aligned with that of the corresponding entity. Coordinate system transformation methods have been fully studied and applied in multiple fields. Their implementation is neither effort nor computation consuming (Bar-Shalom et al. 2001; Du et al. 2014).

It is not difficult to achieve a perfect sensor installation on equipment, whereas there are high requirements on sensor selection for workers on foot for a perfect

installation (e.g., the sensor should be quite integrated and compressed into a small size). In addition, a position slightly higher than the knee is suggested for attaching a sensor and some facilitating devices (e.g., a kneepad) can be considered to fix the sensor in place. The suggested position can better reveal a worker's actual motion characteristics compared with other body parts. For example, the head or shoulders might be turning while the worker is standing still with no velocity.

Quantification of Distance Thresholds

Alert and warning distances are two essential thresholds used in time-sphere and time-cuboid models to identify potential contact collisions. In this section, the principles and methods used to quantify these distances are described.

Alert Zone and Distance

The alert zone is the hazardous area around an entity where no other entities are allowed without authorization. Thus, a contact collision can be efficiently avoided if no intersection of alert zones occurs after the involved entities come to a complete stop. The alert distance between any two entities is a constant value and is not adjusted with the change in entity state. An alert alarm (visual, audible, vibrating, or a combination of these) is generated once the distance between entities is identified as smaller than the corresponding alert distance.

Quantification of the size of the alert zone is an important part of contact collision prevention and is currently garnering much scholarly attention. According to current literature and feedback from onsite construction workers, the size of the equipment alert zone is created by adding a distance (Δ) to the determined equipment size [Eqs. (11)–

(13)]. Three major factors are suggested for consideration in determining Δ : (1) equipment type and operation; (2) equipment blind spots; and (3) continuous, effective, and comfortable eye contact between the equipment operator and workers on foot or between operator and operator (Ray and Teizer 2013; Wang and Razavi 2016a; Proconstruction Guide 2015). An overconservative Δ would be wasteful of space and consequently generate false positives without alarming actual hazardous situations; a too small Δ would not satisfy the previously described three major factors and would result in false negatives. The cuboid height is determined by equipment type. Although accurate quantification of the equipment alert zone is a challenging problem, taking some or all of the suggested factors into account is conducive to better control of unsafe proximities.

$$\text{Sphere radius} = \text{half of equipment length} + \Delta \quad (11)$$

$$\text{Cuboid length} = \text{equipment length} + 2 \times \Delta \quad (12)$$

$$\text{Cuboid width} = \text{equipment width} + 2 \times \Delta \quad (13)$$

For workers on foot, an average 2-m diameter sphere or a $1.4 \times 1.4 \times 2$ -m cuboid is adopted as the alert zone. The 1.4-m distance is the average minimum required between workers (Dagan and Isaac 2015); for safety reasons, the 2-m cuboid height is slightly higher than the average height of an adult male (HHS 2004). To consider the vertical movements of a worker and also to avert intersecting alert zones, the longest side of the cuboid (i.e., cuboid height) or sphere diameter is adopted to define the alert distance.

The alert distance for two pieces of equipment is defined in Eq. (14) and for a worker on foot and equipment is defined in Eq. (15). The quantified alert distance is the minimum that should be kept between entities to avoid their alert zones intersecting.

$$\text{Alert Distance} = (0.5 \times \text{cuboid length}) \text{ or } (\text{sphere radius}) \text{ of ME1} + (0.5 \times \text{cuboid length}) \text{ or } (\text{sphere radius}) \text{ of ME2} \quad (14)$$

$$\text{Alert Distance} = (0.5 \times \text{cuboid height}) \text{ or } (\text{sphere radius}) \text{ of MW} + (0.5 \times \text{cuboid length}) \text{ or } (\text{sphere radius}) \text{ of ME} \quad (15)$$

where ME1 and ME2 represent the different pieces of moving equipment; and MW represents one moving worker on foot.

Warning Distance

Different from the constant alert distance for two specific entities, the warning distance between any two entities is dynamically calculated and adjusted with a change in entity state. It is quantified [Eqs. (16)–(18)] by adding a buffer distance to the quantitatively determined alert distance [Eqs. (11)–(13)]. Three essential distances are comprehensively taken into account to quantify the buffer distance: (1) reaction distance of the worker (RDofW); (2) reaction distance of equipment (RDofE); and (3) braking distance of equipment (BDofE). More details about the calculation of the three essential distances can be found in the work of Wang and Razavi (2016a). The so far developed dynamic quantification methods do not account for the existence of multiple terrain types on sites (e.g., slopes) (Vahdatikhaki et al. 2015). Therefore, this paper presents an improved quantification method that is more robust and applicable to any type of site terrain.

The warning distance for the situation without vertical movements of entities is

expressed in Eqs. (16) and (17). Eq. (16) calculates the warning distance for two pieces of equipment; Eq. (17), for one piece of equipment and one worker on foot.

$$\begin{aligned} \text{Warning Distance} = \sqrt{\{ & [(0.5 \times \text{cuboid length} + \text{RD of E} + \text{BD of E})\text{of ME1} \times \\ & \cos(\text{Pitch1})] + [(0.5 \times \text{cuboid length} + \text{RD of E} + \text{BD of E})\text{of ME2} \times \\ & \cos(\text{Pitch2})\}^2 + \{ & [(0.5 \times \text{cuboid length} + \text{RD of E} + \text{BD of E})\text{of ME1} \times \\ & \sin(\text{Pitch1})] + [(0.5 \times \text{cuboid length} + \text{RD of E} + \text{BD of E})\text{of ME2} \times \\ & \sin(\text{Pitch2})\}^2 \} \end{aligned} \quad (16)$$

$$\begin{aligned} \text{Warning Distance} = \sqrt{\{ & [(0.5 \times \text{cuboid height} + \text{RD of W}) \text{ of MW} \times \cos(\text{Pitch1})] + \\ & [(0.5 \times \text{cuboid length} + \text{RD of E} + \text{BD of E}) \text{ of ME} \times \cos(\text{Pitch2})\}^2 + \{ & [(0.5 \times \\ & \text{cuboid height} + \text{RD of W}) \text{ of MW} \times \sin(\text{Pitch1})] + [(0.5 \times \text{cuboid length} + \text{RD of E} + \\ & \text{BD of E}) \text{ of ME} \times \sin(\text{Pitch2})\}^2 \} \end{aligned} \quad (17)$$

The warning distance for vertical movements of entities is defined in Eq. (18), which is for one piece of equipment and one worker; the worker has vertical movements:

$$\begin{aligned} \text{Warning Distance} = \sqrt{\{ & [(0.5 \times \text{cuboid height})\text{of MW}] + [(0.5 \times \text{cuboid length} + \\ & \text{RD of E} + \text{BD of E})\text{of ME} \times \cos(\text{Pitch2})\}^2 + \\ & \{ & [(0.5 \times \text{cuboid height} + \text{RD of W})\text{of MW} + (0.5 \times \text{cuboid length} + \text{RD of E} + \\ & \text{BD of E})\text{of ME} \times \sin(\text{Pitch2})\}^2 \} \end{aligned} \quad (18)$$

If the distance between entities is smaller than the calculated warning distance, the developed unsafe-proximity query rules described in the next section are used to verify whether an alarm is needed. In this way, false alarms are effectively avoided, and the

dynamic warning distance achieves long-distance detection for higher speed and short-distance detection for lower speed, providing appropriate time for entities to respond.

Unsafe-Proximity Query Rules

Unsafe-proximity query rules are developed to determine whether an alarm is needed. A generated alarm is a true alarm (true positive) if the alert zones are intersected or will be intersected in the future. Therefore, the main idea of these rules is analyzing entities' current states to identify whether their alert zones (i.e., spheres or cuboids) have been intersected or will conflict with each other in the future. Even though many 3D shapes have been used to represent the zone around an entity, a cuboid is the closest to the abstraction of the hazardous zone (alert zone). Therefore, in this paper the intersection of cuboids is considered the relative truth or baseline for comparisons of hazard detection models. The intersection of cuboids around entities has been defined as hazardous in several studies focusing on collision prevention (Cohen et al. 1995; Chang et al. 2010; Vahdatikhaki and Hammad 2015; Vahdatikhaki et al. 2015). Therefore, a true positive is determined if cuboids are identified as intersected at the moment or as being intersected in the future, and a true negative is determined if cuboids are identified as neither intersected at the moment nor being intersected in the future. False positives and false negatives can thus be effectively avoided by the time-cuboid model. The time-sphere model, in which the pairwise 3D unsafe-proximity query is easier to implement, might generate false positives and false negatives. Both models were developed, and their performances were compared through simulation and field experiments in this study.

The developed unsafe-proximity query rules use relative position and velocity to

perform the pairwise 3D unsafe-proximity query. In this process, dimension is reduced by converting the 3D spatial conflict identification and prediction problem to three 2D conflict identification and prediction problems. In one 4D model, the unsafe-proximity query rules implemented in each plane are the same. The overall process of the unsafe-proximity query rules for the two 4D models is explained in Fig. 5. Three points about them are:

- If the states of the involved 3D shapes satisfy Condition 1 (Fig. 5), the unsafe-proximity query rules are used only in the X - Y plane; if the 2D axonometric projections on the X - Y plane have already overlapped or will overlap, the corresponding 3D shapes are also identified as intersected or to be intersected in the future;
- If the 3D shapes are quite close to each other on a slope but do not intersect spatially, it is still possible that their 2D projections in the X - Y plane overlap; this is an exceptional case of Point (1), but because site topography (e.g., steep slope) and falling objects are two identified major factors leading to struck-by accidents (Esmaeili et al. 2015b), such cases are also considered hazardous; therefore, Point (1) is applicable to this case as well; and
- If the states of the involved 3D shapes satisfy Condition 2 (Fig. 5), the unsafe-proximity query rules are used in each projected plane, X - Y , X - Z , and Y - Z , to detect whether the projected 2D shapes are or will be intersected.

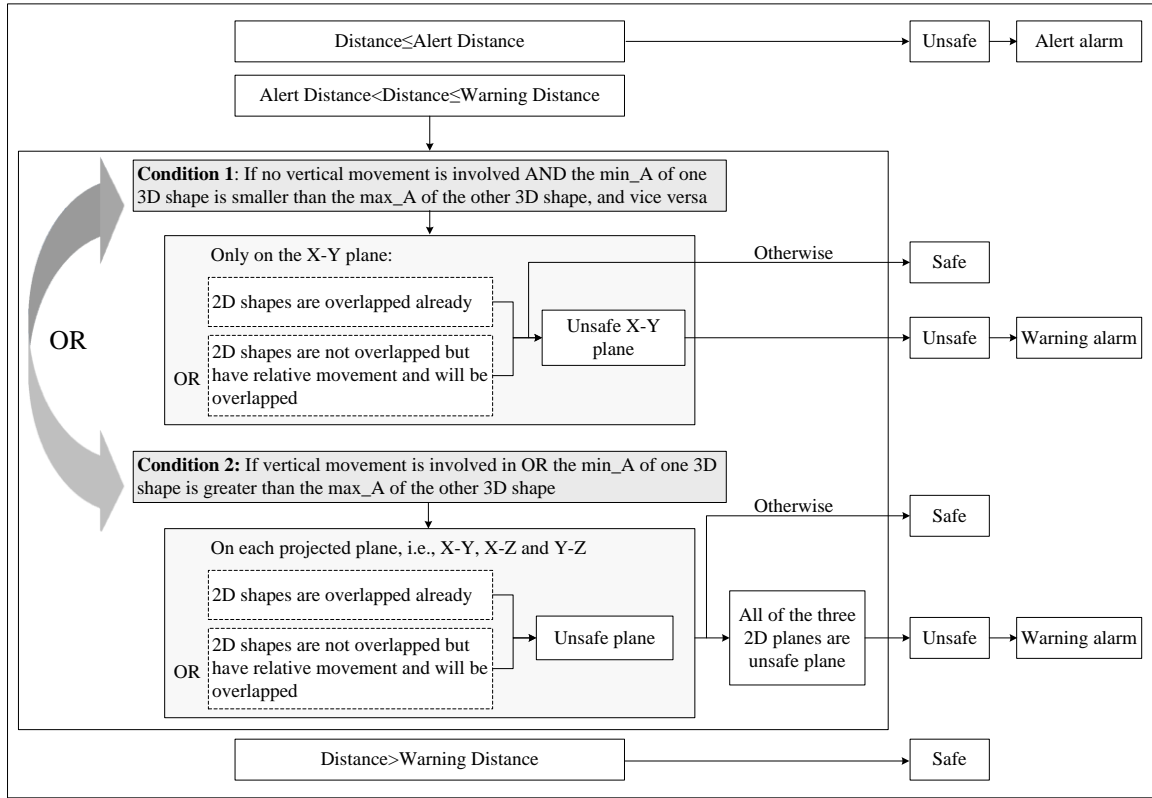


Fig. 5. Overall process of the unsafe-proximity query rules used in the two 4D models (distance = measured distance between centers of two 3D shapes; min_A = minimum altitude of a 3D shape; max_A = maximum altitude of a 3D shape)

As shown in Fig. 5, an alarm is sent out if (1) the distance between the involved 3D shapes is not bigger than the alert distance; (2) under Condition 1, the X-Y plane is identified as unsafe; or (3) under Condition 2, all planes are identified as unsafe.

Unsafe-Proximity Query Rules for the Time-Sphere Model

The projection of a sphere on each plane is a circle with a radius the same as that of the sphere. If the distance between two circle centers is smaller than the sum of the corresponding circle radii, the circles are identified as overlapping. If the projected circles

are not overlapping but their relative velocity is nonzero, the rules shown in Fig. 6 are used to identify their future potential overlap with their current states in this plane.

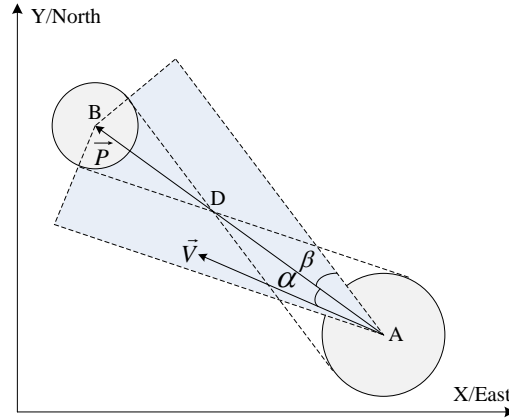


Fig. 6. Unsafe-proximity query rules used in each plane (using the X-Y plane as an example)

In Fig. 6, A and B are two construction entities with corresponding projected circles; D is the distance between the centers of the two projected circles; α is the angle between two vectors of the relative position (\vec{P}) of Entity B with respect to Entity A and the relative velocity (\vec{V}) of Entity A with respect to Entity B; β is calculated using Eq. (19) and 2β (the shaded angle with the dashed boundary) is the range of headings that can eventually cause the moving projected circles to overlap:

$$\beta = \arcsin\left(\frac{\text{radius of A} + \text{radius of B}}{D}\right) \quad (19)$$

If α is smaller than β , the two circles will overlap in the future, and therefore the corresponding plane is considered unsafe. A plane is considered unsafe if the projected

circles have already overlapped or will overlap in the future.

Unsafe-Proximity Query Rules for the Time-Cuboid Model

The projection of a cuboid on each plane is a polygon. There are nine points projected from a cuboid on each plane—eight are the projections of the cuboid vertices and one is projected from the equipped sensor. An algorithm based on a points sweep is developed in this paper to perform the unsafe-proximity query rules. The points sweep repeatedly applies the rules to the points projected from the cuboid vertices one by one until the plane is identified as safe or unsafe. First, the points sweep method analyzes the relative positions of the other projected eight points with respect to the position of the point under study. Using the point under study as the origin, a new and temporary coordinate system is built in which the coordinate axis is parallel to the axis of the local coordinate system. Each point under analysis acts as the origin of its own temporary coordinate system. Based on the calculated and obtained relative positions that are located in different quadrants of the temporary coordinate system, there are six potential cases that the studied point may satisfy. Each point under study meets only one of the six cases. Then a satisfied case for the studied point is determined. Finally, corresponding rules for the determined case are implemented. If a point in a plane is identified or predicted to be inside the other projected polygon, it can be inferred that the two polygons have already overlapped or will overlap soon. In these cases, the query calculation in this plane is stopped, and the plane is considered unsafe. In addition, if one plane is determined as safe, the calculations for the remaining plane(s) are stopped, and the situation is considered safe.

Compared with some other techniques, such as the no-fit polygon method (Burke et al. 2007), the advantage of the developed points sweep method is that not only can the exactly overlapped polygons be detected but the imminent overlap can be identified. Another potential merit of this method is that it speeds up the calculation because the calculation is stopped once a determined condition is met. Analysis of the comparison of calculation speed and other potential techniques is a topic for future study.

There are three potential cases in the situation in which two projected polygons have already overlapped [Figs. 7(a–c)] and three potential cases in the situation in which two projected polygons will overlap [Figs. 8(a–c)]. Figs. 7 and 8, in which each polygon in the X - Y plane is the projection of a cuboid having roll, pitch, and yaw, are explained next.

Situation 1: Two Polygons Have Already Overlapped. If the two projected polygons have already overlapped, at least one point definitely exists for which the projection of a cuboid vertex is within the other polygon. Taking one point as an example, the three following cases can be discussed [Figs. 7(a–c)]:

- If the relative positions of the eight points projected from Entity B's vertices with respect to one point projected from one of Entity A's vertices are found in four quadrants in the temporary coordinate system [Fig. 7(a)], it can be concluded that the two polygons are intersected;
- If the relative positions of the eight points projected from Entity B's vertices with respect to one point projected from one of Entity A's vertices are found in three quadrants [e.g., the first, second, and third quadrants in Fig. 7(b)], and Eq. (20) is

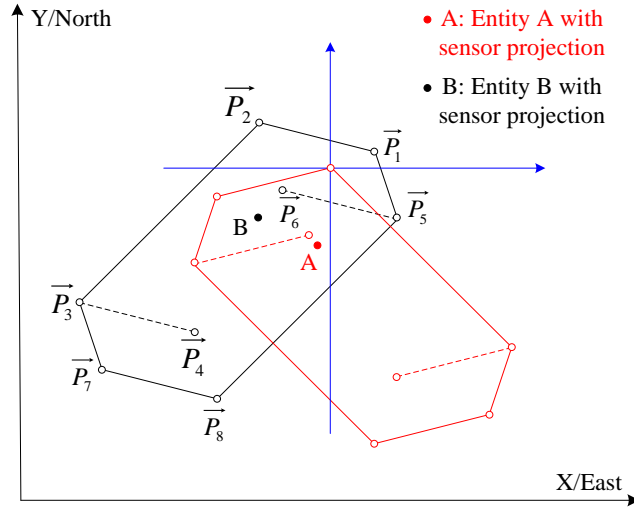
satisfied, it can be concluded that the two polygons are intersected:

$$\sigma \geq \text{Min}(\alpha_i) \quad (20)$$

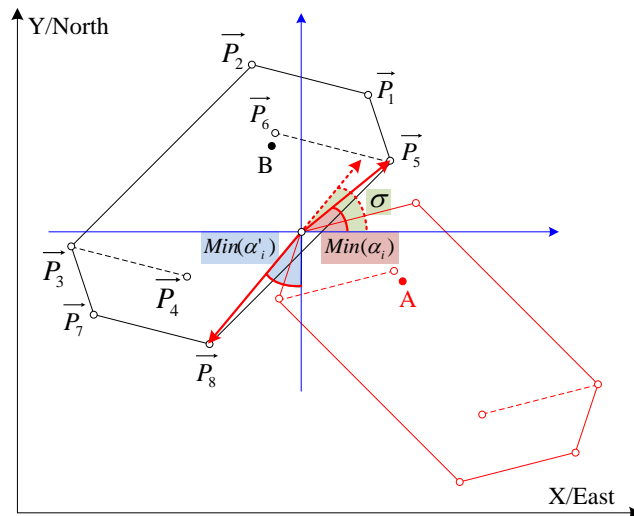
- If the relative positions of the eight points projected from Entity B's vertices with respect to one point projected from one of Entity A's vertices are found in two quadrants [e.g., the first and third quadrants shown in Fig. 7(c)], and Eq. (21) is satisfied, it can be concluded that the two polygons are intersected:

$$\sigma \geq \text{Min}(\alpha_i) \text{ and } \tau \geq \text{Min}(\varphi_i) \quad (21)$$

In Fig. 7, \vec{P}_i ($i = 1, 2, \dots, 8$) is the relative position of each point projected from Entity B's vertices with respect to one point projected from one of Entity A's vertices; α_i is the angle between the vector \vec{P}_i and a unit vector \vec{U}_1 [\vec{U}_1 is (1,0) if \vec{P}_i ($i = 1, 2, \dots, 8$) is within the first, second, and third or the first and third quadrants]; α'_i is the angle between the vector \vec{P}_i and a unit vector \vec{U}_2 [\vec{U}_2 is (0,-1) if \vec{P}_i is within the first, second, and third or the first and third quadrants]; σ is the angle between the corresponding unit vector \vec{U}_1 and the inverse vector of the vector that has the minimum α'_i ; φ_i is the angle between the vector \vec{P}_i and a unit vector \vec{U}_3 [\vec{U}_3 is (-1,0) if \vec{P}_i is within the first and third quadrants]; φ'_i is the angle between the vector \vec{P}_i and a unit vector \vec{U}_4 [\vec{U}_4 is (0,1) if the \vec{P}_i are within the first and third quadrants]; τ is the angle between the corresponding unit vector \vec{U}_3 and the inverse vector of the vector that has the minimum φ'_i .



(a)



(b)

Fig. 7. Cases for already overlapped polygons: (a) four quadrants involved; (b) three quadrants involved; (c) two quadrants involved

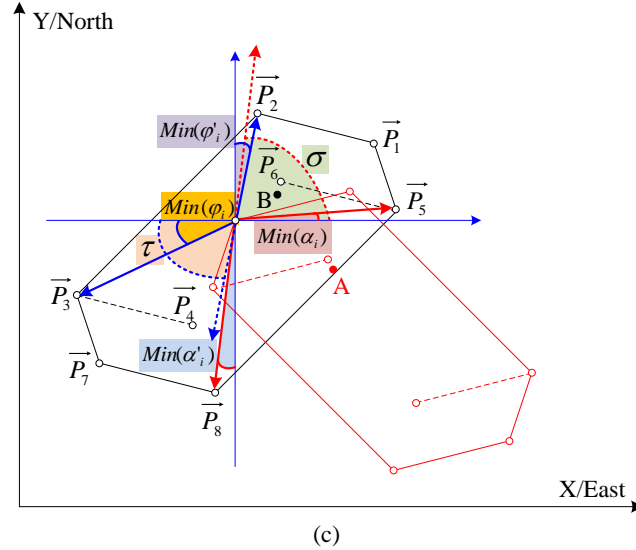


Fig. 7 (Cont'd). Cases for already overlapped polygons: (a) four quadrants involved; (b) three quadrants involved; (c) two quadrants involved

Situation 2: Two Polygons Will Overlap. The situation in which two polygons will overlap also includes three cases. Taking one point as an example, the involved three cases are described as follows [Figs. 8(a–d)]:

- If the relative positions of the eight points projected from Entity B’s vertices with respect to one point projected from one of Entity A’s vertices are found in only one quadrant [taking the second quadrant in Fig. 8(a) as an example], and either one of Eqs. (22) and (23) is met, it can be concluded that the two polygons are to be intersected:

$$\text{The direction of } \vec{V} \text{ is in the second quadrant and } \beta_1 \leq \beta_2 \text{ and } \gamma \leq \gamma_2 \quad (22)$$

$$\text{The direction of } \vec{V} \text{ is in the second quadrant and } \beta_1 > \beta_2 \text{ and } \gamma \leq \gamma_1 \quad (23)$$

All related variables are defined and explained in Fig. 7;

- If the relative positions of the eight points projected from Entity B's vertices with respect to one point projected from one of Entity A's vertices are found in three quadrants [taking the first, second, and third quadrants in Fig. 8(b) as an example], and any one of Eqs. (24)–(26) is met, it can be concluded that the two polygons are to be intersected:

$$\sigma < \text{Min}(\alpha_i), \text{ the direction of } \vec{V} \text{ is in the first quadrant and } \delta \geq \text{Min}(\alpha_i) \quad (24)$$

$$\sigma < \text{Min}(\alpha_i), \text{ the direction of } \vec{V} \text{ is in the third quadrant and } \delta \geq \text{Min}(\alpha'_i) \quad (25)$$

$$\sigma < \text{Min}(\alpha_i) \text{ and the direction of } \vec{V} \text{ is in the second quadrant} \quad (26)$$

- The relative positions of the eight points projected from Entity B's vertices with respect to one point projected from one of Entity A's vertices are found in two quadrants, including the two subcases shown in Figs. 8(c and d); that is,
 - 1) If the two quadrants are consecutive [taking the first and second quadrants shown in Fig. 8(c) as an example] and meet either one of Eqs. (27) and (28), it can be concluded that the two polygons are to be intersected:

$$\text{The direction of } \vec{V} \text{ is in the first or second quadrant and } \beta_1 \leq \beta_2 \text{ and } \gamma \leq \gamma_2 \quad (27)$$

$$\text{The direction of } \vec{V} \text{ is in the first or second quadrant and } \beta_1 > \beta_2 \text{ and } \gamma \leq \gamma_1 \quad (28)$$

- 2) If the two quadrants are nonconsecutive [taking the first and third quadrants in Fig. 8(d) as an example] and meet one of Eqs. (29)–(31), it can be concluded that the two polygons are to be intersected:

$$\begin{aligned} \sigma < \text{Min}(\alpha_i), \tau \geq \text{Min}(\varphi_i), \text{ the direction of } \vec{V} \text{ is in the first quadrant,} \\ \text{and } \delta \geq \text{Min}(\alpha_i) \end{aligned} \quad (29)$$

$$\sigma < \text{Min}(\alpha_i), \tau \geq \text{Min}(\varphi_i), \text{ the direction of } \vec{V} \text{ is in the third quadrant,}$$

$$\text{and } \delta \geq \text{Min}(\alpha'_i) \quad (30)$$

$$\sigma < \text{Min}(\alpha_i), \tau \geq \text{Min}(\varphi_i), \text{ and the direction of } \vec{V} \text{ is in the second quadrant} \quad (31)$$

In Fig. 8, \vec{P}_i , σ , α_i and α'_i ($i = 1, 2, \dots, 8$) have the same definition as in Fig. 7, and the unite vector \vec{U}_1 is (1,0) if \vec{P}_i ($i = 1, 2, \dots, 8$) is within the second or first and second quadrants; \vec{P} is the relative position of the sensor's projection of Entity B with respect to one point projected from one of Entity A's vertices; \vec{V} is the relative velocity of the point projected from Entity A's vertex with respect to the sensor's projection of Entity B; β_1 is the angle between the vector \vec{V} and the unit vector \vec{U}_1 ; β_2 is the angle between the vector \vec{P} and the unit vector \vec{U}_1 ; γ is the angle between the vector \vec{P} and the vector \vec{V} , γ_1 is the angle between the vector \vec{P} and the vector \vec{P}_i which has the maximum α_i , γ_2 is the angle between the vector \vec{P} and the vector \vec{P}_i which has the minimum α_i ; δ is the angle between the vector \vec{V} and the unit vector \vec{U}_1 or \vec{U}_2 . \vec{U}_2 is (0,-1) if \vec{P}_i is within the first, second, and third or first and third quadrants; \vec{U}_1 and \vec{U}_2 are selected depending on the direction of the vector \vec{V} . For example, in Fig. 8(b) and (d), \vec{U}_1 is selected if the direction of \vec{V} is in the first quadrant, and \vec{U}_2 is selected if the direction of \vec{V} is in the third quadrant.

In the examples in Figs. 7 and 8, the points sweep is applied to the projected points from Entity A's vertices. Likewise, the points sweep is repeated and implemented for the projected points from Entity B's vertices. The state information of the analyzed point i ($i = 1, 2, \dots, 8$) projected from Entity A or the analyzed point j ($j = 1, 2, \dots, 8$) projected from Entity B can only meet one of the cases shown in Figs. 7 and 8. Thus, only

one case, not all of the discussed cases, needs to be calculated for the point under study. As soon as one point is found unsafe, the corresponding 2D plane is identified as unsafe and the points sweep calculation for this plane is stopped. A plane can be determined as safe only if the points sweeps for both A and B in this plane are determined to be safe. As soon as one plane is found safe, the points sweep calculation in the remaining plane(s) is stopped and the corresponding situation is identified as safe.

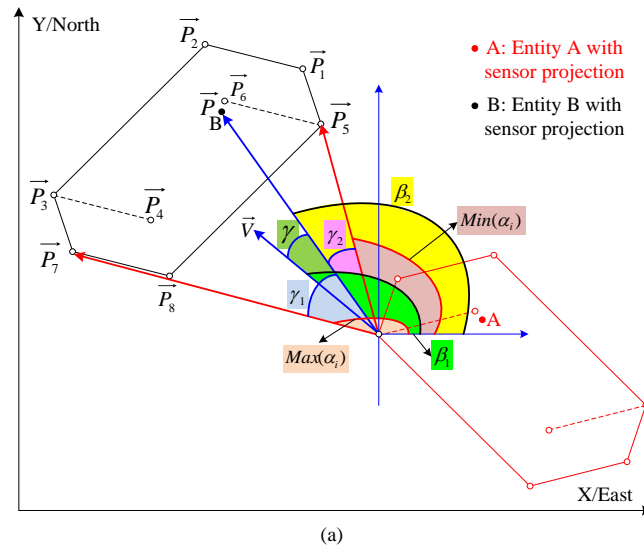
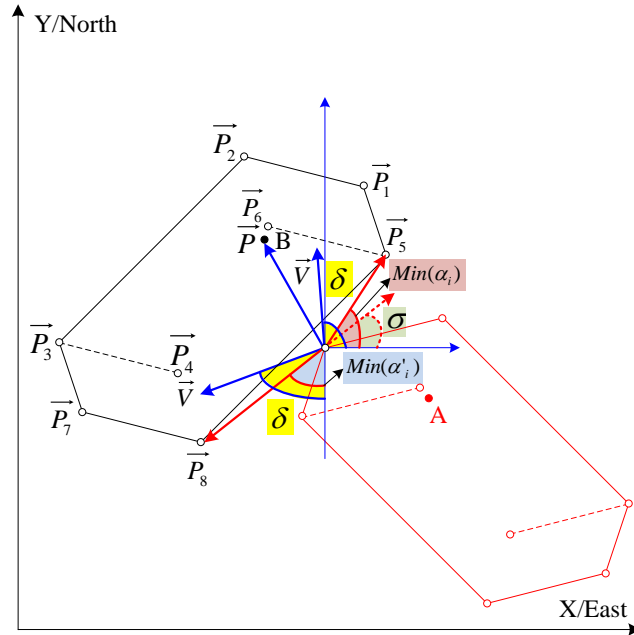
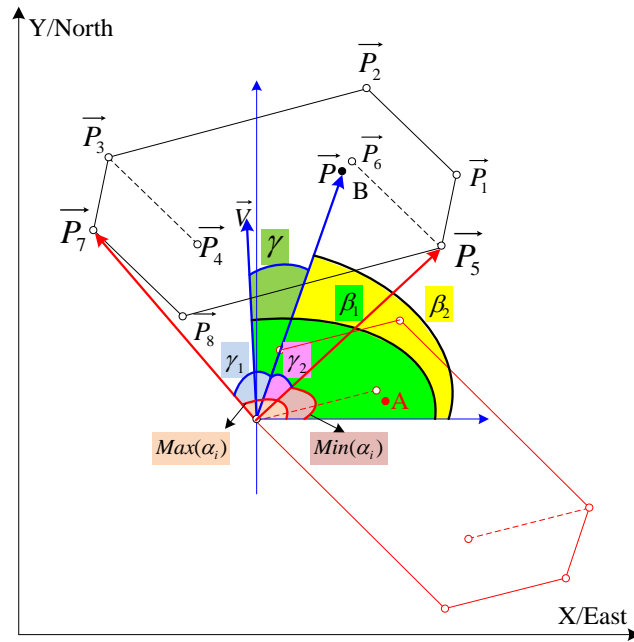


Fig. 8. Unsafe-proximity query rules for polygons that will overlap: (a) one quadrant involved; (b) three quadrants involved; (c) two consecutive quadrants involved; (d) two non-consecutive quadrants involved



(b)



(c)

Fig. 8 (Cont'd). Unsafe-proximity query rules for polygons that will overlap: (a) one quadrant involved; (b) three quadrants involved; (c) two consecutive quadrants involved;

(d) two non-consecutive quadrants involved

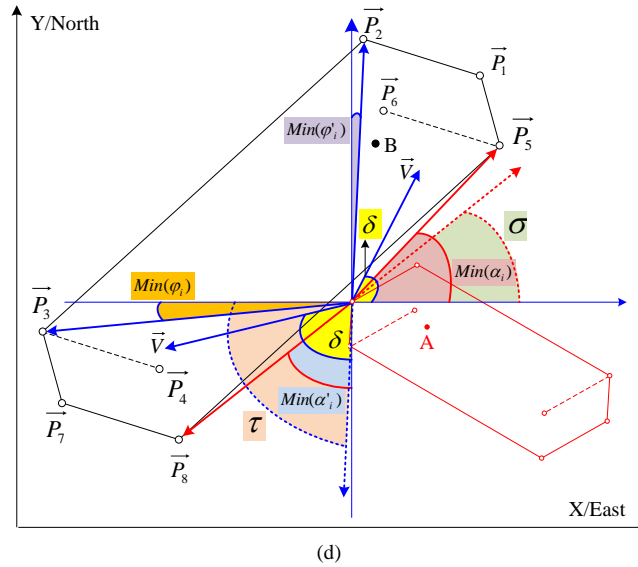


Fig. 8 (Cont'd). Unsafe-proximity query rules for polygons that will overlap: (a) one quadrant involved; (b) three quadrants involved; (c) two consecutive quadrants involved; (d) two non-consecutive quadrants involved

Simulation

Setting

The dimensions of equipment used in the simulation were determined based on a Caterpillar D10 crawler tractor (Caterpillar, Peoria, Illinois) (7.56 m long, 3.64 m wide, and 4.54 m high) and a John Deere 250C articulated dump truck (John Deere, Moline, Illinois) (9.2 m long, 2.8 m wide, and 3.4 m high). As described previously, assigning an appropriate value of Δ to obtain the alert zone for an entity is essential for effective implementation of the developed 4D models. In this paper, to comprehensively evaluate

and compare the models’ effectiveness, Δ was assigned different values in one specific scenario: 1, 1.5, 2, and 3 m. The simulation was run with eight scenarios that included different alert zone sizes, trajectory types, altitudes, movement patterns, and terrains. The eight scenarios are ordered and described in Table 1. Scenarios 3, 4, 5, and 8 are selected as examples and illustrated in Fig. 9, in which the cuboids represent the entity’s updated alert zones over time.

Table 1. Simulated Scenarios

Scenario Number	Involved entities	Trajectory type	Altitude changes for the entity	Altitudes are different between involved entities	Slope	Moving direction	Movement type	Vertical movement	Δ value (m)
1	Crawler tractor	Line	No	No	No	Same	Forward	No	1,1.5,2,3
	Worker on foot	Line	No	No	No	Same	Forward	No	1,1.5,2,3
2	Crawler tractor	Line	No	No	No	Opposite	Forward	No	1,1.5,2,3
	Crawler tractor	Line	No	No	No	Opposite	Backward	No	1,1.5,2,3
3	Dump truck	Line	No	Yes	No	Opposite	Forward	No	1,1.5,2,3
	Dump truck	Line	Yes	Yes	Yes	Opposite	Forward	No	1,1.5,2,3
4	Dump truck	Line	No	Yes	No	—	Forward	No	1,1.5,2,3
	Worker on foot	Line	Yes	Yes	No	—	Downward	Yes	1,1.5,2,3
5	Dump truck	Line	No	Yes	No	—	Forward	No	1,1.5,2,3
	Worker on foot	Line	Yes	Yes	No	—	Static; then up	Yes	1,1.5,2,3
6	Dump truck	Line	No	No	No	Opposite	Forward	No	1
	Dump truck	Seven different lines	No	No	No	Opposite	Forward	No	1
7	Dump truck	Line	No	No	No	—	Forward	No	1
	Dump truck	Two different curves	No	No	No	—	Forward	No	1
8	Worker on foot	Line	No	No	No	—	Random	No	1,1.5,2,3
	Worker on foot	Curve	No	No	No	—	Random	No	1,1.5,2,3
	Dump truck	Curve	No	No	No	—	Random	No	1,1.5,2,3
	Dump truck	Curve	No	No	No	—	Random	No	1,1.5,2,3

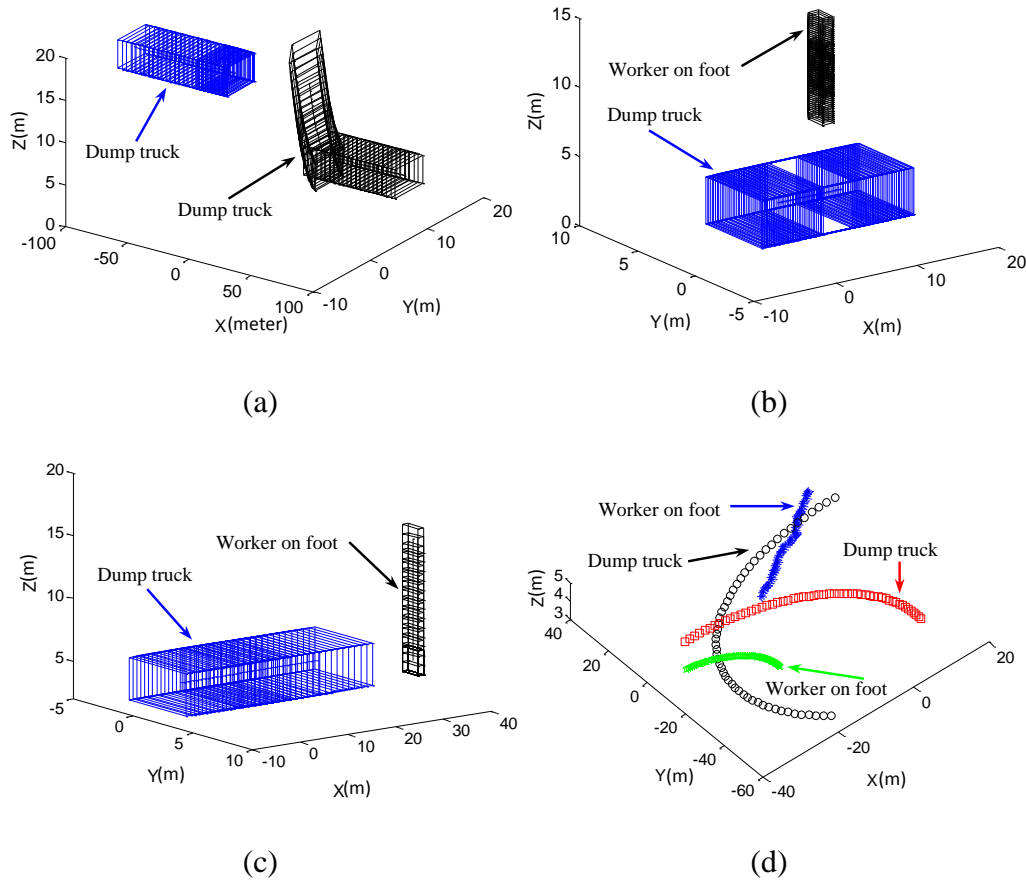


Fig. 9. (a) Scenario 3; (b) Scenario 4; (c) Scenario 5; (d) trajectories in Scenario 8

Results and Analysis

The most prevalent and widely used method that relies solely on distance detection was also implemented in this study as a numerical model and tested in each scenario. Three methods compared were therefore prevalent, time-sphere, and time-cuboid. The major differences between the prevalent method and the developed 4D models is that the latter not only perform distance detection but also (1) take the entity's velocity and orientation into account and (2) use the developed unsafe-proximity query rules. An overconservative warning distance used by the prevalent method produces false

positives, whereas a smaller warning distance than needed may fail to signal actual risks and result in false negatives. Thus, to evaluate the effectiveness of the developed unsafe-proximity query rules in reducing false alarms, the developed warning distance quantification method (i.e., dynamic and adjusted warning distance) was applied to all of the compared methods, including the prevalent method. Three indicators—false positive rate (FPR), false negative rate (FNR), and reduced alarms percentage (RAP)—were used to evaluate and compare model effectiveness. The FPR reflects model effectiveness in reducing false positives. Under the same scenario, the lower the FPR, the more effective the model [Eq. (32)]. The FNR signifies model effectiveness in reducing false negatives. Under the same scenario, the lower the FNR, the more effective the model [Eq. (33)]. Compared with the number of alarms generated by the prevalent method, the developed RAP denotes the overall effectiveness of the two developed 4D models in reducing alarms [Eqs. (34) and (35)].

$$FPR = \frac{\text{false positive}}{\text{false positive} + \text{true negative}} \quad (32)$$

$$FNR = \frac{\text{false negative}}{\text{false negative} + \text{true positive}} \quad (33)$$

$$RAP_{\text{sphere}} = \frac{a_1 - a_{\text{sphere}}}{a_1} \times 100\% \quad (34)$$

$$RAP_{\text{cuboid}} = \frac{a_1 - a_{\text{cuboid}}}{a_1} \times 100\% \quad (35)$$

where a_1 , a_{sphere} , and a_{cuboid} is the number of warning alarms generated by the corresponding method. An alarm (visual, audible, vibrating, or a combination) generated when the distance between entities is greater than the alert distance and smaller than the warning distance is called a warning alarm.

The obtained results are shown in Table 2, in which the last row shows the mean of the obtained FPRs, FNRs, and RAPs. The number of total triggered alarms for each method is the sum of triggered warning alarms and alert alarms. Different from a warning alarm, an alert alarm is triggered when the distance between entities is smaller than their alert distance. The relatively larger number of total alarms generated in Scenarios 6 and 7 results from the higher data collection frequency used.

Table 2. Simulation Results

Basic information		Prevalent method				Time-sphere model				Time-cuboid model									
Scenario	Δ (m)	Total scans	Total triggered alarms	True Negative	True Positive	False Positive	FPR (%)	Total triggered alarms	True Negative	True Positive	False Negative	False Positive	FPR (%)	FNR (%)	RAP (%)	Total triggered alarms	True Negative	True Positive	RAP (%)
1	1	80	16	64	1	15	19	7	73	1	0	6	8	0	60	1	79	1	100
	1.5	80	16	64	2	14	18	8	72	2	0	6	8	0	57	2	78	2	100
	2	80	16	64	8	8	11	8	72	8	0	0	0	0	57	8	72	8	57
2	1	84	7	77	0	7	8	0	84	0	0	0	0	0	100	0	84	0	100
	1.5	84	7	77	0	7	8	0	84	0	0	0	0	0	100	0	84	0	100
	2	84	7	77	0	7	8	0	84	0	0	0	0	0	100	0	84	0	100
3	1	84	9	75	0	9	11	0	84	0	0	0	0	0	100	0	84	0	100
	1.5	34	6	28	0	6	18	0	34	0	0	0	0	0	100	0	34	0	100
	2	34	9	25	0	9	26	4	30	0	0	4	12	0	56	0	34	0	100
4	1	34	12	22	2	10	31	6	28	2	0	4	13	0	60	2	32	2	100
	1.5	40	12	28	0	12	30	0	40	0	0	0	0	0	100	0	40	0	100
	2	40	15	25	0	15	38	0	40	0	0	0	0	0	100	0	40	0	100
5	1	40	19	21	0	19	48	19	21	0	0	19	48	0	0	0	40	0	100
	1.5	40	25	15	0	25	63	25	15	0	0	25	63	0	0	0	40	0	100
	2	30	18	12	0	18	60	0	30	0	0	0	0	0	100	0	30	0	100
6	1	30	19	11	0	19	63	0	30	0	0	0	0	0	100	0	30	0	100
	1.5	30	20	10	0	20	67	0	30	0	0	0	0	0	100	0	30	0	100
	2	30	21	9	0	21	70	10	20	0	0	10	33	0	52	0	30	0	100
7	1	328	305	23	184	121	84	183	144	183	1	0	0	0.5	47	184	144	184	46
	1	328	305	23	40	265	92	181	147	40	0	141	49	0	47	40	288	40	100
	1	328	304	24	36	268	92	178	150	36	0	142	49	0	47	36	292	36	100
8	1	328	304	24	34	270	92	177	151	34	0	143	49	0	47	34	294	34	100
	1	328	304	24	30	274	92	175	153	30	0	145	49	0	47	30	298	30	100
	1	328	304	24	25	279	92	172	156	25	0	147	49	0	47	25	303	25	100
9	1	328	304	24	17	287	92	168	160	17	0	151	49	0	47	17	311	17	100
	1	435	377	58	152	225	80	212	223	152	0	60	21	0	49	152	283	152	67
	1	435	368	67	90	278	81	203	232	90	0	113	33	0	48	90	345	90	80
10	1	54	29	25	7	22	47	9	45	7	0	2	4	0	83	7	47	7	92
	1.5	54	30	24	9	21	47	10	44	9	0	1	2	0	80	9	45	9	84
	2	54	33	21	15	18	46	14	39	14	1	0	0	6.7	76	15	39	15	72
Mean	3	54	37	17	26	11	39	26	28	26	0	0	0	0	50	26	28	26	50
	—	—	—	—	—	—	49	—	—	—	—	—	16	0.2	67	—	—	—	91

Based on the definition of a true alarm (relative truth or baseline) used in this paper, the number of false positives and false negatives generated by the time-cuboid model is zero under all scenarios. The state information corresponding to the generated alarms has been used to verify the correctness of the developed unsafe-proximity query rules as follows:

- The state information corresponding to the alarms (false positives) generated by the time-sphere model, not by the time-cuboid model, shows that for each such alarm the cuboids were not intersected all the time whereas the spheres had intersections;
- The state information corresponding to the alarms (false positives) generated by the prevalent method, not by the time-cuboid model, shows that for each such alarm the cuboids were not intersected all the time whereas the distance was smaller than the associated warning distance;
- The state information corresponding to the alarms generated by the prevalent method, not by the time-sphere model, shows that for each such alarm the spheres were not intersected all the time whereas the distance was smaller than the associated warning distance; and
- The state information corresponding to the alarms (false negatives) generated by the time-cuboid model, not by the time-sphere model, shows that for each such alarm the cuboids were intersected whereas the spheres were not.

More details about the verification process can be found in the work of Wang and Razavi (2016a).

The FPR and FNR of the time-cuboid model are zero for all scenarios. The time-sphere model also has a strong capability to avoid false positives because the average FPR (16%) is much lower than that of the prevalent method (49%). Although the time-sphere model generates false negatives in two scenarios (Table 2), the average FNR is 0.2%, which is very small. An example of a false negative in the X - Y plane is shown in Fig. 10. Generation of false negatives for the prevalent method can be associated with the adopted warning distance, which might be set to a smaller value than needed. Because the dynamic adjusted warning distance was also applied to the prevalent method, the number of false negatives generated by the method is 0 in all scenarios (not shown in Table 2). The obtained RAPs signify that on average 67% of the alarms sent out by the prevalent method can be averted by the time-sphere model and 91% can be avoided by the time-cuboid model.

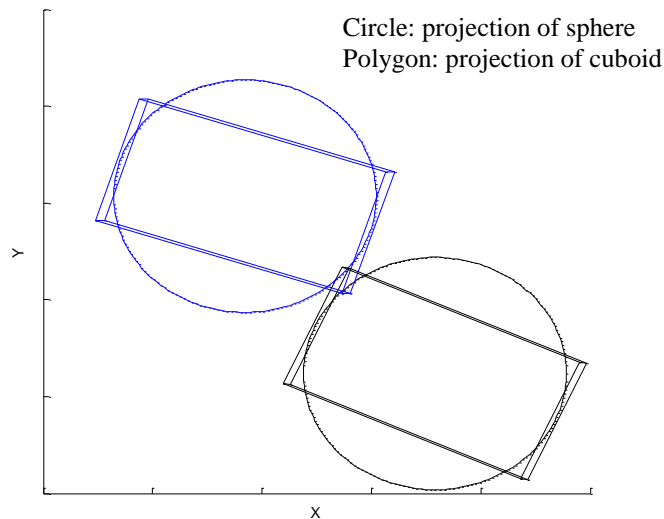


Fig. 10. False negative generated by the time-sphere model

Field Experiments

The effectiveness and feasibility of the developed 4D models were further evaluated via field experiments.

Settings

Three construction yards were provided by an industrial partner to host the field experiments: a material yard with two spoil piles of 60 m (L), 40 m (W), and 10 m (H) and 25 m (L), 20 m (W), and 8 m (H), respectively, which bore heavy truck and loader traffic; and two yards (Yard 1 and Yard 2) adjacent to buildings and roads with busy traffic. Thirteen scenarios were designed and implemented in the experiments, in which only equipment was involved. Three equipment types were adopted: a front-end loader (John Deere, Moline, Illinois) of 8 m (L), 2.6 m (W), and 3.56 m (H); a truck tractor (Mack Trucks, Greensboro, North Carolina) of 8 m (L), 2.6 m (W), and 2.6 m (H); and a lift truck (Caterpillar, Peoria, Illinois) of 3.4 m (L), 2.4 m (W), and 1.4 m (H). The front-end loader was used in two scenarios in the material yard; the truck tractor was used in six scenarios in Yard 1; and the lift truck was used in five scenarios in Yard 2. The experiment scenarios are summarized in Table 3, and the entity movement trajectories are shown in Fig. 11.

A global positioning system–aided inertial navigation system (GPS/INS) (SBG Systems, Rueil-Malmaison, Île-de-France) was affixed to the equipment to collect the required state information: 3D position, orientation, and velocity. Different from widely used RF and Bluetooth sensing technologies, the GPS/INS used includes a microelectromechanical system (MEMS) inertial measurement unit (IMU), a GPS receiver, and a

pressure sensor. Also, it is equipped with an advanced calibration procedure associated with an onboard extended Kalman filter (EKF) to overcome the drift problem even in high dynamic conditions. It thus provides high robustness in data collection but has a small size [36 mm (L), 49 mm (W), and 25 mm (H)], it is lightweight (44 g), and it has low power consumption. For these reasons, it has been widely used in multiple applications, such as unmanned aerial vehicle (UAV) navigation and car motion analysis.

Table 3. Experiment Scenarios

Scenario Number	Involved entities	Trajectory type	Moving direction	Movement type
1	1.1 Loader	Line	Same	Backward
	1.2 Loader	Line	Same	Forward; then static
2	2.1 Loader	—	Random	Forward
	2.2 Loader	—	Random	Backward; then static
3	3.1 Truck tractor	Line	Opposite	Forward
	3.2 Truck tractor	Line	Opposite	Forward; then static
4	4.1 Truck tractor	Line	Same	Forward; then static
	4.2 Truck tractor	Curve	Same	Forward
5	5.1 Truck tractor	Curve	Opposite	Forward
	5.2 Truck tractor	Line	Opposite	Forward; then static
6	6.1 Truck tractor	Line	Opposite	Forward; then static
	6.2 Truck tractor	Line	Opposite	Forward
7	7.1 Truck tractor	Line	Opposite	Forward
	7.2 Truck tractor	Line	Opposite	Forward
8	8.1 Truck tractor	Line and curve	Random	Forward; then backward
	8.2 Truck tractor	Line and curve	Random	Forward
9	9.1 Lift truck	Line and curve	Opposite	Backward
	9.2 Lift truck	Line and curve	Opposite	Backward
10	10.1 Lift truck	Line and curve	Random	Forward
	10.2 Lift truck	Line	Random	Forward; then static
11	11.1 Lift truck	Line and curve	Random	Forward
	11.2 Lift truck	Line and curve	Random	Forward; then static
12	12.1 Lift truck	Line	Opposite	Forward
	12.2 Lift truck	Line	Opposite	Forward; then static
13	13.1 Lift truck	Line and curve	Random	Backward; then forward
	13.2 Lift truck	Curve	Random	Forward, then static

Note: Numbers in the “Involved entities” column represent entities’ trajectories in Fig. 11.

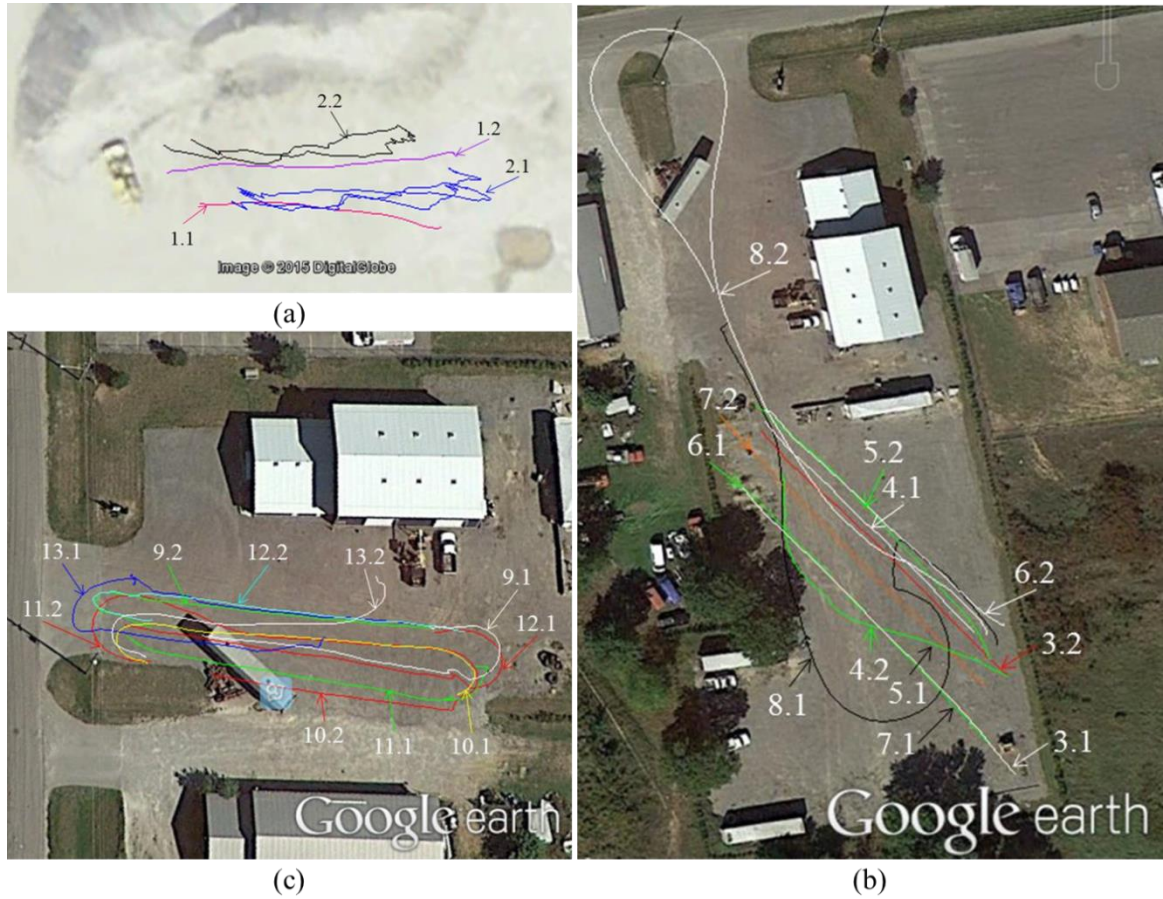


Fig. 11. Entities' movement trajectories (image ©2015 DigitalGlobe Google Earth): (a) front-end loader; (b) truck tractor; (c) lift truck

The developed 4D models can be effectively applied to any scenario regardless of the sensor's installation position. In this study, the GPS/INS was fixed in the front-end loader's cabin, the truck tractor's cabin, and on the platform beside the lift truck's seat, none of which were at any central line of the associated 3D shape [i.e., the case shown in Fig. 4(a)]. The GPS/INS was connected to a data logger to save data, and thereafter the acquired data were transferred to a desktop for post-analysis. In some scenarios, the equipment was controlled to move along trajectories that were marked by strings on the

ground. The distance between the parallel line trajectories in the corresponding scenario was known, which helped in evaluating sensor accuracy in location sensing. No vertical movement was involved in the field experiments.

Results and Analysis

The 3D positions (latitude, longitude, and altitude) were collected from the World Geodetic System 1984 (WGS 84) and converted into the developed local coordinate system (X - Y - Z). The obtained positions were uploaded to Google Earth as shown in Fig. 11. The results on position accuracy are summarized in Table 4, which indicates that the average error in the collected positions is 0.6677 m. As in the simulation described earlier, the prevalent numerical model, the time-sphere model, and the time-cuboid model were applied to the data collected in each scenario, respectively. The collected velocity aligned with the y -axis is the v used in Eqs. (2)–(10) with no conversions. The geometry of the sensor's installation position on each piece of equipment was taken into consideration when applying the 4D models. The alert zone of each entity was calculated using Eqs. (11)–(13), and Δ values of 1, 1.5, 2, and 3 m were tested in each scenario.

The developed warning-distance quantification method (i.e., dynamic and adjusted warning distance) was applied to all compared methods, including the prevalent method. The obtained results are summarized in Table 5, where the last row shows the mean of the obtained FPRs, FNRs, and RAPs. The number of total triggered alarms for each method is the sum of the triggered warning alarms and the alert alarms. In each scenario, the FPR of the prevalent method is higher than the FPRs of the time-sphere and time-cuboid models, which indicates that the two 4D models have a strong capability to

reduce false positives. The average FNR of the time-sphere model is 1.5%, which is very small. As explained earlier, because the dynamic adjusted warning distance was also applied to the prevalent method, the number of false negatives generated by the prevalent method is 0 in all scenarios (not shown in Table 5). On average 63% of the alarms sent out by the current prevalent method can be avoided by the time-sphere model and 71% can be avoided by the time-cuboid model.

In addition, the device used to apply the two 4D models for simulation and experiments was a desktop with an Intel Core i5-2400 CPU (Intel, Santa Clara, California), a 64-bit operating system, and 8 GB of memory. For the field experiments, the average calculation time consumed by the time-sphere model and the time-cuboid model was (5.6×10^{-5}) and (4.0×10^{-4}) s per scan, respectively. The time-cuboid model was more effective but needed relatively more computation time to run. With the obtained results in Tables 2 and 5, other indicators such as true negative rate (specificity) can be calculated for further analysis.

Table 4. Position Accuracy Analysis (m)

Involved trajectories	Distance between marked lines	Average measured distance	Error	Mean error
1.1 versus 1.2	6	5.57	0.43	0.67
3.1 versus 7.2	5	5.8411	-0.8411	
4.1 versus 6.2	3	2.1044	0.8956	
3.2 versus 4.1	1.5	1.5492	-0.0492	
3.1 versus 4.1	10	11.15	-1.15	
6.1 versus 6.2	13	13.2544	-0.2544	
6.1 versus 3.2	8	9.6056	-1.6056	
7.2 versus 3.2	3	3.7645	-0.7645	
9.1 versus 9.2	5	4.4677	0.5323	
10.2 versus 9.1	10	10.2721	-0.2721	
12.1 versus 12.2	5	5.55	-0.55	

Note: Numbers in “Involved trajectories” column correspond to the trajectories shown in Fig. 11.

Table 5. Experimental Results

Basic information		Prevalent method						Time-sphere model						Time-cuboid model					
Scenario	Δ (m)	Total scans	Total triggered alarms	True Negative	True Positive	False Positive	FPR (%)	Total triggered alarms	True Negative	True Positive	False Negative	False Positive	FPR (%)	FNR (%)	RAP (%)	Total triggered alarms	True Negative	True Positive	RAP (%)
1	1	64	30	34	23	7	17	25	39	23	0	2	5	0	71	23	41	23	100
	1.5	64	32	32	29	3	9	27	35	27	2	0	0	6.9	71	29	35	29	43
	2	64	36	28	32	4	13	31	32	31	1	0	0	3.1	71	32	32	32	57
2	3	64	42	22	38	4	15	37	26	37	1	0	0	2.6	71	38	26	38	57
	1	190	183	7	66	117	94	73	117	66	0	7	6	0	60	66	124	66	64
	1.5	190	186	4	70	116	97	85	105	70	0	15	13	0	54	70	120	70	62
3	2	190	188	2	79	109	98	89	101	79	0	10	9	0	54	79	111	79	59
	3	190	189	1	94	95	99	95	95	94	0	1	1	0	59	94	96	94	60
	1	68	17	51	1	16	24	9	59	1	0	8	12	0	47	1	67	1	94
4	1.5	68	17	51	6	11	18	10	58	6	0	4	6	0	50	6	62	6	79
	2	68	17	51	9	8	14	11	57	9	0	2	3	0	50	9	59	9	67
	3	68	19	49	13	6	11	13	55	13	0	0	0	0	50	13	55	13	50
5	1	58	10	48	5	5	9	5	53	5	0	0	0	0	56	5	53	5	56
	1.5	58	10	48	6	4	8	6	52	6	0	0	0	0	50	6	52	6	50
	2	58	14	44	8	6	12	7	50	7	1	0	0	12.5	64	8	50	8	55
6	3	58	25	33	9	16	33	9	49	9	0	0	0	0	80	9	49	9	80
	1	57	12	45	0	12	21	0	57	0	0	0	0	0	100	0	57	0	100
	1.5	57	13	44	0	13	23	0	57	0	0	0	0	0	100	0	57	0	100
7	2	57	15	42	0	15	26	0	57	0	0	0	0	0	100	0	57	0	100
	3	57	17	40	0	17	30	0	57	0	0	0	0	0	100	0	57	0	100
	1	55	12	43	0	12	22	3	52	0	0	3	5	0	75	0	55	0	100
8	1.5	55	13	42	0	13	24	4	51	0	0	4	7	0	69	0	55	0	100
	2	55	13	42	1	12	22	5	50	1	0	4	7	0	62	1	54	1	92
	3	55	14	41	4	10	20	7	48	4	0	3	6	0	50	4	51	4	71
9	1	66	15	51	9	6	11	10	56	9	0	1	2	0	50	9	57	9	60
	1.5	66	15	51	10	5	9	10	56	10	0	0	0	0	50	10	56	10	50
	2	66	16	50	11	5	9	11	55	11	0	0	0	0	50	11	55	11	50
10	3	66	17	49	13	4	8	12	53	12	1	0	0	7.7	50	13	53	13	40
	1	193	15	178	9	6	3	11	182	9	0	2	1	0	50	9	184	9	75
	1.5	193	15	178	9	6	3	11	182	9	0	2	1	0	50	9	184	9	75
11	2	193	17	176	11	6	3	12	181	11	0	1	1	0	56	11	182	11	67
	3	193	17	176	13	4	2	13	180	13	0	0	0	0	57	13	180	13	57
	1	101	14	87	4	10	10	5	96	4	0	1	1	0	90	4	97	4	100
12	1.5	101	14	87	6	8	8	9	92	6	0	3	3	0	63	6	95	6	100
	2	101	16	85	9	7	8	12	89	9	0	3	3	0	50	9	92	9	88
	3	101	19	82	15	4	5	15	86	15	0	0	0	0	44	15	86	15	44
13	1	57	12	45	1	11	20	3	54	1	0	2	4	0	75	1	56	1	92
	1.5	57	13	44	2	11	20	5	52	2	0	3	5	0	62	2	55	2	85
	2	57	13	44	6	7	14	7	50	6	0	1	2	0	55	6	51	6	64
14	3	57	14	43	9	5	10	9	48	9	0	0	0	0	50	9	48	9	50
	1	70	10	60	0	10	14	0	70	0	0	0	0	0	100	0	70	0	100
	1.5	70	11	59	0	11	16	0	70	0	0	0	0	0	100	0	70	0	100
15	2	70	12	58	6	6	9	4	64	4	2	0	0	33.3	80	6	64	6	60
	3	70	13	57	10	3	5	10	60	10	0	0	0	0	33	10	60	10	33
	1	81	11	70	0	11	14	3	78	0	0	3	4	0	73	0	81	0	100
16	1.5	81	11	70	2	9	11	5	76	2	0	3	4	0	67	2	79	2	100
	2	81	11	70	6	5	7	6	75	6	0	0	0	0	63	6	75	6	63
	3	81	14	67	9	5	7	8	72	8	1	0	0	11.1	67	9	72	9	56
17	1	189	24	165	10	14	8	11	178	10	0	1	1	0	57	10	179	10	61
	1.5	189	27	162	18	9	5	18	171	18	0	0	0	0	38	18	171	18	38
	2	189	33	156	25	8	5	25	164	25	0	0	0	0	36	25	164	25	36
18	3	189	45	144	39	6	4	38	150	38	1	0	0	2.6	39	39	150	39	33
	—	—	—	—	—	—	—	19	—	—	—	—	—	—	—	—	—	—	—
	—	—	—	—	—	—	—	—	—	—	—	—	—	—	—	—	—	—	—

Results Comparison and Discussion

Sphere difference, cuboid difference, reduced alarms percentage difference, and ratio (W/L) are metrics developed and used in the results comparison; they are calculated in Eqs. (36)–(41):

$$\text{Sphere difference} = \text{sum of cuboid length} - \text{distance between trajectories} \quad (36)$$

$$\text{Cuboid difference} = \text{sum of cuboid width} - \text{distance between trajectories} \quad (37)$$

$$\text{Reduced alarm percentage difference} = \text{RAP}_{\text{cuboid}} - \text{RAP}_{\text{sphere}} \quad (38)$$

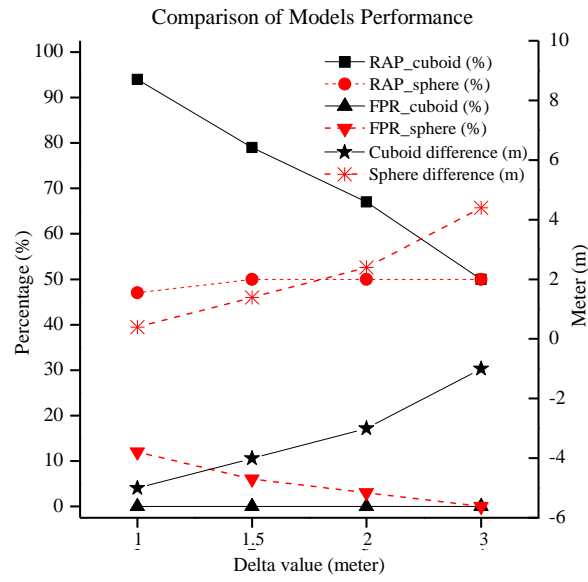
$$\text{Ratio (W/L)} = (\text{sum of cuboid width})/(\text{sum of cuboid length}) \quad (39)$$

$$\begin{aligned} \text{Sum of cuboid length} &= 0.5 \times \text{the longest cuboid side of Entity A} \\ &\quad + 0.5 \times \text{the longest cuboid side of Entity B} \\ &= \text{sphere radius of Entity A} + \text{sphere radius of Entity B} \end{aligned} \quad (40)$$

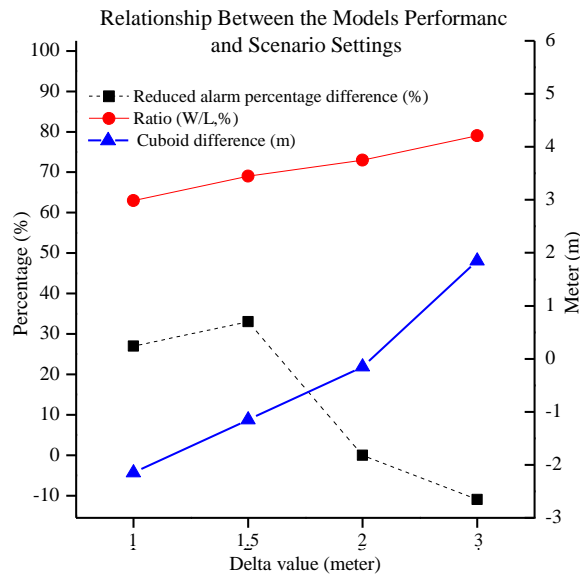
$$\begin{aligned} \text{Sum of cuboid width} &= 0.5 \times \text{cuboid width of entity A} \\ &\quad + 0.5 \times \text{cuboid width of entity B} \end{aligned} \quad (41)$$

where the distance between trajectories is the distance between two parallel-line trajectories. For the field experiments, the distance between trajectories was the average measured distance between lines as given in Table 4.

From the results obtained from the simulation and the field experiments, three major groups of findings can be summarized: model comparison, model analysis, and alert zone dimension. Example results are shown in Fig. 12 to reveal the relationships between the metrics.



(a)



(b)

Fig. 12. Experimental results: (a) Scenario 3; (b) Scenario 12

Model Comparison

Findings from the model comparison are as follows:

- In general, the time-cuboid model performs more effectively than the time-sphere model in reducing false alarms (indicated by FPR) and alarms (indicated by RAP) [Fig. 12(a)]; and
- In the case where the cuboid difference is greater than zero, which means that the entities are close to each other, if the cuboid difference shows an uptrend, the reduced alarm percentage difference shows a downtrend or remains unchanged (i.e., the performance of the time-sphere and time-cuboid models is close) [Fig. 12(b)].

Model Analysis

Findings from the model analysis are as follows:

- In general, if the sphere difference or the cuboid difference shows an uptrend, the corresponding RAP shows a downtrend [Fig. 12(a)]; and
- In the case where the sphere difference or the cuboid difference is smaller than zero, the smaller the difference, the larger and much closer to 1 the corresponding RAP [Fig. 12(a)].

The findings indicate that the developed 4D models greatly assist in reducing alarms, especially when entities are not close to each other.

Alert Zone Dimension

Findings for the alert zone dimension are as follows:

- When the ratio (W/L) is greater than 0.5, if it shows an uptrend, the percentage

difference shows a downtrend or remains unchanged in a majority of scenarios [Fig. 12(b)]; only a few scenarios with false negatives contradict this finding; and

- For all of the simulated and experiment scenarios in which false negatives were generated, only one simulated scenario had the ratio (W/L) smaller than 0.5, all of others had the ratio (W/L) larger than 0.5 [Fig. 12(b)].

The findings indicate that the effectiveness of the two developed 4D models in reducing alarms is similar, particularly when the ratio (W/L) is larger than 0.5. The ratio is essentially determined by the entity's dimension and type.

Limitations and Future Work

In fact, efficient implementations of the developed 4D models in the real world highly rely on near real-time data communication. Based on the field experiments, the computation time consumed by the developed 4D models was extremely trivial. Thus, one substantial challenge in employing the models is to develop near real-time and robust data communication between the utilized devices and the server.

In this study, the intersection of the cuboids was used as the relative truth or baseline for the hazard detection model comparison. Development of more specific definitions regarding the baseline for unsafe situations caused by struck-by hazards is still needed. The alert zone (cuboid or sphere) used in the 4D models is a constant variable once its shape and size are determined. However, dynamic generation of entities' alert zones is needed based on entity types (e.g., excavator), state information, and performed activities and tasks to further improve safety, productivity, and mobility (Dagan and Isaac 2015; Vahdatikhaki and Hammad 2015).

In this paper, the adopted countermeasure on receiving an alarm is braking for equipment and stopping movement for workers on foot. Other responses based on path planning and optimization will be considered and integrated into the 4D models to provide a more comprehensive approach for contact hazard prevention.

The desired situation is that a sensor can be affixed to an entity in a perfect manner. However, particularly for workers on foot on sites, there might be a deviation between the sensor's coordinate system and the associated entity's coordinate system. A small deviation could be neglected and would have no effect on final results. Moreover, small roll and pitch could be disregarded to further speed up the computation without affecting the final results. Quantitative analysis of the negligible range of orientation is another area that needs to be studied in the future.

Conclusions

The high frequency of false alarms has been identified as a main limitation of prevalent methods for preventing struck-by hazards. Three major reasons for the generation of high false alarms are found in the scholarly literature and in practical applications. Aiming to resolve them and reduce false alarms, time-sphere and time-cuboid models were developed. The effectiveness of the two 4D models was evaluated and compared through simulation and field experiments. The obtained false positive and false negative rates indicate that the models have a strong capability to reduce false alarms. In addition, on average 65% of the alarms triggered by the current prevalent method can be averted by the time-sphere model and 81% can be averted by the time-cuboid model. Even though several calculation steps are built into in the 4D models, the

findings can be easily used in practice.

Entities' state information along with time and characteristics are comprehensively monitored and collected. Consequently, over-speed movement and potential rollover accidents can be detected. Detailed post-accident analysis can also be conducted based on records. The developed rigorous 4D models have more applications and can be extended to several types of contact collisions involving temporal and permanent site facilities, materials transported in air, and equipment and workers on foot.

References

- Ahn, C., Lee, S., and Peña-Mora, F. (2015). "Application of low-cost accelerometers for measuring the operational efficiency of a construction equipment fleet." *J. Comput. Civ. Eng.*, 10.1061/(ASCE)CP.1943-5487.0000337, 04014042.
- Awolusi, I. G., Marks, E. D., Pradhananga, N., and Cheng, T. (2015). "Hazardous proximity zone design for heavy construction equipment." *Proc., 5th Inter/11th Construction Specialty Conf.*, Vol. 332, Univ. of British Columbia, Vancouver, BC, Canada, 1–10.
- Bar-Shalom, Y., Li, X. R., and Kirubarajan, T. (2001). *Estimation with applications to tracking and navigation: Theory algorithms and software*, 1st Ed., Wiley, Hoboken, NJ.
- BLS (Bureau of Labor Statistics). (2015). "Census of fatal occupational injuries (CFOI)—Current and revised data." <http://www.bls.gov/iif/oshcfoi1.htm> (Jun. 17, 2015).
- Burke, E., Hellier, R., Kendall, G., and Whitwell, G. (2007). "Complete and robust no-fit

- polygon generation for the irregular stock cutting problem.” *Eur. J. Oper. Res.*, 179(1), 27–49.
- Chae, S., and Yoshida, T. (2010). “Application of RFID technology to prevention of collision accident with heavy equipment.” *Autom. Constr.*, 19(3), 368–374.
- Chang, J., Wang, W., and Kim, M. (2010). “Efficient collision detection using a dual OBB-sphere bounding volume hierarchy.” *Comput.-Aided Des.*, 42(1), 50–57.
- Chavada, R., Dawood, N., and Kassem, M. (2012). “Construction workspace management: The development and application of a novel nD planning approach and tool.” *J. Inf. Technol. Constr. (ITcon)*, 17, 213–236.
- Chen, H., and Huang, T. (1987). “Maximal matching of 3-D points for multiple-object motion estimation.” *Pattern Recognit.*, 21(2), 75–90.
- Cheng, T., and Teizer, J. (2013). “Real-time resource location data collection and visualization technology for construction safety and activity monitoring applications.” *Automation in Construction*, 34, 3–15.
- Choe, S., Leite, F., Seedah, D., and Caldas, C. (2013). “Application of sensing technology in the prevention of backing accidents in construction work zones.” *Proc., Comput. Civ. Eng.*, ASCE, Reston, VA, 557–564.
- Choe, S., Leite, F., Seedah, D., and Caldas, C. (2014). “Evaluation of sensing technology for the prevention of backover accidents in construction work zones.” *Journal of Information Technology in Construction*, 19, 1–19.
- Cohen, J., Lin, M., Manocha, D., and Ponamgi, M. (1995). “I-COLLIDE: An interactive and exact collision detection system for large-scaled environments.” *Proc., 1995*

- Symp. on Interactive 3D Graphics*, Association for Computing Machinery (ACM), New York, 189–196.
- Dagan, D., and Isaac, S. (2015). “Planning safe distances between workers on construction sites.” *Autom. Constr.*, 50, 64–71.
- Du, S., Guo, Y., and Zhang, X. (2014). “Attitude estimation of crane hook based on adaptive complementary filter with outlier rejection.” *Intelligent control and information processing*, IEEE, New York, 498–504.
- Endsley, M. R. (1995). “Toward a theory of situation awareness in dynamic systems.” *Hum. Factors*, 37(1), 32–64.
- Esmaeili, B., Hallowell, M., and Rajagopalan, B. (2015b). “Attribute-based safety risk assessment. I: Analysis at the fundamental level.” *J. Constr. Eng. Manage.*, 10.1061/(ASCE)CO.1943-7862.0000980, 04015021.
- Gürçanlı, G. E., Baradan, S., and Uzun, M. (2015). “Risk perception of construction equipment operators on construction sites of Turkey.” *Int. J. Ind. Ergon.*, 46, 59–68.
- Han, S., Hasan, S., Bouferguène, A., Al-Hussein, M., and Kosa, J. (2014). “Utilization of 3D visualization of mobile crane operations for modular construction on-site assembly.” *J. Manage. Eng.*, 10.1061/(ASCE)ME.1943-5479.0000317, 04014080.
- HEXAGON Mining Safemine. (2015). “Advanced traffic safety solutions for surface mining.” <http://www.safe-mine.com/index.php/products> (May 7, 2015).
- HHS (U.S. Department of Health and Human Services). (2004). “Mean body weight, height, and body mass index.” <http://www.cdc.gov/nchs/data/ad/ad347.pdf> (Jun.

12, 2015).

Hwang, S. (2012). “Ultra-wide band technology experiments for real-time prevention of tower crane collisions.” *Autom. Constr.*, 22, 545–553.

IHSA (Infrastructure Health and Safety Association). (2013). “Can new technologies prevent struck-by injuries?” *IHSA Mag.*, 3(13), 20–21.

Jimenez, P., Thomas, F., and Torras, C. (2001). “3D collision detection: A survey.” *Comput. Graphics*, 25(2), 269–285.

Kim, C., Haas, C., Liapi, K., and Caldas, C. (2006). “Human-assisted obstacle avoidance system using 3D workspace modeling for construction equipment operation.” *J. Comput. Civ. Eng.*, 10.1061/(ASCE)0887-3801(2006)20:3(177), 177–186.

Li, J., Carr, J., and Jobes, C. (2012). “A shell-based magnetic field model for magnetic proximity detection systems.” *Safety Science*, 50(3), 463–471.

Liu, T., and Wang, M. Y. (2005). “Computation of three-dimensional rigidbody dynamics with multiple unilateral contacts using time-stepping and Gauss-Seidel methods.” *IEEE Trans. Autom. Sci. Eng.*, 2(1), 19–31.

Marks, E., and Teizer, J. (2013a). “Evaluation of the position and orientation of (semi-) passive RFID tags for the potential application in ground worker proximity detection and alert devices in safer construction equipment operation.” *Proc., Comput. Civ. Eng.*, ASCE, Reston, VA, 645–652.

Marks, E., and Teizer, J. (2013b). “Method for testing proximity detection and alert technology for safe construction equipment operation.” *Constr. Manage. Econ.*, 31(6), 636–646.

- McFarland, C. J., Harris, Z. J., and Whitcomb, L. L. (2014). “Development of and preliminary results with an extended Kalman filter for the estimation of the translational and angular velocity of underwater vehicles.” *Proc., Oceans–St. John’s*, IEEE, Piscataway, NJ, 1–8.
- Moon, H., Kamat, V. R., and Kang, L. (2014a). “Grid cell-based algorithm for workspace overlapping analysis considering multiple allocations of construction resources.” *J. Asian Archit. Build. Eng.*, 13(2), 341–348.
- Moon, H., Kim, H., Kim, C., and Kang, L. (2014b). “Development of a schedule-workspace interference management system simultaneously considering the overlap level of parallel schedules and workspaces.” *Autom. Constr.*, 39, 93–105.
- Moon, H., Nawood, N., and Kang, L. (2014c). “Development of workspace conflict visualization system using 4D object of work schedule.” *Adv. Eng. Inf.*, 28(1), 50–65.
- Park, J., Marks, E., Cho, Y., and Suryanto, W. (2015). “Performance test of wireless technologies for personnel and equipment proximity sensing in work zones.” *Journal of Construction Engineering and Management*, 10.1061/(ASCE)CO.1943-7862.0001031, 04015049.
- Pradhananga, N., and Teizer, J. (2012). “Spatio-temporal safety analysis of construction site operations using GPS data.” *Construction Research Congress*, ASCE, Reston, VA, 787–796.
- Proconstruction Guide. (2015). “Working safely near construction equipment.” <http://www.proconstructionguide.com/working-near-construction-equipment/>

(Jun. 22, 2015).

- Ray, S. J., and Teizer, J. (2013). “Computing 3D blind spots of construction equipment: Implementation and evaluation of an automated measurement and visualization method utilizing range point cloud data.” *Autom. Constr.*, 36, 95–107.
- Roofigari Esfahan, N., Wang, J., and Razavi, S. (2015). “An integrated framework to prevent unsafe proximity hazards in construction by optimizing spatio-temporal constraints.” *Proc., 5th Int./11th Construction Specialty Conf.*, Univ. of British Columbia, Vancouver, BC, Canada, 1–10.
- Ruff, T. M. (2007). *Recommendations for evaluating and implementing proximity warning systems on surface mining equipment*, Centers for Disease Control and Prevention (CDC), Atlanta, GA.
- Ruff, T. M. (2010). “Overview of proximity warning and technologies and approaches.” *National Institute for Occupational Safety and Health (NIOSH) Workshop on Proximity Warning Systems for Mining Equipment*, Centers for Disease Control and Prevention (CDC), Atlanta, GA.
- Talmaki, S., and Kamat, V. (2014). “Real-time hybrid virtuality for prevention of excavation related utility strikes.” *J. Comput. Civ. Eng.*, 10.1061/(ASCE)CP.1943-5487.0000269, 04014001.
- Talmaki, S., Kamat, V., and Saidi, K. (2015). “Feasibility of real-time graphical simulation for active monitoring of visibility-constrained construction processes.” *Eng. Comput.*, 31(1), 29–49.
- Taneja, S., et al. (2011). “Sensing and field data capture for construction and facility

- operations.” *J. Constr. Eng. Manage.*, 10.1061/(ASCE)CO.1943-7862.0000332, 870–881.
- Tantisevi, K., and Akinci, B. (2007). “Automated generation of workspace requirements of mobile crane operations to support conflict detection.” *Autom. Constr.*, 16(3), 262–276.
- Teizer, J., Allread, B. S., Fullerton, C. E., and Hinze, J. (2010). “Autonomous proactive real-time construction worker and equipment operator proximity safety alert system.” *Autom. Constr.*, 19(5), 630–640.
- Teizer, J., Caldas, C., and Haas, C. (2007). “Real-time three-dimensional occupancy grid modeling for the detection and tracking of construction resources.” *J. Constr. Eng. Manage.*, 10.1061/(ASCE)0733-9364(2007)133:11(880), 880–888.
- Vahdatikhaki, F., and Hammad, A. (2015). “Dynamic equipment workspace generation for improving earthwork safety using real-time location system.” *Adv. Eng. Inf.*, 29(3), 459–471.
- Vahdatikhaki, F., Hammad, A., and Langari, S. M. (2015). “Multi-agent system for improved safety and productivity of earthwork equipment using real-time location systems.” *Proc., 5th Int./11th Construction Specialty Conf.*, Univ. of British Columbia, Vancouver, BC, Canada, 1–10.
- Wang, J., and Razavi, S. (2016a). “Low false alarm rate model for unsafe-proximity detection in construction.” *J. Comput. Civ. Eng.*, 10.1061/(ASCE)CP.1943-5487.0000470, 04015005.
- Wang, J., Zhang, S., and Teizer, J. (2015). “Geotechnical and safety protective equipment

planning using range point cloud data and rule checking in building information modeling.” *Autom. Constr.*, 49, 250–261.

Wu, W., Yang, H., Chew, D, Yang, S., Gibb, A., and Li, Q. (2010). “Towards an autonomous real-time tracking system of near-miss accidents on construction sites.” *Autom. Constr.*, 19(2), 134–141.

Zhang, C., and Hammad, A. (2012). “Multiagent approach for real-time collision avoidance and path replanning for cranes.” *J. Comput. Civ. Eng.*, 10.1061/(ASCE)CP.1943-5487.0000181, 782–794.

CHAPTER 4: RISK AWARENESS

Introduction

The three unsafe-proximity detection models developed in the hazard detection module (Chapters 2 and 3) have been demonstrated effective to improve situational awareness to timely identify hazards on construction sites. However, the risk levels of entities and construction sites pertaining to struck-by-equipment hazard over time are unknown. There has been a need for a method to analyze the dynamic struck-by-equipment risk at both entity and network levels. Through analyzing risk levels over time, safety performance can be evaluated and compared, entities and sites with high levels of risk can be identified, and also insights can be gained into site layout and activity planning. Therefore, the other module of the SA4SR (situational awareness for construction safety risks management) is risk awareness which focuses on monitoring and analyzing safety risks over time to enhance situational awareness.

In the risk awareness module (described in this chapter), a spatiotemporal network-based model was developed to analyze the risk levels of individual entities as well as jobsites with respect to struck-by-equipment hazard. The developed model presented in this chapter can be further extended to analyze the risks of other types of contact collisions on sites. The publication included in this chapter is:

- Wang, J., and Razavi, S. (2018). “**Spatiotemporal Network-Based Model for**

Dynamic Risk Analysis on Struck-by-Equipment Hazard.” *Journal of Computing in Civil Engineering*, 32 (2), DOI: [10.1061/\(ASCE\)CP.1943-5487.0000732](https://doi.org/10.1061/(ASCE)CP.1943-5487.0000732).

The contributions of the co-author include:

- Technical supervision of the study presented in this paper; and
- Review and modification of the manuscript.

Paper #3: Spatiotemporal Network-Based Model for Dynamic Risk Analysis on Struck-by-Equipment Hazard

Abstract

Having an approach that can analyze and identify safety risks in dynamic and hazardous construction environments is one of the key steps to the success of health and safety plans. Struck-by-equipment hazard is one of the leading causes of construction injuries and fatalities. Therefore, the primary objective of this paper is to investigate and provide an effective method of safety risk analysis on struck-by-equipment hazard. A spatiotemporal network-based model is developed in this paper which performs dynamic risk analysis on the struck-by-equipment hazard at both entity and network levels. The developed model is capable of performing safety risk analysis in a real-time and proactive manner by considering the spatiotemporal interactions among all construction entities (equipment and workers on foot) across the jobsite. Three risk factors of struck-by-equipment hazards were selected, including proximity, blind spots, and velocity. The interactions of the selected factors between entities are quantified and used to generate the network. Three safety leading indicators, i.e., degree centrality, eigenvector centrality, and relative risk score, are adopted to represent the risk levels of individual entities and jobsites. The implementation and evaluation of the network-based model with the three leading indicators are conducted and illustrated based on four simulated jobsites. Accordingly, the derived practical applications for risk analysis and hazard identification and prevention are described. The work presented in this paper enables the quantification

and analysis of the struck-by-equipment risk of both individual entities and jobsites from multiple perspectives. Further insight is gained into the temporal aspects of risk and the safety performance of entities as well as jobsites, to proactively identify and prevent hazards.

Keywords: Construction Safety; Dynamic Risk Analysis; Network Analysis; Struck-by Hazard; Safety Leading Indicator; Spatiotemporal Interaction

Introduction

Construction remains a high-risk industry for occupational safety and health. Among all construction injuries and fatalities, it is worth noting that struck-by-equipment hazard is one of the leading causes. In the U.S., 15% of the total fatal occupational injuries resulted from struck-by hazards involving equipment and objects in 2014 (BLS 2016b). Approximately 75% of struck-by fatalities involved heavy equipment such as trucks, as published by the United States Department of Labor (OSHA 2016). Struck-by-equipment accidents often result from specific conditions inherent to construction sites which strain workers' situational awareness, leaving them vulnerable. Thus having a proactive system that can identify risks on construction sites is the key to the success of health and safety plans in dynamic and hazardous construction environments. Therefore, the focus of this paper is on developing and evaluating a model for safety risk analysis on the struck-by-equipment hazard. It should be noted that struck by the falling parts of equipment (e.g., the collapsed boom or other falling parts of cranes) and the swing booms of cranes are not included in this study.

A struck-by-equipment hazard is the consequence of mutual interactions of multiple risk factors among construction entities (equipment and workers on foot). Extensive studies focusing on proximity detection to prevent struck-by-equipment hazards have been conducted through utilizing different technologies (Park et al. 2015; Teizer and Cheng 2015; Choe et al. 2014; Ruff 2010). However, studies on the impact of dynamic spatiotemporal interactions of multiple factors (not limited to proximity) among entities in struck-by-equipment hazard remain lacking. Also, there has been a need for a systematic risk analysis method for struck-by-equipment hazard (Isaac and Edrei 2016; Esmaeili et al. 2015a). As thus, a comprehensive method to evaluate the risk of struck-by-equipment hazard by considering the dynamic spatiotemporal interactions of multiple factors among all entities is developed in this paper. Herein, comprehensive refers to a method that is capable of performing safety risk analysis and identification at multiple levels (i.e., entity level and network level) in a real-time and proactive manner. Entity-level analysis mainly aims to detect and capture risk-related entities, for example, entities with a higher risk of being involved in hazards. Unlike the entity-level analysis, the network-level analysis focuses on evaluating the overall risk level of the network pertinent to the hazard, i.e., the global risk level of the spatiotemporal interactions among all entities on the jobsite. Two entity-level indicators (i.e., degree centrality and eigenvector centrality) and one network-level indicator (i.e., relative risk score) are used in this paper to represent the risk levels of entities and jobsites, respectively.

Different from the existing studies investigating the interactions (e.g., proximity) between paired entities individually, this paper takes a step forward by integrating all of

the entities on the jobsite into a connected network as a system in which the dynamic interrelationships and interactions among all entities are not overlooked. Consequently, more advanced insight is gained into the temporal aspects of risk and the safety performance of individual entities as well as the whole system. The implementation and evaluation of the developed model with the three safety leading indicators for the risk analysis pertinent to struck-by-equipment hazard are conducted and explained in detail in this paper.

The technical novelties of this study are: (i) using three risk factors of struck-by-equipment hazards to capture and quantify the dynamic spatiotemporal interactions among entities to assess safety risk; and (ii) performing safety risk analysis at both entity and network levels considering all interactions and interrelationships that coexist in the network.

The remainder of the paper is organized as follows. A literature review identifies research gaps; following is a discussion of research needs and objectives and then a discussion of the development, implementation, and evaluation of the network-based model for risk analysis. Ending the paper are contributions, limitations and future work, and concluding remarks.

Literature Review

Struck-by Hazard Identification and Risk Analysis

The general factors associated with struck-by hazards were summarized as workforce age, construction activity, equipment type, human factor, and environmental factor (Hinze et al. 2005). More specific factors such as close proximity, high machine

speed, a right-facing orientation, and blind spots were identified as main causes of struck-by-equipment hazards by a number of studies (Ray and Teizer 2016; Bartels et al. 2009). Accordingly, several studies were conducted aiming to eliminate the struck-by-equipment risk by providing solutions to some of the above-identified risk factors.

Various emerging technologies such as computer vision, global positioning system (GPS), and radar-based sensors have been employed for construction safety monitoring and proximity-detection system development (Zhu et al. 2016; Seo et al. 2015; Choe et al. 2014; Ruff 2010). However, a majority of current proximity warning methods only consider proximity or a very limited number of risk factors (e.g., proximity along with equipment speed). For example, systems based on radio-frequency identification (RFID), magnetic, and Bluetooth were developed and tested respectively for personnel and equipment proximity sensing in work zones, by only considering the distance between two entities (Park et al. 2015).

Another limitation of most of the existing methods for struck-by-equipment hazard awareness, also including the above-mentioned methods, is that they mainly focus on entity-level hazard identification. For example, a system based on computer vision and fuzzy inference was developed to assess the risk level for each entity (Kim et al. 2016). The three models (e.g., time-cuboid model) developed by Wang and Razavi (2016a, b) to reduce false alarms are other examples of entity-level risk identification. Another example is a method developed on behavior-based safety (BBS) to investigate three types of unsafe human behaviors for each worker (Li et al. 2015b). Nevertheless, a full understanding of the risk at different aspects enables safety managers to superiorly

achieve proactive hazard identification and prevention. In the work conducted by Luo et al. (2016), the hazard exposure was quantified and used to assess the proximity risk. The safety risk trends from multiple perspectives including worker, hazard, and project can be obtained and compared. However, only data on the location of equipment and workforce were considered.

In addition, there has been a need for a systematic risk analysis method for struck-by hazards, particularly on proactive monitoring and predictive assessment. Esmaili et al. (2015a) developed generalized linear models to predict the probability of occupational fatality in regard to struck-by accidents. A statistical model for dynamic safety risk control was developed by Isaac and Edrei (2016) to provide proactive alerts to site managers if workers are within the pre-defined statistical zones. Bobadilla et al. (2014) proposed and developed a methodology based on information spaces to proactively monitor and predictively assess struck-by hazards. The existing studies shed lights on further systematic risk analysis on struck-by-equipment hazard.

Review of the current literature shows that the development of a method which considers multiple risk factors to proactively monitor and evaluate the struck-by-equipment risk at multiple levels is substantially needed.

Interaction Analysis

An incident/accident is the consequence of spatiotemporal interactions generated by risk factors, work tasks, and involved entities, among others (Teizer and Cheng 2015; Hallowell et al. 2011). Therefore, investigating the encompassed spatiotemporal interactions is essential in assessing safety risk and avoiding injuries/fatalities.

Herein, three example studies are selected and described to illustrate the study of spatiotemporal interactions for safety risk analysis and hazard identification. As identified in the work by Hallowell et al. (2011), spatiotemporal interactions among work tasks were overlooked in the quantitative safety risk analysis. Therefore, Hallowell et al. (2011) utilized the Delphi method to quantify six hundred safety risk interactions among work tasks for highway construction projects. It can be seen that the study of spatiotemporal interactions has been applied to the quantitative safety risk analysis. Teizer and Cheng (2015) concluded that in studies of proximity hazard identification, evaluation of interactions among workers on foot and equipment in particular is still lacking. Thus, a proximity hazard indicator method was developed to capture near-miss interactions between workers on foot and equipment and geo-referenced hazardous areas (Teizer and Cheng 2015). However, only the position-based interactions among entities were considered in that work. Another method, heat map generation, which considered the interactions of multiple risk factors (e.g., proximity and equipment orientation) was developed to prevent struck-by hazards between workers on foot and equipment (Golovina et al. 2016). A hazard index that can be visualized in the generated heat map was developed to further determine the root causes. However, the role of an entity in the occurrence of an incident/accident, considering all entities' interactions and interrelationships on the jobsite, was not further explored. From the work of Teizer and Cheng (2015) and Golovina et al. (2016), it can be seen that investigating the spatiotemporal interactions amongst entities can be used to identify struck-by-equipment hazards.

As the studies described and limitations identified above, fully considering the spatiotemporal interactions of multiple factors among all entities on a site is a promising approach to proactively analyzing and identifying the risk pertinent to struck-by-equipment hazard.

Research Needs and Objectives

Struck-by-equipment hazard is the consequence of mutual interactions among entities that result from multiple risk factors. Based on the shortfalls identified in the literature, a comprehensive model that can assess and identify the safety risk pertaining to struck-by-equipment hazard is needed. A full understanding of the risk at different aspects assists to proactively identify and prevent hazards in the dynamic and hazardous construction environment. As thus, the objectives of this study are as follows:

- Development of a network-based model to analyze and identify the struck-by-equipment risk at both entity and network levels;
- Selection of risk factors causing struck-by-equipment hazards using historical data and current literature;
- Quantification of the dynamic interactions among entities that result from each selected risk factor; and
- Evaluation and illustration of the developed network-based model with the safety leading indicators for real-time and proactive safety risk analysis.

Model Development

This paper develops a network-based model for the dynamic risk analysis on struck-by-equipment hazard. Four primary steps were included in the developed model

(Fig. 1) to assess risk in a comprehensive way, based on monitoring and capturing the spatiotemporal interactions among all entities:

Step 1: Select the major risk factors causing struck-by-equipment hazards;

Step 2: Quantify the dynamic interaction associated with each selected risk factor over time;

Step 3: Conceptualize and model all of the involved entities and their interactions and interrelationships as a dynamic weighted network; then calculate the determined safety leading indicators (i.e., degree centrality, eigenvector centrality, and relative risk score); and

Step 4: Utilize the computed safety leading indicators to identify the dynamic risk of individual entities (i.e., entity level) and jobsites (i.e., network level).

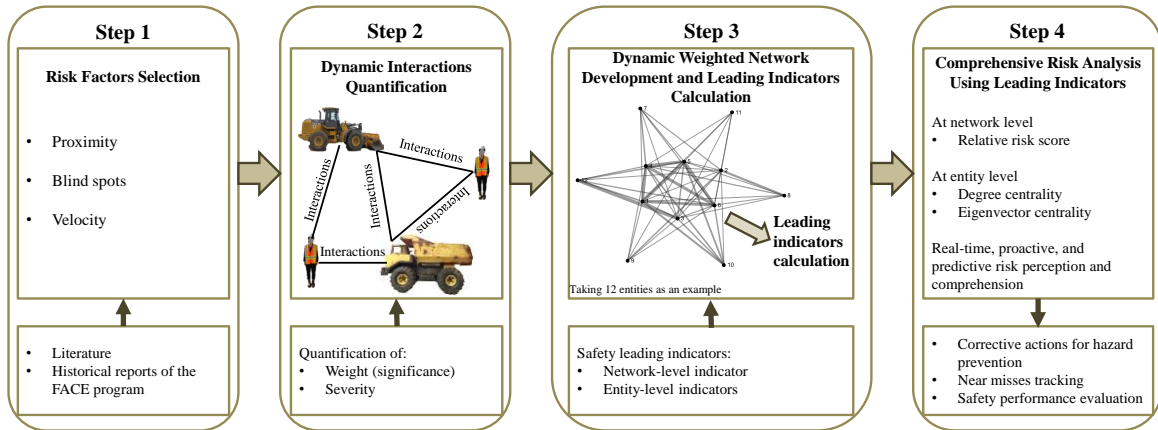


Fig. 1. Network-based struck-by-equipment risk analysis model (adapted from Wang and Razavi 2017a; the images of workers and equipment in Step 2 are adopted from Wang and Razavi 2016b)

The dynamic interactions between connected entities are quantified and updated according to the monitored situation on the site. The dynamics of the site can be monitored by attaching sensors to individual entities to acquire their real-time states (i.e., position, velocity and orientation). The sensed data are wirelessly transmitted to the cloud or server for further analysis (Wang and Razavi 2016b; Wang et al. 2016). Real-time data collection and transition have been extensively studied (Wang et al. 2016; Jiang et al. 2014) and are not within the scope of this paper. The analysis of the sensed data using the developed model in the cloud or on a server is the focus of this paper. In this way, a real-time weighted network is created that intellectualizes the causal relationships and interdependencies among entities. The outputs of the created network are the calculated leading indicators which deliver the information regarding the risk levels of jobsites (i.e., network level) and entities (i.e., entity level). The essential steps are explicated in detail in subsequent sections.

Step 1: Risk Factors Selection

The occurrence of a struck-by-equipment incident/accident is the consequence of mutual interactions of multiple risk factors. In this study, both the literature and the historical reports were used for the risk factors selection. The distance between entities has been widely adopted as an indicator to denote their close proximity so that potential collisions can be detected (Park et al. 2015; Vahdatikhaki and Hammad 2015). However, only considering the proximity of entities cannot fully reveal the real situations on a dynamic jobsite (Wang and Razavi 2016b). Therefore, along with the proximity of entities, another two essential risk factors, i.e., blind spots and velocity, were selected

from the literature and the historical records and used in this paper (Ray and Teizer 2016; Golovina et al. 2016). Thoroughly considering the selected risk factors assists to reveal entities' real-time dynamics in a more accurate way and thus to capture and quantify the interactions and interdependences among them more precisely.

The historical records used in this paper are 118 detailed struck-by-equipment accident reports extracted from the Fatality Assessment and Control Evaluation program (FACE program), which includes the National Institute for Occupational Safety and Health FACE reports (NIOSH FACE reports) and the State FACE reports (NIOSH 2016). From the FACE program (i.e., the NIOSH FACE reports and the State FACE reports), three categories, Construction, Machine Construction, and Highway Work Zones were reviewed to extract struck-by-equipment accident reports. The accident locations were not limited to construction sites, and a total of 118 struck-by-equipment accident reports were extracted. The supreme advantage of the FACE program database compared with other databases is the extraordinarily detailed information recorded about the accidents. The reports are expressed in a narrative format to reveal the circumstances before, during, and after accidents. The recorded detailed information includes but not limited to the description of the accident process, time of accident, age of victim, activities performed on the site, involved equipment, weather, accident causes with corresponding suggestions, contractor introduction, involved personnel's safety training and records, the position of the victim when the accident happened, and other related information. The detailed reports also provided valuable information that was further used for the interactions quantification (explained in the following section). The work presented in this paper is

also meant to motivate the related participants and organizations to investigate and record near misses, incidents, and accidents with high levels of detail for further effective safety management.

In the process of risk factors selection, the literature on struck-by-equipment hazard was studied to extract risk factors. The extracted factors included proximity, velocity, blind spots, orientation, weather, equipment type, safety training, and worker's age. Afterward, each report extracted from the FACE program was fully read and analyzed to obtain and record information about the risk factors taken from the literature. The causes of death and the factors reported in the recommendation section in each report were fully recorded. Also recorded was information regarding other factors such as victim age and working hours. As a result, the frequency of each factor was obtained from the historical reports. The obtained frequencies of the representative risk factors are summarized in Table 1 which supported and assisted to select the risk factors for this study. Based on Table 1, proximity, blind spots, and velocity are the risk factors with relatively high frequency. The region relative to equipment also played an important role in the occurrence of hazards and is considered in the severity quantification for blind spots (explained in the Severity Quantification section). Therefore, by comprehensively considering the leading factors suggested by the literature and Table 1, proximity, blind spots, and velocity were selected and studied in this paper. The selected three factors are explained in more detail in the following sections. Quantifying and integrating other representative factors such as weather, equipment type, workforce age, and working hours into the developed model are the focus of future work.

Table 1. Summary of Frequencies of Factors

Factors	Description	Frequency
Proximity	—	0.64
Blind spots	—	0.41
Equipment velocity	—	0.19
Region relative to equipment	Front	0.24
	Front left	0.03
	Front right	0.05
	Left side	0.04
	Right side	0.06
	Back	0.34
	Back left	0.05
	Back right	0.08
Equipment type (big category)	Truck (e.g., dump truck, pick-up truck etc.)	0.51
	Loader (e.g., skid-steer loader)	0.1
	Excavator and backhoe	0.14
	Others (e.g., forklift, roller, scraper etc.)	0.33
Safety training	Low ^a	0.30
	Moderate ^b	0.21
	Good ^c	0.31
Age of victim	<20	0.05
	[20,30)	0.18
	[30,40)	0.27
	[40,50)	0.23
	[50,60)	0.20
	≥60	0.06
Working hours on accident day ^d	<2	0.002
	[2,4)	0.003
	[4,6)	0.002
	[6,8)	0.001
	≥8	0.001

^aNo training or had warning, incident, accident etc. records.

^bUncomprehensive training.

^cComprehensive training and training records maintained.

^dNumber of hours between time of accident and time that victim started work on that day.

- Proximity

The published statistics show that locating or working in close proximity to heavy equipment is a leading cause of construction injuries and fatalities (NIOSH 2016). As mentioned earlier, monitoring and detecting the distance between entities has been broadly used as a manner to avert struck-by hazards.

- Equipment blind spots

Limited equipment operators' visibility due to blind spots also is another significant cause of struck-by-equipment accidents (Ray and Teizer 2016). Camera systems, radar, and other technologies have been employed to increase operators' visible regions around equipment. The blind spots of multiple types of equipment have been studied and summarized by the Center for Disease Control and Prevention (CDC 2009). Compared with existing manual or semi-automated blind spots identification methods, automated and real-time measurement of blind spots is attracting more interest (Ray and Teizer 2016; Teizer et al. 2010).

- Velocity

Studies such as the work of Bartels et al. (2006) have shown that a machine with high velocity poses itself at a relatively higher risk of striking an entity. Also, a moving entity on the ground with higher velocity has more kinetic energy, which generally results in a more severe collision outcome (Golovina et al. 2016; Alexander et al. 2015). Investigating the relative velocity of entities supports determining whether the dynamic entities are getting closer to each other (Wang and Razavi 2016a) and further quantifying the impact of a potential collision.

Step 2: Dynamic Interactions Quantification

The interactions between entities associated with the above-selected risk factors are quantified over time by monitoring entities' real-time states, including position, velocity, and orientation. The stronger the interactions between entities, the greater the possibility of a collision.

The dynamic interactions between each pair of involved entities (i.e., equipment and equipment, or equipment and workers on foot) are quantified using Equation (1). The risk factor i ($i = 1,2,3$) refers to the respective risk factor including proximity, blind spots, and velocity. The eventual interaction level is the sum of the interactions resulted from the three factors. The interaction resulted from each factor is calculated using Equation (2), which is the production of the weight and severity of each factor. Equation (2) is adopted from the method proposed and used by Golovina et al. (2016), where the weight assigned to each factor ($weight_i$) is determined based on the estimated frequency that the corresponding factor is about to happen on the site. In this study, it is assumed that the states of risk factors are monitored in real time, as thus the weight assigned to each risk factor is modified and considered as the significance of the factor compared with that of other risk factors in causing a collision (Shapira et al. 2012). Thus, the interaction is the production of the weight (significance) of each factor and the severity of the real-time detected state of that factor. In summary, the interactions between entities are quantified from different perspectives by analyzing entities' motions. The quantifications of the weight and severity in the context of struck-by-equipment hazard are explained in detail below.

$$\text{Interaction level of pair } x \text{ and } y = \sum_{i=1}^3 \text{interaction of risk factor } i \quad (1)$$

$$\text{Interaction of risk factor } i = \text{weight}_i \times \text{severity}_i \quad (2)$$

where $x = 1, 2, \dots, p$ and $y = 1, 2, \dots, q$; p is the total number of pieces of equipment; and q is the total number of entities (workers on foot and equipment) on the site.

Weight Quantification

In this paper, the weight of a risk factor is quantified and determined in Equation (3) by using the lagging indicator, i.e., loss of time. The loss of time is calculated by analyzing the information extracted from the historical records of the FACE program [Equation (4)].

$$\text{Weight of factor } i = \frac{\sum_{j=1}^{Num_i} \text{loss of time of accident } j}{\sum_{k=1}^{Num} \text{loss of time of accident } k} \quad (3)$$

$$\text{Loss of time} = (\text{age of off work} - \text{victimage}) \times \text{working weeks per year} \quad (4)$$

where Num is the total number of accident records under analysis; and Num_i is the number of accidents caused by factor i . In Equation (4), the age of off work is adopted as 70 (CPWR 2012a), and the average working weeks per year is 45.2 (CPWR 2012b).

Severity Quantification

The resulting severity of each risk factor (i.e., proximity, blind spots, and velocity) is determined based on the real-time monitored state of the factor, justified as follows.

- Severity of proximity

The severity of proximity is quantified using Equation (5), which is adopted and

modified from the work by Golovina et al. (2016). An adaptive distance rather than a constant value [which was used by Golovina et al. (2016)] is adopted in this paper. The adaptive distance is the required traveling distance that the involved entities need to come to a complete stop upon realizing an unsafe proximity. The adaptive distance is adjusted and determined by multiple factors such as equipment speed and braking distance and worker reaction distance (Wang and Razavi 2016b). The severity is quantified by measuring the ratio of the monitored distance between entities and their adaptive distance.

$$Severity_proximity = e^{-\frac{Monitoreddistance}{Adaptivedistance}} \quad (5)$$

- Severity of blind spots

The area around any equipment is divided into eight regions as shown in Table 1. The different regions relative to equipment can have different severity levels of consequence (NIOSH 2016; Golovina et al. 2016). The blind spots around equipment can be measured and recorded in multiple ways, as reported in studies such as Ray and Teizer (2016) and CDC (2009). Hence, if an entity is identified within the blind spots of equipment, the severity associated with that specific region will be adopted. The severity associated with each region is quantified using Equation (6) (Lee et al. 2012). The obtained severity for each region is summarized in Table 2.

$$Severity\ associated\ with\ region\ t = \frac{\sum_{j=1}^{Num_t} loss\ of\ time\ of\ accident\ j}{Num_t} \quad (6)$$

where Num_t is the number of accidents occurred in the region t ($t = 1, 2, \dots, 8$). The loss of time is calculated using Equation (4) by analyzing the historical records.

Table 2. Severity of Different Regions Relative to Equipment

Region	Severity
Front	0.76
Left	0.1
Right	0.88
Rear	0.47
Front left	0.26
Front right	0.54
Rear left	0.3
Rear right	0.9

- Severity of velocity

Entities' relative velocity is used to quantify severity with respect to velocity. Equations (7) and (8) will be applied if the involved entities are identified as getting closer to each other at the moment (Wang and Razavi 2016a). The equations produce severity of more than 1 if the magnitude of the obtained relative velocity is greater than the allowed maximum relative velocity between the entities (i.e., between equipment and equipment or between equipment and workers on foot).

$$Severity_velocity = \frac{\|Relative\ velocity\|}{Max_E_E} \quad (7)$$

$$Severity_velocity = \frac{\|Relative\ velocity\|}{Max_E_W} \quad (8)$$

where the Max_E_E is the allowed maximum relative velocity between equipment and equipment on the site; and the Max_E_W is the allowed maximum relative velocity between equipment and workers on foot. The allowed maximum relative velocity is a value determined and set by users in advance, according to site characteristics (e.g., size,

layout, terrain, and soil type), equipment type, entity maximum speed, and others. For example, the maximum speed of a piece of equipment on a site can be determined based on its specification, site terrain, soil type, and others. Afterward, the maximum magnitude of the relative velocity between two entities is the sum of the determined maximum speed of each entity on the site. The maximum magnitude of the relative velocity, if needed, can be further modified based on the number of entities on the site, site layout, and others to finalize the allowed maximum relative velocity.

Step 3: Dynamic Weighted Network Development and Leading Indicators Calculation

The generation of the dynamic network for risk analysis and the adopted three safety leading indicators are described in this section.

Network Generation and Analysis

The weighted network is adopted to model entities and their interactions and interrelationships for risk analysis. As discussed earlier, the dynamic interactions between entities are captured and quantified in real time. As such, a jobsite and its entities are modeled as a dynamic weighted network where each entity is represented as a node and the interactions between each pair of entities are presented as the link between them. The quantified interactions between entities present the intensity of the connection between them and are used as the weight of the corresponding link [the weight of a link is different from the weight expressed in Equation (2)].

Leading Indicators: Entity Level and Network Level

Two levels of network analysis are performed in this study, i.e., entity level and network level, to obtain a comprehensive and multi-perspective risk analysis. The entity-level analysis focuses on performing safety risk analysis for entities involved in the network. The network-level analysis focuses on evaluating the overall risk level of the generated network, or in other words, the global risk level of the interactions among all entities on a jobsite. The following three metrics are adopted to represent the risk at the entity and network levels:

- Degree centrality (entity-level)

Degree centrality is the most straightforward measure of node centrality. The method developed by Opsahl et al. (2010), which considers both the number of links and their weights, is adopted in this paper. A degree score for each node signifying its centrality and node strength is calculated. The higher the degree score, the more intensive the interactions and connections with other nodes (i.e., the node has more strength). The nodes with relatively higher degree centrality scores indicate that the corresponding entities have a higher probability of causing struck-by-equipment hazards.

- Eigenvector centrality (entity-level)

Eigenvector centrality evaluates node importance by incorporating the importance (centrality) of the node's neighbors (Spizzirri 2011). The eigenvector centrality adopts the eigenvector (e) corresponding to the largest eigenvalue (λ) of the network adjacency matrix (A), as expressed in Equation (9) (Carreras et al. 2007). Through examining the nodes' eigenvector centrality, the entities which are interacting with risky (important)

entities can be identified. The identified entities have a relatively higher probability of being involved in an incident/accident. In some cases, the top entities in the degree centrality ranking and the eigenvector centrality ranking might have some in common (Zafarani et al. 2014).

$$A \cdot e = \lambda e \quad (9)$$

where A is the adjacency matrix of the network; λ is the largest eigenvalue (Canright and Engø-Monsen 2004); and e is the eigenvector of A with respect to λ .

- Relative risk score (network-level)

In this paper, the global risk level of a jobsite (i.e., network level analysis) is evaluated by investigating how well the generated network is connected and interacting. The more intensive and extensive the connections in the network are, the higher the overall jobsite risk is. The relative risk score is developed based on a measurement named algebraic connectivity (AC). The algebraic connectivity is a direct and widely used indicator to reflect how well a network is connected. The higher the calculated algebraic connectivity, overall the higher the jobsite risk. The algebraic connectivity is defined as the second smallest eigenvalue of the Laplacian matrix of the network (Wei and Sun 2011). The Laplacian matrix for a weighted network is defined in Equation (10). It should be noted that the algebraic connectivity is an evaluation of the overall risk level rather than capturing individual risk-related entities. As because the dynamic interactions among all entities are monitored and quantified in real time, the algebraic connectivity of the monitored situation can be calculated in real time.

$$L = D - A \quad (10)$$

where L is the Laplacian matrix of a weighted network; and D is the network degree matrix, which is a diagonal matrix containing information about the degree of each node. The degree of a node is the number of links attached to it.

As pointed by Wei and Sun (2011), in weighted networks the weight of each link should be bounded by an upper limit as a weighting scale without an upper limit normally is not applicable in practice. More insight can be gained from an obtained number if users know the limit that number should not exceed. Taking the interactions between entities as an example, the strength of the interactions should be bounded by an upper limit as hazards might happen if the interactions between entities exceed the upper limit. Therefore, to gain further insight about the output risk level (i.e., algebraic connectivity) of the monitored situation, the index of relative risk score [Equation (11)] is developed and utilized (Hallowell and Gambatese 2009; Baradan et al. 2006). The relative risk score is the ratio of the algebraic connectivity of the monitored situation ($AC_{monitored}$) and the risk tolerance of the jobsite ($AC_{tolerance}$). The algebraic connectivity of the monitored situation is calculated based on the interactions quantified from real-time observations. While the risk tolerance of the jobsite is the algebraic connectivity of the generated network in which the interactions between entities are at their upper limits. The upper limit defines a tolerance of the interactions that should not be exceeded between entities. Correspondingly, the calculated algebraic connectivity is taken as the risk tolerance of the jobsite. In this way, the output of Equation (11) enables users to better understand the risk of the monitored situation at the network level.

$$\text{Relative Risk Score} = \frac{\text{Risk level of the monitored situation}}{\text{Tolerance of risk level}} = \frac{AC_monitored}{AC_tolerance} \quad (11)$$

Step 4: Comprehensive Risk Analysis Using Leading Indicators

This section explains how to use the developed network-based model with the three leading indicators for comprehensive safety risk analysis on struck-by-equipment hazards.

The model implementations are conducted and explained based on four different simulated jobsites. Multiple characteristics, including backing up equipment, trajectory, velocity, and moving area, were taken into consideration in the simulation, as described and summarized in Table 3. On each jobsite, a total of 2000 seconds (one frame per second) were simulated with six trucks and six workers on foot. Totals of collisions and near misses between all entities in the 2000 frames were used to preliminarily represent the risk level of each jobsite. Therefore, entities' trajectories (curves and lines), velocities, and moving areas (constrained area or entire site) were designed to have the four sites with different levels of risk (Table 3). The total collisions on sites #1 and #4 (more than 1000) greatly differed from the total collisions on sites #2 and #3 (less than 1000). For sites #1 and #4, the moving area of entities on site #1 was more constrained compared with the moving area on site #4. For sites #2 and #3, site #2 had backing-up equipment whereas site #3 did not. The four sites were purposely simulated in the way, as summarized in Table 3, to potentially include the representative characteristics of real jobsites. Furthermore, the settings aided the comparison analysis of the network-level risk.

All selected risk factors (proximity, blind spots, and velocity) were taken into account in the calculation and analysis.

Table 3. Description of Simulated Jobsites

Characteristic	Jobsite			
	1	2 ^d	3 ^d	4
Backing up ^a	Y/1	Y/1	N	Y/1
Trajectory	Curve and line	Curve and line	Curve and line	Curve and line
Total near misses ^b	2042	583	15	1034
Total collisions ^c	6737	717	0	3393
Velocity	Not constant	Not constant	Not constant	Not constant but on average higher than other sites
Jobsite occupied by entities	Constrained area	Entire site	Entire site	Entire site

^a Y = equipment backing up; N=no equipment backing up; Y/1 = 1 piece of equipment backing up;

^b A near miss = distance between entities is 2-4 meters;

^c A collision = distance between entities is smaller than 2 meters;

^d No actual collisions simulated or involved on sites #2 and #3.

Network-Level Analysis: Relative Risk Analysis

The network-level analysis aims to evaluate the overall risk level of struck-by-equipment hazards for the entire jobsite [Equation (11)]. As explained earlier, the weight of each link between two entities (i.e., the interactions between two entities) is calculated using Equations (1) and (2), in which the resulting severity of each factor changes over time and determines the eventual weight of a link. Therefore, the threshold of the severity pertinent to each risk factor determines the upper limits of interactions between entities (i.e., thresholds of link weights in the network), which are the basis to calculate the risk tolerance [the denominator in Equation (11)]. Two methods to define the severity

threshold are adopted and employed in this paper:

- The severity thresholds for all risk factors are a constant value, regardless of the situation presented on the jobsite. The constant value can be any number between 0 and 1, i.e., (0, 1]. A smaller value indicates that the risk tolerance for the jobsite is lower, so a higher relative risk score is produced for a given situation.
- The severity threshold for each risk factor is adjusted and updated based on the real situation presented on the jobsite. For each risk factor, the monitored situation can be categorized into one of the user-defined categories. For example, (a) the magnitude of the monitored relative velocity is larger than, say, 80%, of its allowance or not for velocity; (b) the region in which an entity is located relative to equipment is the equipment's front, left, or other position for blind spots. Such categories and the severity threshold for each category are defined and determined by users in advance. The monitored situation will fall into one of the categories and accordingly, the severity threshold of the category will be adopted and applied in the calculation. A more hazardous situation (category) pertinent to the specific risk factor will be assigned with a relatively lower severity threshold, and consequently, a higher relative risk score will be obtained for the monitored situation.

The obtained results with analysis are presented below, followed by the derived applications based on the monitored and analyzed network-level leading indicator.

Result I: One Jobsite

Taking the simulated jobsite #4 as an example, the relative risk scores over the simulation time period under different risk tolerances can be calculated (Fig. 2). The assigned severity thresholds for all risk factors were 1, 0.8, and 0.6, respectively, in Fig. 2(a)-(c). Updated thresholds were applied in Fig. 2(d).

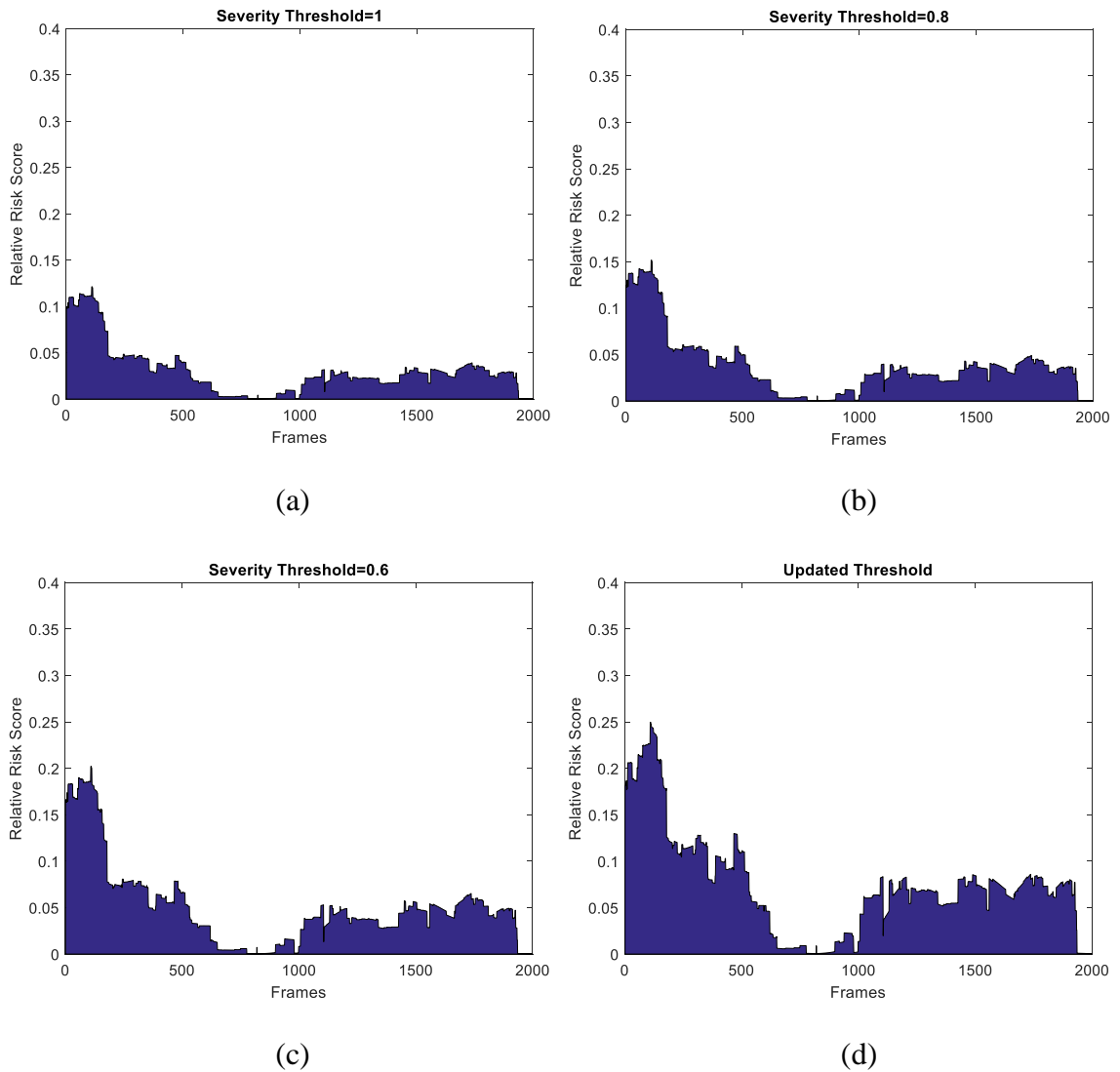


Fig. 2. Relative risk scores of jobsite #4 using severity thresholds as: (a) 1; (b) 0.8; (c) 0.6; and (d) adjusted and updated

Result II: Multiple Jobsites

Adopting the same risk tolerance, e.g., a constant value 0.6, as the severity threshold for the selected risk factors, the relative risk scores for the simulated four jobsites during the 2000 frames were calculated. The results are shown in Fig. 3.

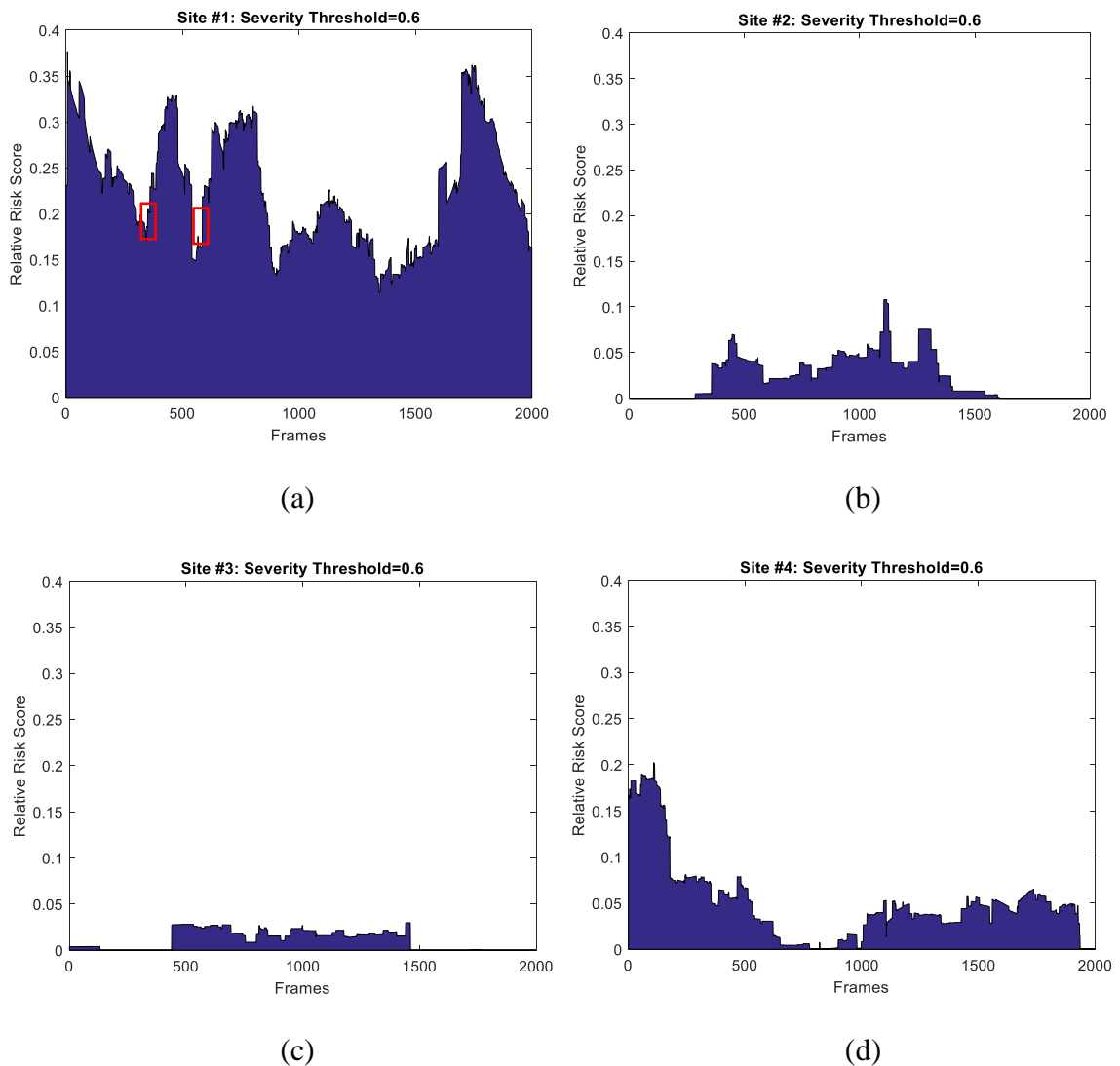


Fig. 3. Relative risk scores of jobsite (a) #1; (b) #2; (c) #3; and (d) #4 using the same severity threshold

Analysis of Network-Level Results

The analysis of the results (Figs. 2 and 3) at the network level is summarized.

- Overall, jobsite #1 presented the highest struck-by-equipment risk; conversely, jobsite #3 maintained a safer environment (Fig. 3). The results are compatible with the truth described in Table 3.
- For the same situation at one specific frame, a higher relative risk score was gained if the adopted jobsite risk tolerance was lower [Fig. 2(a)-(c)]. Users can adopt the desired severity threshold selection method to perform risk monitoring and analysis (Fig. 2).
- Even though the notion of relative risk is developed and utilized, it does not mean that relatively lower values represent safe situations and that hazards are only associated with high values. Based on the conducted work and obtained results (e.g., Figs. 2 and 3), the magnitude of the relative risk score is generally less than 50%. For example, four situations in Fig. 3 are selected and shown in Fig. 4 with their respective relative risk score. Collisions were included in Fig. 4(a) with 37.66% of the relative risk score, whereas a relatively safer situation is presented in Fig. 4(d) for which the relative risk score is 2.97%. Entities' trajectories are shown as the black lines in Fig. 4.

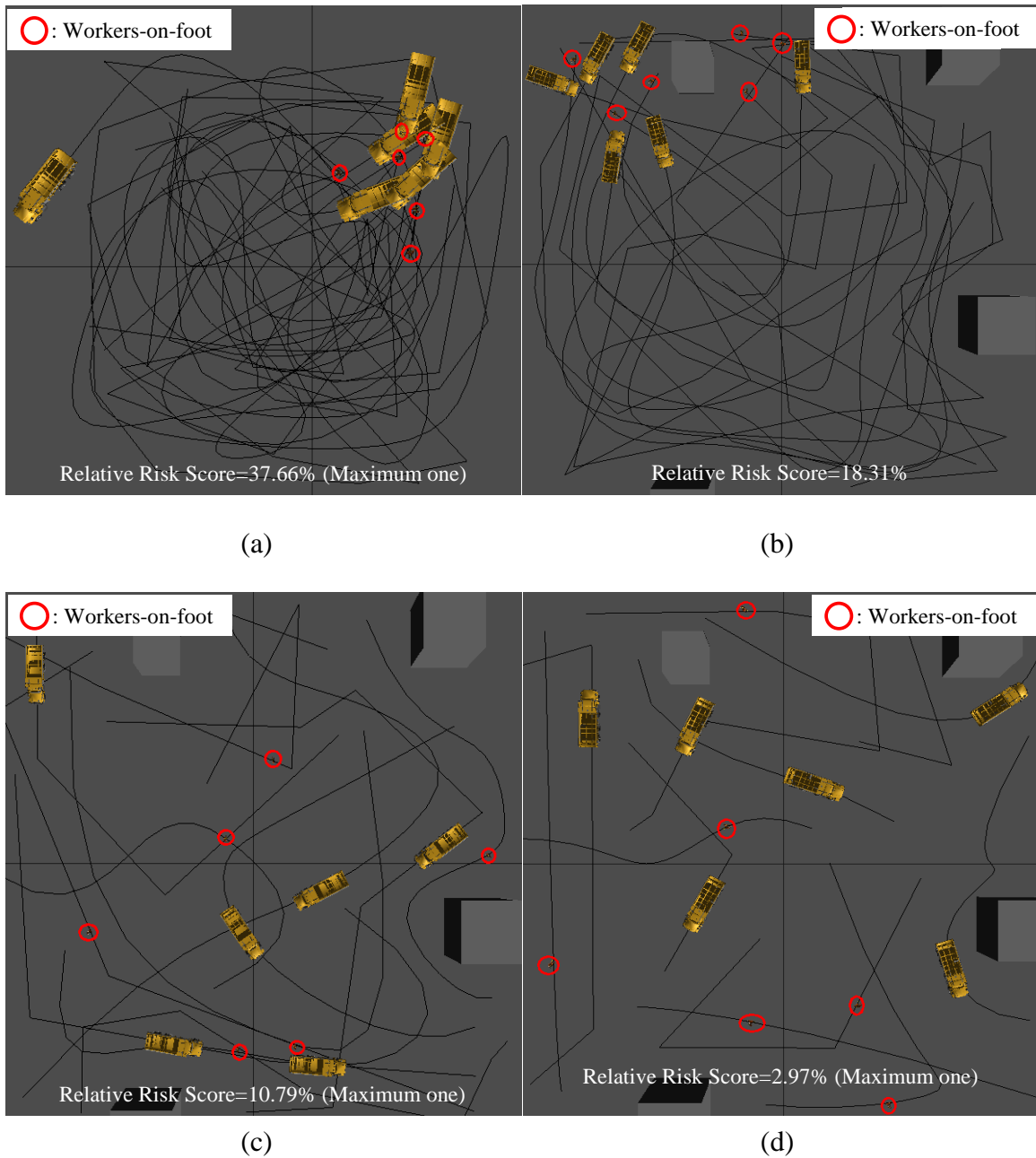


Fig. 4. Illustration of the situation at (a) frame 7 in Fig. 3(a); (b) frame 13 in Fig. 3(d); (c) frame 1117 in Fig. 3(b); and (d) frame 1441 in Fig. 3(c)

- Users can set and adopt a relative risk score threshold when the severity threshold

for each factor is determined. In this way, the frames with the relative risk score higher than the set threshold can be identified. For example, if 18% was set as the relative risk score threshold when the severity threshold was 0.6 (Fig. 3), consequently, the frames in Fig. 3(a) with relative risk scores over 18% can be timely identified. In addition, attention is drawn to a relative risk score approaching the set threshold, e.g., some frames marked in Fig. 3(a). The 18% is temporally adopted as in Figs. 3 and 4, in general, situations with relative risk score higher than 18% presented the high potential of occurrences of collisions in the near future, with all entities gathering and locating close to each other on the site [e.g., Fig. 4(b)] (no actual collisions were simulated on sites #2 and #3 and all entities were distributed across the entire site). A more robust way to set the relative risk score threshold will be explored based on the implementations of the model in the real world (Tchiehe and Gauthier 2017).

Applications

Through monitoring and analyzing relative risk scores over time, several applications can be derived with respect to proactive monitoring and predictive assessment for struck-by-equipment hazard, explained as follows.

For one specific jobsite (e.g., Fig. 2):

- If the monitored relative risk score at one moment exceeded the set threshold, the results obtained from the real-time entity-level analysis will be utilized (described in the next section). Therefore, this model can be applied to real-time hazard monitoring and detection.

- The following two applications are more focused on proactive risk analysis to avoid occurrences of struck-by-equipment hazards in the future:

(1) During a defined time period (e.g., one day), the periods of time that a jobsite tends to have higher relative risk scores (e.g., from 9 am to 10 am) can be found.

If this phenomenon is repeated over time, especially if the monitored relative risk scores are close to the set threshold, more attention must be paid and necessary actions taken.

(2) Through monitoring and analyzing the evolution and trending of the relative risk scores, actions can be taken to prevent potential hazardous outcomes.

For multiple jobsites (e.g., Fig. 3):

- Overall, jobsites can be ranked with respect to the struck-by-equipment risk, and the ones with better performance can be identified and rewarded. For example, in Fig. 4 the practices in maintaining a safer environment that implemented on jobsite #3 are worth being promoted. As the relative risk score is adopted in this study, the safety performance of different jobsites or a jobsite in different time periods can be compared.

Entity-Level Analysis

The entity-level analysis focuses on investigating individual entities' risk from different aspects, i.e., degree centrality and eigenvector centrality. Some of the obtained results are presented below, followed by the applications derived and gained from the results analysis.

Result I: Real-Time Monitoring

The leading indicators can be calculated and monitored in real time. Taking frame 3 of jobsite #2 as an example, the corresponding simulated situation is described in Fig. 5. The width of the link in Fig. 5(b) indicates the strength of the interactions between nodes. The results with respect to each leading indicator are shown in Figs. 6 and 7. In Fig. 6(b), a larger node indicates a higher degree centrality score. In Fig. 7(b), the eigenvector centrality scores are expressed in the generated network using different colors.

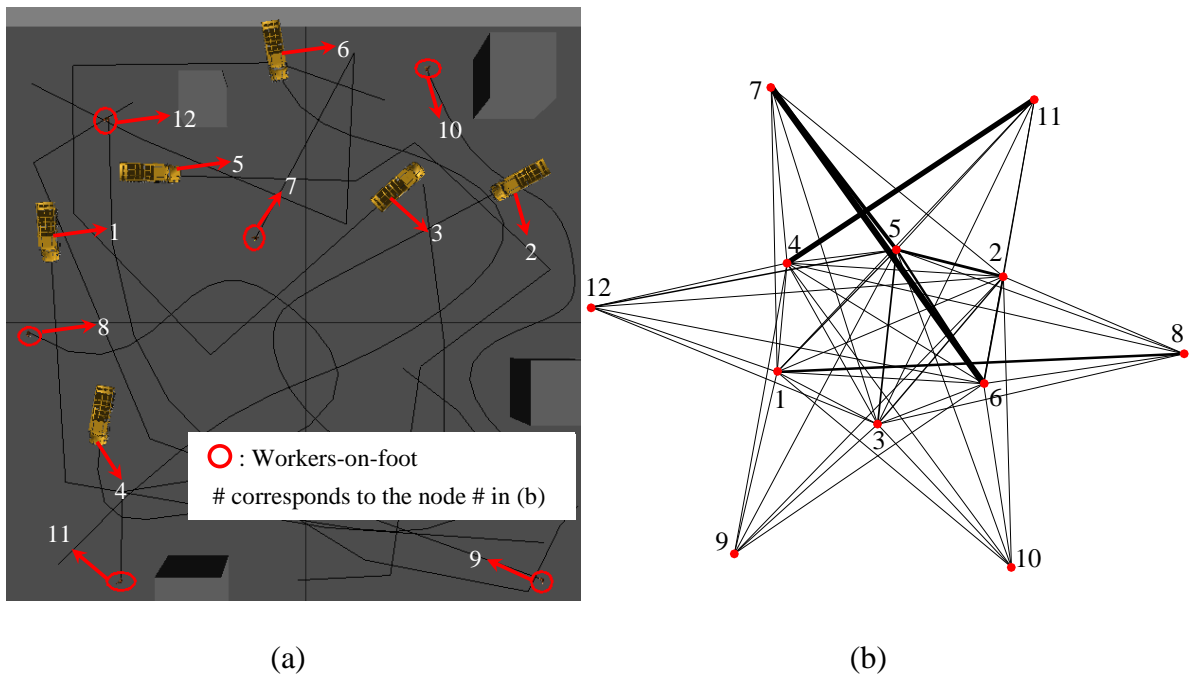


Fig. 5. Illustration of the situation at frame 3: (a) layout of entities on the jobsite and (b) quantified interactions presented in the network

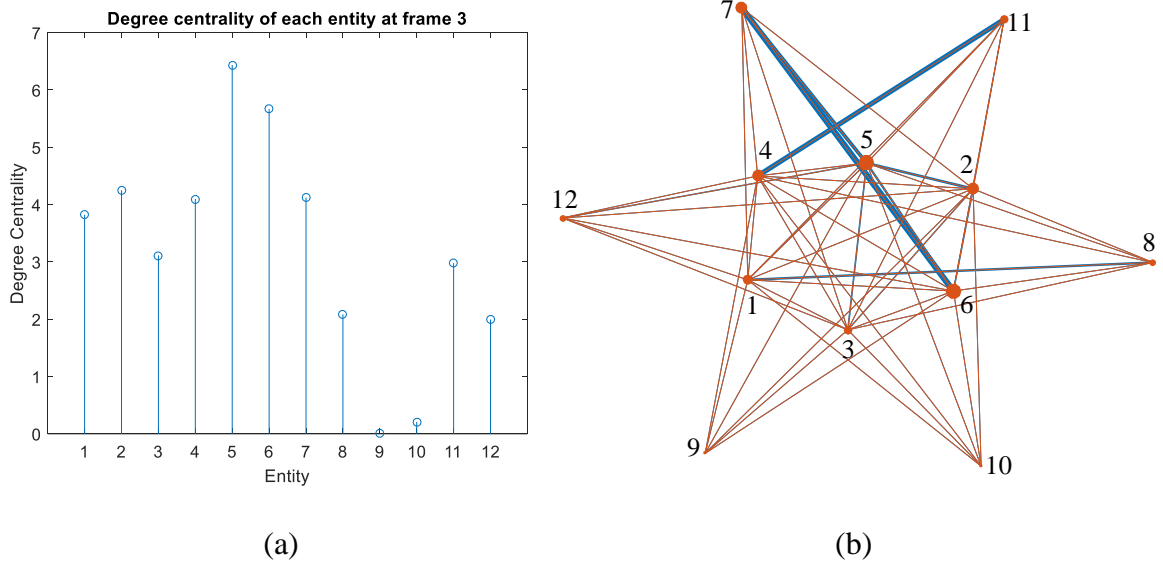


Fig. 6. Degree centrality results: (a) score of each entity and (b) degree centrality expressed in the weighted network

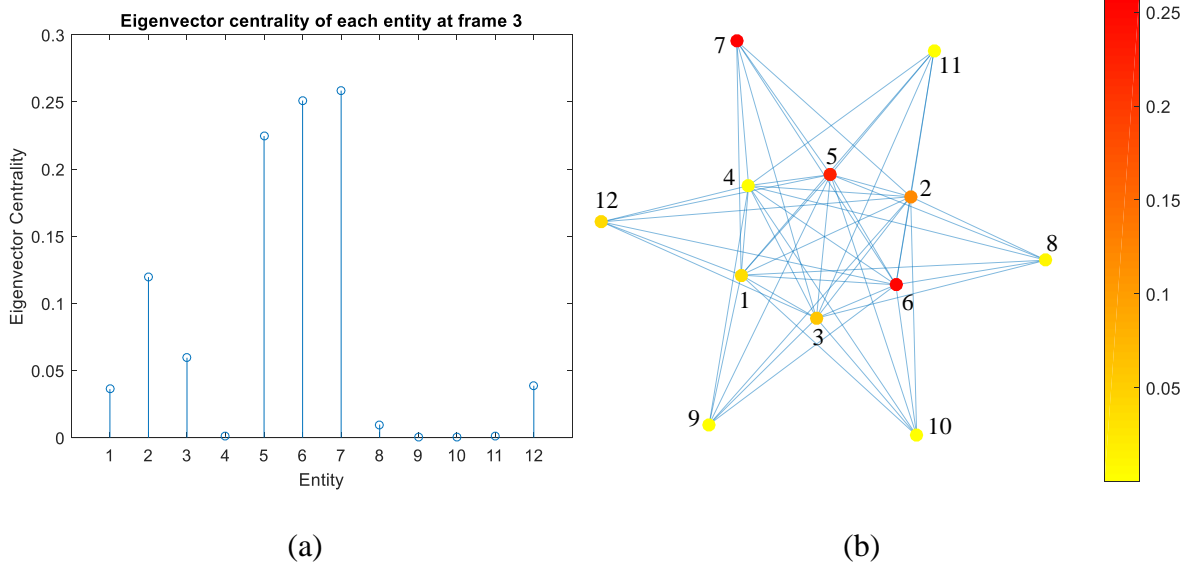


Fig. 7. Eigenvector centrality results: (a) score of each entity and (b) eigenvector centrality expressed in the network

Result II: Overall Performance

The evolution of individual entities’ risk over time can be tracked and analyzed for proactive hazard prevention. Taking jobsite #1 as an example, some of the obtained results are shown in Figs. 8 and 9.

The entities having the highest centrality (degree and eigenvector) at each frame are identified and displayed in Figs. 8(a) and 9(a). For one specific entity, its centrality ranking over time is expressed in Figs. 8(b) and 9(b), where 12 in the y-axis means the entity has the highest centrality compared with other entities, and 1 indicates the minimum centrality is gained by the entity.

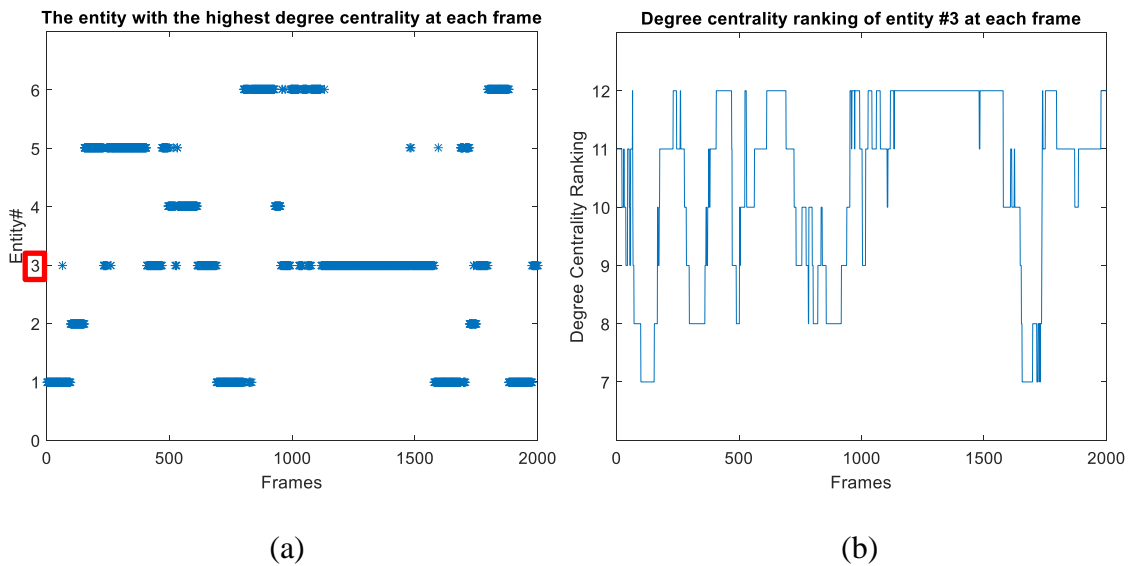


Fig. 8. Degree centrality over time: (a) entity with the highest degree centrality at each frame and (b) degree centrality ranking of one specific entity at each frame

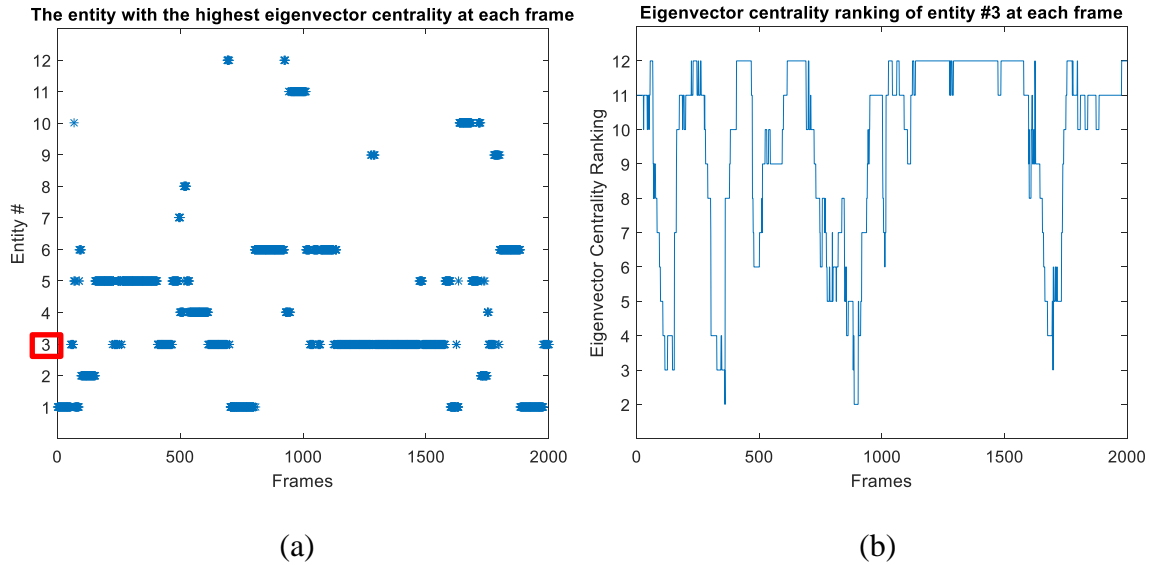


Fig. 9. Eigenvector centrality over time: (a) entity with the highest eigenvector centrality at each frame and (b) eigenvector centrality ranking of one specific entity at each frame

Analysis of Entity-Level Results

The major findings obtained from Figs. 5-9 are presented as follows.

- The calculated scores of the entity-level indicators can indicate the risk levels of individual entities. In Fig. 6, entities #5 and #6 are identified with higher degree centrality scores, indicating that they had a relatively higher probability of causing hazards compared with other entities on the site at frame 3. In Fig. 7, entities #7, #6, and #5 are identified with higher eigenvector centrality scores, indicating they had a higher probability of being involved in hazards compared with other entities. As mentioned earlier, the top entities in the degree centrality ranking and the eigenvector centrality ranking might have some in common. Frame 3 was selected merely to illustrate the application and meanings of entity-level indicators for risk

analysis, even though the relative risk score of frame 3 is very low [Fig. 3(b)].

- During the monitoring period of jobsite #1 [Figs. 8(a) and 9(a)], it is observed that the entity #3 had the maximum number of frames with the highest degree centrality and the highest eigenvector centrality [marked in Figs. 8(a) and 9(a) using a rectangle]. Therefore, most of the time entity #3, which can be considered a risk-prone entity, took more actions that cause hazards [Fig. 8(a)] and presented a higher probability to be involved in hazards [Fig. 9(a)].
- Project managers and safety personnel can clearly capture the trend of centrality evolution for each entity [Figs. 8(b) and 9(b)]. For example, the eigenvector centrality of entity #3 overall trended upward (became more risk-prone) after frame 900 and stayed high until frame 1600 [Fig. 9(b)].

Applications

Multiple applications are derived based on monitoring the leading indicators.

- The results obtained from the entity- and network-level analyses can be combined for real-time hazard identification. For example, if the monitored relative risk score exceeded its threshold, priority countermeasures could be selected and applied to the entities which are identified with higher centrality [e.g., Figs. 8(a) and 9(a)].
- Similarly, a threshold for degree centrality can be defined. By comparing the monitored centrality with the defined threshold, entities with high risk of collisions can be identified and controlled effectively. For example, the degree centrality of a piece of equipment that had amassed a total of 960 collisions

(defined in Table 3) over the simulated 2000 frames ranged [5.0, 24.6] with an average of 12.7, whereas the degree centrality of another piece of equipment which had no collisions over the 2000 frames ranged [2.0, 5.6] with an average of 3.1. In the next step of this study, the statistical analysis of entity-level indicator scores, relative risk scores, number of collisions at each frame, and others for more jobsites will be conducted to determine the corresponding indicator's threshold. In addition, through monitoring the evolution of each indicator, interventions can be implemented to prevent it from increasing.

- More important, entities' performance can be evaluated from the following two perspectives so that specialized and proactive safety training can be provided for specific entities:
 - (1) Entities that had more risk-related actions over time can be identified [e.g., Figs. 8(a) and 9(a)]; and
 - (2) For each entity, periods of time having non-low relative risk scores during which the entity exhibited risk-prone actions can be identified [e.g., Figs. 8(b) and 9(b)].
- Based on the combined analysis at the entity and network levels, near-miss events can be tracked and recorded for further safety training and hazard prevention.

Discussions

Compared with the existing methods that rely solely on detecting the proximity between entities to prevent struck-by-equipment hazards, the developed network-based model considers the dynamic interactions of multiple factors that coexist on an entire

jobsite. Even though real-time interactions between entities can be monitored and used alone to detect hazards, the focus of this paper is to demonstrate the capability and advantages of the network-based model in multi-level safety risk analysis. Furthermore, the risk evolution of each entity and the network can be tracked and analyzed for risk prediction.

It is worth emphasizing that the methodology of the network-based model with its implementation is the primary focus and contribution of this paper. Afterward, a powerful and robust cyber-physical system that automatically and smartly performs the above-mentioned comprehensive analysis, including results visualization and countermeasures actuation, will be developed as the continuation of the present work.

Contributions

The primary contribution of this paper is the development of a network-based model for the risk analysis of struck-by-equipment hazard. Other contributions are as follows:

- Consideration and quantification of the dynamic spatiotemporal interactions among entities resulting from the selected risk factors including proximity, blind spots, and velocity, to assess struck-by-equipment risk;
- Assessment of the overall risk of the interactions coexisting on the entire jobsite by applying network-level risk analysis;
- Investigation of the different roles that entities are playing in the occurrences of struck-by-equipment hazards by applying entity-level risk analysis; and
- Provision of a systematic methodology for the safety management of struck-by-

equipment hazards, including safety performance assessment, safety training, and collection of data on near misses.

Limitations and Future Work

The quantification of interactions among entities involves a variable, i.e., the weight of each considered risk factor in causing hazards [Equations (1)-(3)]. In this paper, determination of the weight of each factor relied on the information extracted from the historical records of the FACE program. Currently, available detailed reports regarding struck-by-equipment hazard are very limited. Therefore, the quantified weight of each factor will be adjusted and improved with more collected detailed reports regarding near miss, injury, and fatality. Assistance from both industry and academia on tracking and recording hazard details of near miss, injury, and fatality will significantly aid the full implementation of the developed model (Shen et al. 2015; Wu et al. 2010).

Equipment blind spots are included in the developed model. In this paper, the blind spots of the adopted equipment were provided by the CDC (2009), which studies blind spots for a vast number of equipment types. Nonetheless, real-time automatic measurement of blind spots can be utilized and integrated into the developed model (Ray and Teizer 2016; Teizer et al. 2010). In this way, the applicability and flexibility of the developed model will be greatly enhanced.

To further explore the practical applications of the developed network-based model with the safety leading indicators (such as risk prediction), more analysis on the indicators' scores and evolution will be conducted. In addition, validation of the developed network-based model on real jobsites is needed and will be conducted in the

next step of this study.

Conclusion

A spatiotemporal network-based model is developed in this paper for comprehensive and dynamic risk analysis on struck-by-equipment hazard. Three major risk factors—proximity, blind spots, and velocity—were selected for model development. The dynamic interactions of the selected factors among entities are quantified by considering (i) the weight of each risk factor in causing hazards and (ii) the corresponding resulting severity of the real-time monitored situation. The comprehensive safety risk analysis and its derived practical applications are further discussed using four simulated jobsites. The developed network-based model is capable of performing entity-level and network-level risk analysis in real-time and proactive manners. Further insight into the safety performance of individual entities as well as jobsites to proactively identify and prevent hazards was gained. The work presented in this paper provides a methodology for the safety management of struck-by-equipment hazard.

References

- Alexander, D., Hallowell, M. and Gambatese, J. (2015). “Energy-based safety risk management: using hazard energy to predict injury severity.” *Proc., 5th Inter/11th Construction Specialty Conf.*, Vol. 214, Univ. of British Columbia, Vancouver, Canada, 1-10.
- Baradan, S. and Usmen, M. (2006). "Comparative Injury and Fatality Risk Analysis of Building Trades." *J. Constr. Eng. Manage.*, 10.1061/(ASCE)0733-9364(2006)132:5(533), 533-539.

- Bartels, J., Ambrose, D. and Gallagher, S. (2006). “Analyzing factors influencing struck-by accidents of a moving mining machine by using motion capture and DHM simulations.” *SAE Int. J. Passenger Cars, Electron Electr Syst*, 1, 599-604.
- BLS (Bureau of Labor Statistics). (2016b). “Census of fatal occupational injuries (CFOI)- Current and revised data.” <<http://www.bls.gov/iif/oshcfoi1.htm>> (Aug. 18, 2016).
- Bobadilla, L., Mostafavi, A., Carmenate, T., and Bista, S. (2014). “Predictive Assessment and Proactive Monitoring of Struck-By Safety Hazards in Construction Sites: An Information Space Approach.” *Comput.in Civ. and Build. Eng.*, 989-996.
- Canright, G. and Engø-Monsen, K. (2004). “Roles in networks.” *Science of Computer Programming*, 53(2), 195–214.
- Carreras, I., Miorandi, D., Canright, G. and Engø-Monsen, K. (2007). “Eigenvector centrality in highly partitioned mobile networks: principles and applications.” In: Dressler, F. and Carreras, I. (Eds) *Advances in Biologically Inspired Information Systems*. 1st Ed., Springer, Berlin, 123-145.
- CDC (2009). “Construction Equipment Visibility” <<http://www.cdc.gov/niosh/topics/highwayworkzones/bad/imagelookup.html>> (June 19, 2016).
- Choe, S., Leite, F., Seedah, D., and Caldas, C. (2014). “Evaluation of sensing technology for the prevention of backover accidents in construction work zones.” *Journal of Information Technology in Construction*, 19, 1–19.
- CPWR (Center for Construction Research and Training) (2012a). “Worker Age in Construction and Other Industries.” *The construction chart book*, 14, 1-2.

- CPWR (Center for Construction Research and Training) (2012b). "Hours Worked, Overtime, and Time Use in Construction and Other Industries." *The construction chart book*, 29, 1-2.
- Esmaeili, B., Hallowell, M., and Rajagopalan, B. (2015a). "Attribute-Based Safety Risk Assessment. II: Predicting Safety Outcomes Using Generalized Linear Models." *Journal of Construction Engineering and Management*, 10.1061/(ASCE)CO.1943-7862.0000981,04015022.
- Golovina, O., Teizer, J. and Pradhananga, N. (2016). "Heat map generation for predictive safety planning: Preventing struck-by and near miss interactions between workers-on-foot and construction equipment." *Autom. Constr.*, 71, 99–115.
- Hallowell, M., Esmaeili, B. and Chinowsky, P. (2011). "Safety risk interactions among highway construction work tasks." *J. Constr. Manage. Econ.*, 29(4), 417–429.
- Hallowell, M. and Gambatese, J. (2009). "Activity-Based Safety Risk Quantification for Concrete Formwork Construction." *J. Constr. Eng. Manage.*, 10.1061/(ASCE)CO.1943-7862.0000071, 990-998.
- Hinze, J., Huang, X., and Terry, L. (2005). "The Nature of Struck-by Accidents." *J. Constr. Eng. Manage.*, 10.1061/(ASCE)0733-9364(2005)131:2(262), 262-268.
- Isaac, S. and Edrei, T. (2016). "A statistical model for dynamic safety risk control on construction sites." *Autom. Constr.*, 63, 66–78.
- Jiang, H., Lin, P., Fan, Q., and Qiang, M. (2014). "Real-time safety risk assessment based on a real-time location system for hydropower construction sites." *The Scientific World J.*, 1-14.

- Kim, H., Kim, K., and Kim, H. (2016). “Vision-Based Object-Centric Safety Assessment Using Fuzzy Inference: Monitoring Struck-By Accidents with Moving Objects.” *Journal of Computing in Civil Engineering*, 10.1061/(ASCE)CP.1943-5487.0000562,04015075.
- Lee, H., Kim, H., Park, M., Ai Lin Teo, E., and Lee, K. (2012). “Construction Risk Assessment Using Site Influence Factors.” *J. Comput. Civ. Eng.*, 10.1061/(ASCE)CP.1943-5487.0000146, 319-330.
- Li, H., Lu, M., Hsu, S.-C., Gray, M., and Huang, T. (2015b). “Proactive behavior-based safety management for construction safety improvement.” *Safety Science*, 75, 107-117.
- Luo, X., Li, H., Huang, T., and Skitmore, M. (2016). “Quantifying Hazard Exposure Using Real-Time Location Data of Construction Workforce and Equipment.” *Journal of Construction Engineering and Management*, 10.1061/(ASCE)CO.1943-7862.0001139,04016031.
- NIOSH (National Institute for Occupational Safety and Health) (2016). “Fatality Assessment and Control Evaluation (FACE) program.” <https://www.cdc.gov/niosh/face/> (Apr. 18, 2016).
- Opsahl, T., Agneessens, F. and Skvoretz, J. (2010). “Node centrality in weighted networks : Generalizing degree and shortest paths.” *Social Networks*, 32(3), 245–251.
- OSHA (Occupational Safety and Health Administration). (2016). “Construction eTool- Struck by.”

<<https://www.osha.gov/SLTC/etools/construction/struckby/mainpage.html>> (Aug. 18, 2016).

Park, J., Marks, E., Cho, Y., and Suryanto, W. (2015). "Performance test of wireless technologies for personnel and equipment proximity sensing in work zones." *Journal of Construction Engineering and Management*, 10.1061/(ASCE)CO.1943-7862.0001031, 04015049.

Ray, S and Teizer, J. (2016). "Dynamic blindspots measurement for construction equipment operators." *Safety Science*, 85, 139–151.

Ruff, T. M. (2010). "Overview of proximity warning and technologies and approaches." *National Institute for Occupational Safety and Health (NIOSH) Workshop on Proximity Warning Systems for Mining Equipment*, Centers for Disease Control and Prevention (CDC), Atlanta, GA.

Seo, J., Han, S., Lee, S., and Kim, H. (2015). "Computer vision techniques for construction safety and health monitoring." *Advanced Engineering Informatics*, 29(2), 239-251.

Shapira, A., Simcha, M., and Goldenberg, M. (2012). "Integrative Model for Quantitative Evaluation of Safety on Construction Sites with Tower Cranes." *J. Constr. Eng. Manage.*, 10.1061/(ASCE)CO.1943-7862.0000537,1281-1293.

Shen, X. and Marks, E. (2015). "Near-Miss Information Visualization Tool in BIM for Construction Safety." *J. Constr. Eng. Manage.*, 10.1061/(ASCE)CO.1943-7862.0001100, 04015100.

Spizzirri, L. (2011). "Justification and Application of Eigenvector Centrality." *Algebra in*

Geography: Eigenvectors of Networks, 1-12.

- Tchiehe, D. and Gauthier, F. (2017). “Classification of risk acceptability and risk tolerability factors in occupational health and safety.” *Safety Science*, 92, 138-147.
- Teizer, J., Allread, B. and Mantripragada, U. (2010). “Automating the blind spot measurement of construction equipment.” *Autom. Constr.*, 19(4), 491–501.
- Teizer, J. and Cheng, T. (2015). “Proximity hazard indicator for workers-on-foot near miss interactions with construction equipment and geo-referenced hazard areas.” *Automation in Construction*, 60, 58–73.
- Vahdatikhaki, F. and Hammad, A. (2015). “Risk-based look-ahead workspace generation for earthwork equipment using near real-time simulation.” *Autom. Constr.*, 58, 207–220.
- Wang, J., Du, S., and Razavi, S. (2016). “An integrated INS-GPS-Raspberry Pi system using the time-sphere model for real-time identification of struck- by-equipment hazard.” *Proceedings of the 33rd ISARC*, International Association for Automation and Robotics in Construction (IAARC), 1032-1040.
- Wang, J., and Razavi, S. (2016a). “Low False Alarm Rate Model for Unsafe-Proximity Detection in Construction.” *J. Comput. Civ. Eng.*, 10.1061/(ASCE)CP.1943-5487.0000470, 04015005.
- Wang, J., and Razavi, S. (2016b). “Two 4D Models Effective in Reducing False Alarms for Struck-by-Equipment Hazard Prevention.” *J. Comput. Civ. Eng.*, 10.1061/(ASCE)CP.1943-5487.0000589, 04016031.
- Wang, J., and Razavi, S. (2017a). “A Comprehensive Spatio-Temporal Network-Based

Model for Dynamic Risk Analysis on Struck-by-Equipment Hazard.”

International Workshop on Computing in Civil Engineering, ASCE, Reston, VA.
384-391.

Wei, P. and Sun, D. (2011). “Weighted algebraic connectivity: An application to airport transportation network.” *IFAC Proceedings Volumes*, 44(1), 13864–13869.

Wu, W., Gibb, A. and Li, Q. (2010). “Accident precursors and near misses on construction sites: An investigative tool to derive information from accident databases.” *Safety Science*, 48(7), 845–858.

Zafarani, R., Abbasi, M. and Liu, H. (2014). *Social Media Mining: An Introduction*, Cambridge University Press, Cambridge.

Zhu, Z., Park, M., Koch, C., Soltani, M. and Hammad, A. (2016). “Predicting movements of onsite workers and mobile equipment for enhancing construction site safety.” *Autom. Constr.*, 68, 95–101.

CHAPTER 5: CONCLUSIONS

Summary, Contributions, and Impacts

The continuously high number of injuries and fatalities in construction indicates that safety is one of the foremost challenges faced by the construction industry. Improved situational awareness in construction environments contributes to identifying hazardous situations and avoiding accidents. To enhance construction safety and reduce injuries and fatalities, this thesis presents a comprehensive study on improving situational awareness to prevent struck-by-equipment hazards (workers on foot struck by equipment or equipment struck by equipment) on construction sites. Two identified solutions to improve situational awareness include (i) effective detection of unsafe proximities between construction entities in near real time and (ii) analysis of risk levels over time. Therefore, the study, i.e., situational awareness for construction safety risks management (SA4SR), presented in this thesis includes two modules: hazard detection and risk awareness.

Hazard detection: The existing methods for unsafe-proximity detection have a major and common limitation which is the high frequency of false alarms generated. Thus, the hazard detection module (Chapters 2 and 3) in the SA4SR focuses on identifying struck-by-equipment hazards with reduced false alarms in a timely manner. The primary contribution was the development of the three models, including a 3D model and two 4D models (time-sphere model and time-cuboid model) to detect hazards with a low false

alarm rate. The 3D model (described in Chapter 2) considered construction entities' motions and alert zones in a two-dimensional space. To depict real situations on sites and identify safety hazards more accurately, the time-sphere and time-cuboid models (described in Chapter 3) improved the 3D model and considered entities' three-dimensional motions and alert zones. Different from most of the existing methods which only consider the distance between entities for hazard detection, the developed unsafe-proximity query rules (which were termed safety rules in the developed 3D model in Chapter 2) in each model considered entities' positions, velocity, and orientation altogether. Furthermore, the developed models can identify not only the occurring unsafe situations but also the imminent unsafe proximities. The obtained results demonstrated the effectiveness of the three models in reducing false alarms in the struck-by-equipment hazard detection. Based on the characteristics of sites and entities, the appropriate model can be selected and applied.

Risk awareness: In addition to the near real-time hazard detection between paired entities (Chapters 2 and 3), the overall risk levels of each entity (entity-level risk) and the whole jobsite (network-level risk) regarding struck-by equipment hazards also need to be investigated for proactive hazard prevention. One of the identified gaps in the literature was that no such systematic risk analysis methods had been developed particularly for struck-by hazards. Therefore, to fill the identified gap, in the risk awareness module (Chapter 4) of the SA4SR, a network-based model including four major steps was developed to analyze the dynamic struck-by equipment risk at both entity and network levels. The developed network-based model filled the gap by considering all entities and

their quantified interactions that coexist on a site as a network for the systematic risk analysis. The monitoring and analysis of the struck-by-equipment risk levels over time assist to evaluate and compare safety performance, identify entities/sites with high-risk levels, and provide insight into activity and site layout planning. Furthermore, the obtained outcomes can also provide insight into or be integrated with other fields of studies, such as human-in-the-loop cyber-physical systems and construction workers' behaviors.

The SA4SR: The situational awareness can be improved by using the developed analytical models in the SA4SR combined with technologies (e.g., motion tracking sensors and data communication platforms). Accordingly, struck-by-equipment hazards can be proactively prevented and injuries and fatalities on construction sites will be reduced. The SA4SR provides a systematic methodology for researchers and industrial professionals who are interested in struck-by-equipment hazard prevention. The detailed contributions and impacts of the SA4SR are summarized as below:

- Three models for false alarm reduction in proximity-hazard detection are developed. Reducing false alarms will reduce interruptions to work and maintain site mobility, and consequently improve construction productivity.
- An integrated individual and site risk analysis method is developed. Analyzing risk at both entity and network levels will assist to make decisions and take corrective actions from both entity and system levels to proactively prevent hazards.
- The expected outcomes of the SA4SR are to alleviate safety concerns in

construction and further lead to a greener and sustainable construction system.

- Improved construction safety will reduce the associated delays and cost incurred by accidents on jobsites, and accordingly, will achieve projects' goals in cost, schedule, and quality.
- The applications of the SA4SR are also expected to induce social and economic benefits that can influence the quality of life of the public, such as the decreased insurance claims and hospitalizations.

Although the work presented in this thesis mainly focuses on the struck-by-equipment hazard, the SA4SR can be further extended and applied to other types of contact collisions on construction sites and in work zones. For example, based on the developed network-based risk analysis model in Chapter 4, a framework for network-based comprehensive safety risk analysis for contact collisions in construction was proposed and developed [the work has been developed and submitted as another journal article of Wang and Razavi (2017b)]. The methodology for construction safety risks management developed in this thesis integrates data acquisition, processing, analysis, and communication, which contributes to the future development of smart construction.

Recommendations for Future Work

In this thesis, the advantages and limitations of existing proximity detection technologies were investigated and summarized to provide insight into real-world applications. However, the implementation and testing of the developed hazard detection and risk analysis models on real construction sites were not conducted. To fully and effectively employ the developed SA4SR on real construction sites, a reliable and robust

system integrating computation, sensing, visualization, actuation, and wireless data communication needs to be developed. The development of such a system involves and stimulates rich interdisciplinary studies. To achieve the system development goal, some exploratory work has been conducted during my Ph.D. study. Herein, two pieces of the conducted work with the corresponding yielded future work are described.

- i. Smartphone construction safety awareness system: a cyber-physical system approach (Genders et al. 2016)

In this work, a cyber-physical system (CPS) approach was used to design and develop a smartphone-based system to alert hazardous proximities of entities and improve construction site safety awareness. The developed smartphone-based system functioned on a client-server model between smartphone clients (construction entities) and a central server. The field testing showed that the smartphone GPS measurement error and the system responsiveness were two limiting issues that needed to be resolved before real-world deployment. The GPS error is hardware dependent, and the trend for decades has been continuous technological improvements. The requirements for hardware and software need to be further investigated for the system utilization on real sites. The development of the smartphone-based system presented strong evidence that the common and cost-effective technology can be programmed to perform highly specialized tasks to improve construction safety (Yoon et al. 2016).

- ii. An integrated INS-GPS-Raspberry Pi system using the time-sphere model for real-time identification of struck-by-equipment hazard (Wang et al. 2016)

In this work, an integrated inertial navigation system (INS)-GPS-Raspberry Pi

system was developed to timely identify and alarm struck-by-equipment hazards. The integrated system (INS-GPS-Raspberry Pi) was aimed to be equipped by each dynamic entity. The developed time-sphere model described in Chapter 3 was embedded in another Raspberry Pi which was the central data processing unit to analyze the collected states of entities for unsafe-proximity identification. Visual warnings were triggered for the identified unsafe entities, i.e., the light on the corresponding INS-GPS-Raspberry Pi system started flashing, if an unsafe proximity was identified.

However, in this work, the developed integrated system was not suitable to be worn by workers on foot due to its size ($17 \times 13.5 \times 7$ cm). Thus, the hazard type of workers on foot struck by equipment was not included or tested in the controlled field experiment. More compacted devices need to be explored and developed for workers on foot to use. Also, in recent years cameras have been introduced to construction sites and used for surveillance and site monitoring. For example, in the studies of Zhu et al. (2017), Kim et al. (2016), and Park et al. (2012), on-site camera systems were used to track the motions of workforce and equipment; in the work of Han and Golparvar-Fard (2017), Ham et al. (2016), and Yang et al. (2015), using visual data to monitor construction progress was presented. Thus, cameras present high promise to be used to collect construction entities' motions which will be sent to the server with the developed hazard detection and risk analysis models for processing. In addition, more reliable and advanced actuation mechanisms (not limited to visual, audible and vibrant warnings) need to be studied for the complex construction environments.

In addition to the future work presented in chapters 2 to 4 (i.e. individual papers),

another two future research plans based on this thesis are suggested and described below:

Human-in-the-loop cyber-physical systems for construction safety: In this thesis, construction entities' motions were tracked and entities were assumed to apply preventive actions upon receiving alarms and notifications to avoid hazards. However, in the real world, compliance of workers with the assigned and instructed actions or recommended behaviors is a problem with high levels of uncertainties. A majority of construction accidents are related to workers' unsafe behaviors (Jiang et al. 2015). Human behavior is a complex interplay of three components, including cognitions, emotions, and actions (IMOTIONS 2017). Monitoring and analysis of workers' behaviors in a timely and smart manner by considering the above-mentioned three components enables to investigate the potential causes of unsafe behaviors and to improve safety performance in construction site environments (Luo et al. 2016; Li et al. 2015b). It should be noted that the cyber-physical systems approach has been introduced to the construction domain, and some studies have been conducted for safer construction sites, such as the work conducted by Kan et al. (2017), Yuan et al. (2016), and Barro-Torres et al. (2012). Therefore, further studies can integrate the element of human behaviors into the cyber-physical systems, i.e., human-in-the-loop cyber-physical systems to prevent safety hazards on sites. One of the challenges involved in this research plan is to understand and determine the types of behaviors and the human-in-the-loop controls to be included and studied in the human-in-the-loop cyber-physical systems. Another expected challenge is the modeling of workers' behaviors due to the complex physiological, psychological, and behavioral aspects of human beings (Munir et al. 2013).

Multi-layer network-based safety risks analysis in construction: This research focuses on evaluating the safety performance of a construction project to avoid undesirable consequences. In this thesis, the developed weighted network for struck-by-equipment risk analysis modeled construction entities and put entities and the real-time quantified risk factors in the same network layer. However, some aspects such as entities' attributes were not considered and included in the modeled network. For a construction project, the levels of safety risks are determined by multiple aspects, including but not limited to entities' attributes, safety communication, safety risk factors, construction environments, and organizational behavior (McCabe et al. 2017; Jitwasinkul et al. 2016; Namian et al. 2016; Kines et al. 2010). Thus, instead of modeling all the aspects in the same layer, the multi-layer networks can be adopted. The multi-layer networks can be composed of attribute-based layers, entity-based layers, risk factor-based layers, environment-based layers, and some other layers. Such networks conceptualize and quantify the above-mentioned aspects and their interactions, interrelationships, and uncertainties to fully model the safety performance. The network analysis techniques used in Chapter 4 can be further explored for multi-layer networks analysis, and more network metrics can be developed to reflect the levels of safety risks. Furthermore, other perspectives such as the resilience of the safety networks of a project can be analyzed.

The expected outcome of this research is the development of an adaptive method to analyze, address, and control the safety risks with high levels of uncertainty and complexity in construction.

REFERENCES

- Albert, A. and Hallowell, M. (2014) “Modeling the role of social networks in situational awareness and hazard communication.” *Construction Research Congress*, ASCE, Reston, VA, 1752–1761.
- AWCBC (Association of Workers Compensation Boards of Canada). (2016). 2015 Injury Statistics across Canada <http://awcbc.org/?page_id=14 > (Accessed on Sept. 28, 2017).
- Barro-Torres, S., Fernandez-Carams, T.M., Prez-Iglesias, H.J., and Escudero, C.J. (2012). “Real-time personal protective equipment monitoring system.” *Computer Communications*, 36 (1), 42-50.
- Behzadan, A. H., Aziz, Z., Anumba, C. J., and Kamat, V. R. (2008). “Ubiquitous location tracking for context-specific information delivery on construction sites.” *Automation in Construction*, 17(6), 737–748.
- BLS (Bureau of Labor Statistics). (2016a). Census of fatal occupational injuries (CFOI). <<https://www.bls.gov/iif/oshcfoi1.htm#2015>> (Accessed on Sept. 28, 2017).
- BLS (Bureau of Labor Statistics). (2016b). “Census of fatal occupational injuries (CFOI)- Current and revised data.” <<http://www.bls.gov/iif/oshcfoi1.htm>> (Aug. 18, 2016).
- Cheng, T., and Teizer, J. (2013). “Real-time resource location data collection and visualization technology for construction safety and activity monitoring applications.” *Automation in Construction*, 34, 3–15.
- Choe, S., Leite, F., Seedah, D., and Caldas, C. (2014). “Evaluation of sensing technology for the prevention of backover accidents in construction work zones.” *Journal of*

Information Technology in Construction, 19, 1–19.

Endsley, M.R. (2000). “Theoretical underpinnings of situation awareness: a critical review.” *Situation Awareness analysis and Measurement*, 3-32.

Esmaeili, B., Hallowell, M., and Rajagopalan, B. (2015a). “Attribute-Based Safety Risk Assessment. II: Predicting Safety Outcomes Using Generalized Linear Models.” *Journal of Construction Engineering and Management*, 10.1061/(ASCE)CO.1943-7862.0000981,04015022.

Genders, W., Wang, J., and Razavi, S. (2016). “Smartphone Construction Safety Awareness System: A Cyber-Physical System Approach.” *The 16th International Conference on Computing in Civil and Building Engineering*, Osaka University, Japan, 1697-1704.

Guo, H., Li, H., Chan, G., and Skitmore, M. (2012). “Using game technologies to improve the safety of construction plant operations.” *Accident Analysis & Prevention*, 48, 204-213.

Ham, Y., Han, K.K., Lin, J.J. and Golparvar-Fard, M. (2016). “Visual monitoring of civil infrastructure systems via camera-equipped Unmanned Aerial Vehicles (UAVs): a review of related works.” *Visualization in Engineering*, 4(1), 1-8.

Han, K., and Golparvar-Fard, M. (2017). “Potential of big visual data and building information modeling for construction performance analytics: An exploratory study.” *Automation in Construction*, 73, 184–198.

Hasanzadeh, S., Esmaeili, B., and Dodd, M. (2016). “Measuring construction workers’ real-time situation awareness using mobile eye-tracking.” *Construction Research*

Congress, ASCE, Reston, VA, 2894–2904.

HSE (Health and Safety Executive). (2015). “Leadership and worker involvement toolkit.”

<<http://www.hse.gov.uk/construction/lwit/assets/downloads/situational-awareness.pdf>> (Accessed on Feb. 9, 2018)

Hinze, J. W., and Teizer, J. (2011). “Visibility-related fatalities related to construction equipment.” *Safety Science*, 49(5), 709–718.

Hu, Z.Z. and Zhang, J.P. (2011). “BIM- and 4D-based integrated solution of analysis and management for conflicts and structural safety problems during construction: 1. Principles and methodologies.” *Automation in Construction*, 20(2), 155-166.

IHSA (Infrastructure Health and Safety Association). (2013). “Can new technologies prevent struck-by injuries?” *IHSA Magazine*, 3(13), 20–21.

IHSA (Infrastructure Health and Safety Association). “Struck-by Hazards.” <http://www.ihsa.ca/Topics_Hazards/Struck_Bys.aspx> (Accessed on Sept. 29, 2017).

IMOTIONS. (2017). “Human Behavior: The Complete Pocket Guide.” <<https://imotions.com/>> (Accessed on Nov. 2, 2017)

Irizarry, J., Gheisari, M., Williams, G., and Walker, B.N. (2013). “InfoSPOT: a mobile augmented reality method for assessing building information through a situation awareness approach.” *Automation in Construction*, 33, 11-23.

Jiang, Z., Fang, D., and Zhang, M. (2015). “Understanding the causation of construction workers’ unsafe behaviors based on system dynamics modeling.” *Journal of Management in Engineering*, 10.1061/(ASCE)ME.1943-5479.0000350, 04014099.

- Jitwasinkul, B., Hadikusumo, B. H., and Memon, A. Q. (2016). “A Bayesian Belief Network model of organizational factors for improving safe work behaviors in Thai construction industry.” *Safety Science*, 82(2), 264-273.
- Kan, C., Anumba, C. J., and Messner, J. I. (2017). “Potential Use of Cyber-Physical Systems (CPS) for Planning and Operation of Mobile Cranes on Construction Sites.” *International Workshop on Computing in Civil Engineering 2017*, ASCE, Reston, VA, 139-146.
- Kannan, M.R. and Santhi, M.H. (2013). “Constructability assessment of climbing formwork systems using building information modeling.” *Procedia Eng.*, 64, 1129-1138.
- Kim, H., Kim, K., and Kim, H. (2016). “Vision-Based Object-Centric Safety Assessment Using Fuzzy Inference: Monitoring Struck-By Accidents with Moving Objects.” *Journal of Computing in Civil Engineering*, 10.1061/(ASCE)CP.1943-5487.0000562,04015075.
- Kines, P., Andersen, L.P., Spangenberg, S., Mikkelsen, K.L., Dyreborg, J., and Zohar, D. (2010). “Improving construction site safety through leader-based verbal safety communication.” *Journal of Safety Research*, 41 (5), 399-406.
- Kochovski, P and Stankovski, V. (2018). “Supporting smart construction with dependable edge computing infrastructures and applications.” *Automation in Construction*, 85, 182–192.
- Li, H., Lu, M., Chan, G., and Skitmore, M. (2015a). “Proactive training system for safe and efficient precast installation.” *Automation in Construction*, 49, 163-174.

- Li, H., Lu, M., Hsu, S.-C., Gray, M., and Huang, T. (2015b). “Proactive behavior-based safety management for construction safety improvement.” *Safety Science*, 75, 107-117.
- Li, J., Carr, J., and Jobes, C. (2012). “A shell-based magnetic field model for magnetic proximity detection systems.” *Safety Science*, 50(3), 463–471.
- Luo, X., Li, H., Huang, T., and Skitmore, M. (2016). “Quantifying Hazard Exposure Using Real-Time Location Data of Construction Workforce and Equipment.” *Journal of Construction Engineering and Management*, 10.1061/(ASCE)CO.1943-7862.0001139,04016031.
- McCabe, B.Y., Alderman, E., Chen, Y., Hyatt, D.E., Shahi, A. (2017). “Safety Performance in the Construction Industry: Quasi-Longitudinal Study.” *Journal of Construction Engineering and Management*, 10.1061/(ASCE)CO.1943-7862.0001260.
- Munir, S., Stankovic, J.A., Liang, C.-J.M., and Lin, S. (2013). “Cyber physical system challenges for human-in-the-loop control.” *Feedback Computing*.
- Namian, M., Albert, A., Zuluaga, C. M., and Behm, M. (2016). “Role of safety training: Impact on hazard recognition and safety risk perception.” *Journal of Construction Engineering and Management*, 10.1061/(ASCE)CO.1943-7862.0001198, 04016073.
- OSHA (Occupational Safety and Health Administration). Top Four Construction Hazards. <<https://www.osha.gov/Publications/3216-6N-06-english-06-27-2007.html>> (Accessed on Sept. 28, 2017).

- Park, J., Marks, E., Cho, Y., and Suryanto, W. (2015). “Performance test of wireless technologies for personnel and equipment proximity sensing in work zones.” *Journal of Construction Engineering and Management*, 10.1061/(ASCE)CO.1943-7862.0001031, 04015049.
- Park, M., Koch, C., and Brilakis, I. (2012). “Three-dimensional tracking of construction resources using an on-site camera system.” *Journal of Computing in Civil Engineering*, 10.1061/(ASCE)CP.1943-5487.0000168, 541–549.
- Pinto, A., Nunes, I.L., and Ribeiro, R.A. (2011). “Occupational risk assessment in construction industry – Overview and reflection.” *Journal of Safety Science*, 49, 616-624.
- Statistics Canada. (2017). Labour force survey estimates (LFS), by North American Industry Classification System (NAICS), sex and age group. CANSIM Database, Table 282-0008.
- Teizer, J. and Cheng, T. (2015). “Proximity hazard indicator for workers-on-foot near miss interactions with construction equipment and geo-referenced hazard areas.” *Automation in Construction*, 60, 58–73.
- Teizer, J., Cheng, T., and Fang, Y. (2013). “Location tracking and data visualization technology to advance construction ironworkers’ education and training in safety and productivity.” *Automation in Construction*, 35, 53-68.
- Vahdatikhaki, F., Hammad, A., and Langari, S. M. (2015). “Multi-agent system for improved safety and productivity of earthwork equipment using real-time location systems.” *Proc., 5th Int./11th Construction Specialty Conf.*, Univ. of British

Columbia, Vancouver, BC, Canada, 1–10.

- Wang, C., and Cho, Y.K. (2015). “Smart scanning and near real-time 3D surface modeling of dynamic construction equipment from a point cloud.” *Automation in Construction*, 49, 239-249.
- Wang, D., Chen, J., Zhao, D., Dai, F., Zheng, C., and Wu, X. (2017). “Monitoring workers' attention and vigilance in construction activities through a wireless and wearable electroencephalography system.” *Automation in Construction*, 82, 122-137.
- Wang, J., and Razavi, S. (2016a). “Low False Alarm Rate Model for Unsafe-Proximity Detection in Construction.” *Journal of Computing in Civil Engineering*, DOI: 10.1061/(ASCE)CP.1943-5487.0000470
- Wang, J., and Razavi, S. (2016b). “Two 4D Models Effective in Reducing False Alarms for Struck-by-Equipment Hazard Prevention.” *Journal of Computing in Civil Engineering*, DOI: 10.1061/(ASCE)CP.1943-5487.0000589
- Wang, J., and Razavi, S. (2017b). “A Framework for Network-based Comprehensive Safety Risk Analysis in Construction.” *Submitted to the Canadian Journal of Civil Engineering* on Sept. 12, 2017.
- Wang, J., Du, S., and Razavi, S. (2016). “An integrated INS-GPS-Raspberry Pi system using the time-sphere model for real-time identification of struck- by-equipment hazard.” *Proceedings of the 33rd ISARC*, International Association for Automation and Robotics in Construction (IAARC), 1032-1040.
- WSIB (Workplace Safety and Insurance Board). (2017). 2016 WSIB Statistical Report

By the Numbers. <<http://www.wsibstatistics.ca/>> (Accessed on Sept. 28, 2017)

- Yang, J., Park, M-W., Vela, P. A., and Golparvar-Fard, M. (2015). “Construction performance monitoring via still images, time-lapse photos, and video streams: Now, tomorrow, and the future.” *Advanced Engineering Informatics*, 29(2), 211–224.
- Yang, K., Ahn, C. R., Vuran, M. C., and Aria, S. S. (2016). “Semi-supervised near-miss fall detection for ironworkers with a wearable inertial measurement unit.” *Automation in Construction*, 68, 194–202.
- Yoon, H., Ham, Y., Golparvar-Fard, M., and Spencer, B. F. (2015). “Forward-Backward Approach for 3D Event Localization Using Commodity Smartphones for Ubiquitous Context-Aware Applications in Civil and Infrastructure Engineering.” *Computer-Aided Civil and Infrastructure Engineering*, 31(4), 245–260.
- Yuan, X., Anumba, C.J., Parfitt, M.K. (2016). “Cyber-physical systems for temporary structure monitoring.” *Automation in Construction*, 66, 1–14.
- Zhang, S., Teizer, J., Lee, J.-K., Eastman, C. M., and Venugopal, M. (2013). “Building information modeling (BIM) and safety: Automatic safety checking of construction models and schedules.” *Automation in Construction*, 29(1), 183–195.
- Zhou, W., Whyte, J., and Sacks, R. (2012). “Construction safety and digital design: A review.” *Automation in Construction*, 22(1), 102–111.
- Zhu, Z., Ren, X, and Chen, Z. (2017). “Integrated detection and tracking of workforce and equipment from construction jobsite videos.” *Automation in Construction*, 81, 161–171.